Title
The Identification and Characterization of Chondrodysplasias Resulting from Cartilage Extracellular Matrix Abnormalities

Author
Balasubramanian, Karthika

Publication Date
2017

Peer reviewed|Thesis/dissertation

UNIVERSITY OF CALIFORNIA

Los Angeles

The Identification and Characterization of Chondrodysplasias Resulting from Cartilage Extracellular Matrix Abnormalities

A dissertation submitted in partial satisfaction of the

requirements for the Doctor of Philosophy

in Molecular, Cell and Developmental Biology

by

Karthika Balasubramanian

2017

ABSTRACT OF THE DISSERTATION

The Identification and Characterization of Chondrodysplasias Resulting from Cartilage Extracellular Matrix Abnormalities

by

Karthika Balasubramanian

Doctor of Philosophy in Molecular, Cell and Developmental Biology

University of California, Los Angeles, 2017

Professor Daniel H. Cohn, Chair

The chondrodysplasias are a group of genetic disorders resulting from profound defects in cartilage development. Two mild chondrodysplasias, Multiple Epiphyseal Dysplasia (MED) and Stickler Syndrome (STL), result from reduced synthesis and/or altered structure of cartilage extracellular matrix (ECM) proteins, which provide a scaffold for the organization of the chondrocytes in the endochondral growth plate.

Individuals affected with MED exhibit mild short stature, joint pain, and early-onset osteoarthropathy. Dominantly inherited mutations in 5 genes, *COMP*, *MATN3*, *COL9A1*, *COL9A2*, and *COL9A3*, and recessively inherited mutations in *SLC26A2* result in a MED phenotype, and the mutations in these genes account for the molecular basis of disease in 80-85% of the cases. Using exome sequencing, I endeavored to identify the molecular basis of the disease in cases with an unknown etiology. I identified two cases with a clinically distinct recessively-inherited form of MED due to mutations in *CANT1*, a gene involved in ECM biosynthesis. As this form of MED only accounts for a subset of the uncharacterized cases, there is further locus heterogeneity among patients with this phenotype.

Type IX collagen, a heterotrimeric collagenous ECM protein comprised of three procollagen chains, α1(IX), α2(IX), and α3(IX), is involved in the pathogenesis of both MED and STL. STL is characterized by mild short stature, craniofacial defects, sensorineural hearing loss, and myopia, and recessive loss-of-function mutations in all three human type IX procollagen genes have been identified in STL. Previous studies have indicated that the loss of α1(IX) results in a functional knockout of type IX collagen, but similar studies have not been conducted for α2(IX) and α3(IX). Through the generation of a *Col9a2* $^{-/-}$ mouse, I determined that the loss of α2(IX) also results in total loss of type IX collagen, and the resulting mouse phenocopies STL.

Through the study of MED and type IX collagen, I have gained a better understanding of the mechanisms of pathogenesis in a subset of chondrodysplasias of the cartilage ECM.

The dissertation of Karthika Balasubramanian is approved.

Deborah Krakow

Karen M. Lyons

Matteo Pellegrini

Daniel H. Cohn, Committee Chair

University of California, Los Angeles

2017

To my family

TABLE OF CONTENTS

LIST OF TABLES AND FIGURES

Chapter 1

Chapter 2

Chapter 3

ACKNOWLEDGEMENTS

Throughout my graduate career, I have been very lucky to work with some of the most kind, intelligent and all-around generous individuals.

First and foremost, I would like to thank my mentor, Dr. Daniel Cohn, for taking me on as his first graduate student and helping me grow and develop into a strong, independent scientist. Under Dr. Cohn's mentorship, I have gained a wide-array of skills, including both computational analytical skills and molecular biology wet-lab techniques, which have really provided me with a strong foundation for the future. He has always been very supportive of my long-term career goals and has assisted me in all possible ways to achieve those goals. I will always consider myself very fortunate that Dr. Cohn was my mentor in graduate school.

I would also like to thank the members of doctoral committee, Dr. Deborah Krakow, Dr. Karen Lyons, and Dr. Matteo Pellegrini, for all of the guidance you have provided me with over the years. Both Dr. Krakow and Dr. Lyons have felt like second mentors to me and have truly helped me navigate through all of the different hurdles I've encountered.

I also am very fortunate to have worked with so many knowledgeable experts in bioinformatics, cartilage development, and skeletal genetics in the Cohn, Krakow and Lyons labs. I would like to thank all of the past and present members of the Cohn lab—Bing Li, Felipe Marques, Lisette Nevarez, Michael Weinstein, Stuart Tompson, and Wenjuan Zhang, the Krakow lab—Fabi Csukasi, Ivan Duran-Jimenez, Jen Zieba, Jorge Martin, Paige Taylor, and Sulin Wu, and the Lyons Lab—Weiguang Wang, for all of the knowledge and support you have passed on to me. Everyone has taught me so many skills and techniques, and I would need an

entire book to detail everything that they have helped me with. I owe a special thanks to all of the undergraduate students who have assisted me with my projects—Patric Ho, Julia Ainsworth and Jorge Ortiz, without whom I would not have made so much progress.

Finally, I would like to thank my parents, Kamala and P.N. Balasubramanian, and my sister, Archana, for all of your love and support over the last six years. You have been my strength and emotional rocks through all of the obstacles that I have encountered. Without my family, I would not have been able to reach this goal. Thank you for always being here for me.

VITA

2006-2009	University of California, San Diego Degree: Bachelor of Science, Human Biology
2009-2010	University of California, San Diego Degree: Master of Science, Biology
Winter 2010	Nutrition Teaching Assistant Division of Biological Sciences University of California, San Diego
Spring 2010	Introductory Genetics Teaching Assistant Division of Biological Sciences University of California, San Diego
Winter 2012	Introductory Genetics Teaching Assistant Department of Life Sciences University of California, Los Angeles
Fall 2012	Introductory Genetics Teaching Assistant Department of Life Sciences University of California, Los Angeles
December 2014	MCDB Research Conference Poster Award Winner
Summer 2015	Biomedical Sciences Enrichment Program Laboratory Instructor Undergraduate Research Center Sciences University of California, Los Angeles

PUBLICATIONS

Zhiyun, W., Zhang, K., Wen, G., **Balasubramanian, K.,** Shih, P.B., Rao, F., Friese, R.S., Miramontes-Gonzalez, J.P., Schmid-Schoenbein, G.W., Kim, H., Mahata, S.K., and O'Connor, D.T. (2013). "*Heredity and cardiometabolic risk: naturally occurring polymorphisms in the human neuropeptide Y(2) receptor promoter disrupt multiple transcriptional response motifs*." J Hypertens. 31(1):123-33.

MANUSCRIPTS IN PREPARATION

Balasubramanian, K., Nevarez, L**.,** Lachman, R.S., Nickerson, D.A., Bamshad, M., University of Washington Center for Mendelian Genomics Consortium, Krakow, D.,and Cohn, D.H. (2017). "*Recessive Mutations in CANT1 Result in a Clinically Distinct Multiple Epiphyseal Dysplasia, Expanding the CANT1 Phenotypic Spectrum."*

Balasubramanian, K., Weis, M., Wang, J., Vangala, S., Friedman, R.A., Eyre, D.R. and Cohn, D.H. (2017). "*Loss of α2(IX) Also Results in a Functional Knockout of Type IX Collagen.*"

POSTER PRESENTATIONS

Balasubramanian, K. and Cohn, D.H. (2015). "Type IX Collagen Trimerization in the Absence of the Alpha-2 Chain." Poster presented at the MCDB Research Conference 2015: Lake Arrowhead, CA.

Balasubramanian, K. and Cohn, D.H. (2014). "Is the Alpha-2 Chain of Type IX Collagen Essential for Trimer Assembly?" Poster presented at the MCDB Research Conference 2014: Lake Arrowhead, CA.

Balasubramanian, K., Bamshad, M.J., Nickerson, D.A., University of Washington Center for Mendelian Genomics, Lachman, R.S., and Cohn, D.H. (2014). "Exome Sequencing Identifies Locus Heterogeneity in Multiple Epiphyseal Dysplasia." Poster presented at the 64th Annual Meeting of the American Society of Human Genetics 2014: San Diego, CA.

Balasubramanian, K., Ho, P., Li, B., and Cohn, D.H. (2013). "Search for Novel Variants Resulting in Multiple Epiphyseal Dysplasia." Poster presented at the MCDB Research Conference 2013: Lake Arrowhead, CA.

Candolfi, M., Yagiz, K., **Balasubramanian, K**., Puntel, M., King, G.D., Mineharu, Y., Muhammad, A.K.M.G., Foulad, D., Barnett, N., Kroeger, K.M., Lowenstein, P., and Castro, M.G. (2011). "Anti-Glioma Immune Response Induced by Conditional Cytotoxic/Immune-Stimulatory Gene Therapy Requires pDC Activation Triggered by Circulating Brain Tumor DNA." Poster presented at the 14th Annual Meeting of the American Society of Gene and Cell Therapy 2011: Seattle, WA.

CHAPTER ONE

Introduction

The Skeletal Dysplasias

The skeletal dysplasias are a diverse group of inherited genetic diseases primarily affecting the growth and development of the human skeleton. Currently, 436 clinically distinct skeletal dysplasias have been recognized, and 364 of these diseases are associated with a mutated gene[1]. The identification and examination of the functional consequences of the mutations that result in the skeletal dysplasias has provided insight into the functions of the molecules and mechanisms that are essential for the development of the human skeletal system.

The skeletal dysplasias can be classified into three main groups of disorders: the osteodysplasias, the chondrodysplasias, and dysostoses. The osteodysplasias primarily involve defects in the development and maintenance of bone, resulting in alterations in mineralization that ultimately affect bone mineral density[2]. The chondrodysplasias result from defective chondrocyte differentiation and proliferation, leading to abnormalities in skeletal patterning and linear growth that result in short stature and skeletal deformities. Lastly, the dysostoses affect the patterning, sizes and shapes of individual bones or a specific group/type of bones[3-5].

Collectively the occurrence of skeletal dysplasias is relatively common, with an incidence of 1 in every 5,000 births, but at the level of individual diseases the frequency of each is low[4]. The severity of these disorders ranges from perinatal lethal diseases[6] to mild affectation in adulthood[7], primarily resulting in delayed skeletal growth[8, 9]. Prenatal diagnosis of a skeletal dysplasia can occur as early as 12 weeks of gestational age, when defects in skeletal length, morphology, and ossification can be observed by ultrasonography[10, 11]. Typically, the earlier in development defects in skeletogenesis are observed, the higher likelihood these defects result from mutations in genes that are essential to skeletal patterning and development, and ultimately result in a perinatal lethal skeletal dysplasia[11].

In order to accurately diagnose skeletal dysplasias, clinicians, radiologists, and researchers use a combination of clinical and radiographic data to assess the age of onset and severity of the phenotype[12]. This includes three key diagnostic tools: radiographs to assess the skeletal defects, family history to assess the mode of inheritance, and clinical evaluation to indentify additional non-skeletal features that may be diagnostic for particular diseases. A full genetic skeletal survey provides detailed information including but not limited to bone age, ossification defects, and unique radiographic features that lead to the identification of the underlying disorder[12]. For example, the presence of a double-layered patella in a lateral knee radiograph is a clinically distinct feature of recessive Multiple Epiphyseal Dysplasia, distinguishing this phenotype from the autosomal dominant forms of the disease [13]. Next, a study of the family history will aid in determining the mode of inheritance, which can be autosomal or X-linked dominant or recessive [1]. Additional unusual inheritance patterns have been observed including dominant mutations inherited by somatic and germline mosaicism and recessive phenotypes with digenic inheritance[4, 5]. Lastly, secondary clinical phenotypes arising from developmental defects in other organ systems such as the brain[14], heart[15], kidney[16], liver[17], eye[18] and ear[19, 20] can aid in clinical diagnosis. For example, the type II collagenopathies can exhibit profound vision and hearing defects, which assist in distinguishing the observed skeletal anomalies from other disorders with similar radiographic features[21]. Combined, the unique clinical and radiographic features of each disorder illustrate the genetic diversity among the skeletal dysplasias and the complex biochemical and molecular mechanisms associated with skeletal development. As identification of the molecular basis of the majority of these disorders has been accomplished, this information has also facilitated the use of

molecular testing as an important diagnostic tool for accurately diagnosing these disorders for the benefit of patients.

Chondrodysplasias

The chondrodysplasias are a subset of about 200 of the skeletal dysplasias that have primary effects on cartilage development. Defects in cartilage development result in abnormal formation of the limbs, trunk and/or skull, often leading to disproportionate short stature[3]. The genes associated with the chondrodysplasias encode proteins with a diverse array of functions including but not limited to the formation of the cartilage extracellular matrix (ECM) by structural proteins[18, 22-24], signaling by a variety of signaling receptors and their ligands[25], and transcription factors involved in skeletal development[26-28], attesting to the complexity of these disorders and their underlying causes. In some cases the genes are expressed in a wide variety of tissues, but their defects lead to an especially profound effect on cartilage, as in the case of the spectrum of chondrodysplasias resulting from reduced enzymatic function of the sulfate transporter encoded by *SLC26A2*[29]. However, in about one third of the chondrodysplasias, the defects are in genes that are selectively expressed in cartilage, including the genes encoding the major extracellular matrix structural proteins.

Through transcriptome profiling studies of normal human, mouse and rat cartilage, a subset of genes that are selectively expressed in the tissue have been identified, several of which have been previously implicated in cartilage development or associated with a chondrodysplasia[30-32]. These include many well-characterized genes such as the cartilage collagens (types II, XI and IX) and other ECM structural proteins including aggrecan and the matrilins and a wide array of additional genes known or implicated as important for skeletal development[30]. In the study by Funari et al. 2007, 161 genes were determined to be cartilage

selective based on significant expression in cartilage and low expression in non-cartilaginous tissues, with 25 genes known to be associated with chondrodysplasias [30]. Many of the genes also possessed novel, uncharacterized functions in cartilage, creating a list of potential loci for chondrodysplasias with an unidentified molecular basis of disease. Because many of the chondrodysplasias result from mutations in cartilage selective genes, the use of next generation techniques, such as exome or genome sequencing, in combination with cartilage gene expression studies, can assist in the identification of novel disease loci[21].

Endochondral Ossification

Study of the pathogenesis in the chondrodysplasias has demonstrated that the phenotypes are due to defects in the mechanisms underlying the formation of cartilage and bone [3]. Most elements of the axial skeleton, including the rib cage and vertebrae, and most of the appendicular skeleton, including the upper and lower limbs and the pelvic girdle, all are formed via endochondral ossification, the formation of bone via a cartilage template. By contrast, the skull and portions of the mandible, lateral clavicles and pubis form via intramembranous ossification, the direct differentiation of precursor mesenchymal cells into bone without a cartilage intermediate[33].

During human fetal development, the skeletal elements arise from precursor mesenchymal stem cells which cluster and condense to pattern the early skeleton[34]. For bones that develop via endochondral ossification, the mesenchymal condensations undergo chondrogenesis and become chondrocytes and then align along the axis of growth to form the growth plates [34-36]. During endochondral bone formation, linear growth occurs by a tightly regulated developmental process in which chondrocytes proliferate, expand in size, and mature into terminally differentiated cells that secrete an extracellular matrix that becomes mineralized,

after which the cells undergo apoptosis[34]. The endochondral growth plate can be divided according to the stages of chondrocyte differentiation. The zones, in order from least differentiated to most differentiated, are the reserve, proliferative, pre-hypertrophic and hypertrophic zones. Chondrocytes in each zone exhibit a characteristic size, morphology, and organization. Once the chondrocytes undergo apoptosis, osteoblasts (bone forming cells) invade the mineralized cartilage template and replace the cartilage matrix with a mineralized bone matrix [33, 37, 38] (Figure 1.1).

The process of endochondral ossification is highly regulated by numerous transcription factors and signaling molecules. The master transcriptional regulator of chondrogenesis, SOX9 (SRY-related high-mobility-group-box 9), determines the cell fate of chondrocytes and drives the differentiation of mesenchymal stem cells into cartilage forming cells [38, 39]. SOX9 is expressed in mesenchymal stem cells, reserve chondrocytes and proliferative chondrocytes [35, 39], and modulates the expression of many genes selectively expressed in cartilage. During chondrogenesis, active SOX9 forms a homodimer and binds to paired heptameric consensus sequences, which are specific to cartilage expressed genes [40]. Multiple SOX9 response elements have been identified in the cartilage selective genes *COL2A1*, *COL9A1, COL9A2*, *COL11A2*, and *ACAN*, and alterations to the consensus sequence and surrounding nucleotides in the response elements result in reduced binding of SOX9 and decreased target gene expression[41-43]. Additional studies have shown that SOX9 induces the temporal-dependent expression of the cartilage specific transcription factors SOX5 and SOX6 during endochondral ossification, further emphasizing the critical role of SOX9 in determining cartilage selectivity and chondrocyte growth and differentiation[44].

One of the critical functions of growth plate chondrocytes is the ability to synthesize structural proteins to create the cartilage ECM. The ECM functions as a scaffold for chondrocytes in the growth plate and assists in maintaining the organization and polarity of the columnar proliferative and hypertrophic chondrocytes along the longitudinal growth axis [45]. As observed in human chondrodysplasias or phenotypes in mouse models, perturbation of the expression of the genes encoding ECM proteins, or alterations in their structures, can result in abnormalities in chondrocyte proliferation and growth plate architecture [46, 47]. In some cases, these alterations in protein synthesis lead to induction of the unfolded protein response, increased cell stress and chondrocyte apoptosis, with reduced growth plate size [46, 48]. As the length of the endochondral growth plate can correlate to the height of an individual, the resulting shorter growth plates reflect the disproportionate short stature observed in many skeletal dysplasia patients.

The Cartilage Extracellular Matrix

The ECM provides structure to the growth plate, as well as tensile strength and elasticity to the tissue, all of which is mediated by the tight network of the fibrillar and extrafibrillar matrix[47]. The fibrillar matrix is primarily composed of type II collagen fibrils interspersed with type XI collagen, which forms a scaffold for the developing chondrocytes in the growth plate [45, 47, 48]. In contrast, the extrafibrillar matrix is comprised of a variety of sulfated proteoglycans, with the chondroitin sulfate proteoglycan aggrecan as the major structural protein, providing structural integrity and mechanostability to the cartilage[49]. Interactions between the fibrillar and the extrafibrillar matrix are mediated by adaptor proteins such as the cartilage oligomeric matrix protein, matrilin-3, and type IX collagen[48] (Figure 1.2). Each of these proteins exerts a unique function in the maintenance and homeostasis of the ECM, as determined by the structures of these collagenous and non-collagenous proteins.

The principal component of the fibrillar matrix, type II collagen, and the minor component, type XI collagen, together cooperate to form the scaffolding of the ECM. Both of these collagens, known as the fibrillar collagens, form long, uninterrupted triple helixes to perform this function [50]. Type II collagen exists as a homotrimer of the α1(II) procollagen chain, while type XI is comprised of a heterotrimer of the α1(XI), α2(XI), and α1(II) procollagen chains[50]. These chains trimerize and the triple helical domain contains a conserved Gly-X-Y amino acid motif, which is altered in many of the chondrodysplasias resulting from Glycine mutations *[18, 50]*. Minor amounts of type IX collagen, which is a heterotrimer of α1(IX), α2(IX), and α3(IX)[51], serve a dual function in the matrix: molecules are covalently cross-linked to the fibrillar collagen in an antiparallel orientation at conserved lysine residues to regulate the diameter of collagen fibrils[52], and they also serve as bridging molecules between the fibrillar and extrafibrillar matrix[53]. As a fibril-associated collagen with interrupted triple helices (FACIT), type IX collagen contains three collagenous domains (COL1-3) that are flanked by four non-collagenous domains (NC1-4), each of which serves a unique function in the ECM[53]. The NC1, NC2, COL1 and COL2 domains are involved in regulating the collagen fibril diameter while the NC3 domain functions as a hinge, pointing the COL3 and NC4 domains into the matrix, enabling the bridging/adaptor function [54]. Since all three selectively expressed collagenous proteins share structural roles in the ECM, mutations in all of the genes encoding these proteins can result in the chondrodysplasia Stickler Syndrome, which will be discussed later in this chapter. The close interactions among all three collagen molecules in the ECM is required for the development and maintenance of the matrix, and even mild alterations in the amount or structures of these proteins can result in a skeletal dysplasia.

To create stability between the fibrillar and extrafibrillar cartilage matrix, noncollagenous adaptor proteins such as cartilage oligomeric matrix protein (COMP) and the matrilin family of proteins mediate interactions between the collagen fibrils and the proteoglycan (aggrecan) matrix[48, 55]. Here the type IX collagen bridging function is most notable, as COMP and matrilin-3 interact with the COL3 and NC4 domains pointing into the matrix[47]. While loss of either *COMP* or *MATN3* do not result in a dysplasia in mice [56-58], structurally abnormal proteins due to dominant negative mutations in both of these genes and the genes encoding the three type IX procollagen chains can result in the mild disease Multiple Epiphyseal Dysplasia (MED)[59]. MED, as detailed below, is one of the more common skeletal dysplasias, and the study of MED patients has provided a deeper understanding of the cellular responses to abnormal protein synthesis.

Multiple Epiphyseal Dysplasia

Multiple Epiphyseal Dysplasia (MED) is a chondrodysplasia that is characterized by mild short stature, joint pain, and early-onset osteoarthropathy. Patients can also present with mild to moderate brachydactyly and genu valgum (knock-knees) or genu varum (bow-legs) [59, 60]. Radiographic features include epiphyseal dysplasia at the hip or knee joints, delayed carpal ossification in the hands, and in some cases mild platyspondyly and/or irregularly-shaped vertebral bodies[59, 61] (Figure 1.3). Autosomal dominant mutations in *COMP*[62, 63], *MATN3*[64], *COL9A1*[65],*COL9A2*[66], and *COL9A3*[67] account for the molecular basis of disease in approximately 70-75% of the cases. All of these genes encode structural proteins of the cartilage extracellular matrix that are selectively expressed in the tissue[47]. A clinically distinct recessive form of the disease, which is caused by homozygosity or compound heterozygosity for mutations in *SLC26A2*, the diastrophic dysplasia sulfate transporter, is characterized by epiphyseal dysplasia at the hips, advanced carpal ossification, and a double-

layered patella observed by x-ray and accounts for an additional 10-15% of MED cases [68]. The molecular basis of disease remains unknown in approximately 15-20% of MED cases.

The mechanisms underlying the pathogenesis of MED in both the dominant and recessive forms are vastly different due to the fundamental natures of the proteins encoding the disease-associated genes. In all of the dominant disease loci, the genes encode multimeric structural proteins of the ECM that are selectively expressed in cartilage[47]. Because the patients are heterozygous for their mutations, 50% of the synthesized monomers are abnormal, resulting in proteins composed of a mixture of normal and mutant monomers in varying stoichiometries. In the case of COMP, the mature protein is a homopentamer, and heterozygosity for a structural mutation would predict that 31/32 pentamers will contain at least one abnormal chain. Each COMP monomer contains 4 domains—an oligomerization domain at the amino terminal, EGF-like repeats/type II repeats, calmodulin-like repeats/type III repeats, and a globular C-terminal domain[69, 70]. Identified mutations in COMP are missense or small in-frame deletions and typically are found in the type III repeats/calmodulin-like repeats or in the C-terminal domain, which result in impaired binding to Ca2+ molecules and protein misfolding [71, 72]. Matrilin-3 monomers also have 4 domains—a signal peptide, a von Willebrand factor A domain, EGF-like repeats, and an oligomerization domain[73]—and form homotrimers, homotetramers, or heterotetramers with matrilin-1[74] with 7/8 mutant homotrimers, 15/16 mutant homotetramers, and 3/4 mutant heterotetramers synthesized. All MED-associated mutations in MATN3 cluster in the von Willebrand factor A domain, resulting in misfolding of the alpha and beta sheets of the protein [75, 76]. Lastly, as described earlier, type IX collagen is a heterotrimer composed of a procollagen chain encoded by each of the type IX collagen genes and contains 3 collagenous domains—COL1-3—which are flanked by four noncollagenous domains—NC1-4[54]. Disease

producing mutations in the type IX procollagen genes are all splicing mutations that lead to exon skipping and a 12 bp deletion targeting the COL3 domain, producing 50% mutant trimers [60, 66] (Figure 1.4). All of the dominant mutations exert their phenotypic effect through a dominant negative mechanism, either leading to synthesis and intracellular retention of structurally abnormal proteins within the rough endoplasmic reticulum (RER) or the secretion of mutant proteins into the ECM [75-79]. In addition to disrupting the matrix, accumulation of abnormal proteins within the RER can induce an unfolded protein response and lead to secondary abnormalities, including apoptosis [80, 81].

In contrast to AD MED, in recessive MED the mutations result in reduced enzymatic activity of the diastrophic dysplasia sulfate transporter encoded by *SLC26A2*. This enzyme imports inorganic sulfate into the cells for posttranslational modification of ECM proteoglycans[82] and in MED, the decreased enzymatic activity ultimately leads to decreased sulfation of chondroitin sulfate proteoglycans, including ECM proteins[83, 84]. Because both the dominant and recessive MED loci share a common function of maintaining the structural integrity of the cartilage extracellular matrix (ECM), mutations in these genes result in a similar radiographic phenotype, even though the underlying mechanisms are different.

Collectively, mutations in these six genes accounts for the molecular basis of disease in 80-85% of the cases. Linkage studies have excluded mutations in the known genes in cases with an unknown molecular basis of disease, but novel loci have not yet been identified[85]. Using the exome sequencing tool, I endeavored to identify mutations in novel loci that result in MED in cases of unknown molecular basis. As the current loci are all involved in ECM biosynthesis, I hypothesized that a novel locus might also share a similar function. Chapter 2 will highlight the

results of this study and the identification of mutations in *CANT1,* a gene involved in proteoglycan synthesis, that have been found in a clinically distinct recessive form of MED.

Stickler Syndrome

While the defects observed in AD MED result from structural abnormalities in proteins of the ECM, Stickler syndrome (STL), which is an arthroopthalmopathy with involvement of the skeletal, ocular, and auditory systems, results primarily from loss of function defects in ECM proteins. Affected individuals present with mild short stature, myopia, vitreoretinal degeneration, retinal detachment, midface hypoplasia, micrognathia, cleft palate, epiphyseal dysplasia, and sensorineural hearing loss [86] (Figure 1.5). Similar to MED, there is extensive locus heterogeneity in STL, with dominant mutations in *COL2A1[87]*, *COL11A1[88]*, and *COL11A2[89]* and recessive mutations in *COL9A1[19]*, *COL9A2[20]*, and *COL9A3[90]* all resulting in a similar clinical phenotype. Since type IX collagen functions as a bridging molecule with a role in the fibrillar matrix structure and as an adaptor protein, the observed defects in STL may relate more closely to its structural role in the fibrillar matrix.

While significant locus heterogeneity exists in STL, the frequency at which the mutations are observed is not equal among the various genes. About 80-90% of the cases arise from mutations in *COL2A1*, 10-20% from defects in the type XI collagen genes, and only 6 cases have been observed that result from type IX collagen gene mutations [86]. The mutations in type II collagen are dominantly inherited and primarily result in premature termination codons leading to haploinsufficiency, demonstrating that a 50% reduction in type II collagen produces a milder phenotype than the dominant negative mutations observed in the other type II collagenopathies[18]. However, type II collagen Stickler syndrome is still the most severe phenotype on the STL spectrum[86]. *COL11A1* STL results from missense, splicing, and small

insertion/deletion mutations that produce structurally abnormal proteins[91]. The phenotype in these patients resembles the *COL2A1* Stickler phenotype, but the defects are milder [86]. *COL11A2* mutations, which result from in-frame deletions and also lead to structurally abnormal proteins [91], produce a clinically distinct phenotype as these patients lack ocular defects, reflecting that the gene is not expressed in the vitreous of the eye [92]. Lastly, all of the type IX collagen Stickler syndrome cases are recessive and result from homozygosity or compound heterozygosity for nonsense mutations that result in a loss of type IX collagen [19, 20, 90]. Although type IX collagen is not a major component of the ECM, it is likely that the frequency of type IX collagen Stickler is lower because the phenotype is recessive. In addition, there is a very low carrier frequency of type IX collagen gene null alleles observed in public databases such as the NCBI Exome Variant Server [93] and the Exome Aggregation Consortium [94]. This may reflect purifying selection against null alleles for these genes, which may be an additional reason so few cases have been observed [95].

Among the different forms of Stickler syndrome, the type IX collagen cases exhibit profound vision and hearing defects, but the observed skeletal defects are relatively mild in comparison to the type II and type XI collagen Stickler phenotypes [90] (Table 1.1). Studies in the *Col9a1* $^{-/-}$ mouse have demonstrated that the loss of *Col9a1* results in a functional knockout of type IX collagen [96] and the mouse model phenocopies Stickler syndrome with abnormal growth plate organization[97], early-onset osteoarthritis[98], and hearing loss[99]. It has been assumed that a similar phenomenon occurs with α2(IX) and α3(IX), an inference supported by the fact that loss of function mutations in *COL9A2* or *COL9A3* result in Stickler syndrome, but no functional studies have been completed to determine the validity of this assumption[20, 90].

Also relevant in this context, biochemical analysis of the stoichiometry of chain composition required for type IX collagen trimerization has demonstrated that α1(IX) is essential to producing a functional protein, but the data are less clear for α2(IX) and α3(IX). *In vitro* expression of various combinations of α1(IX), α2(IX) and α3(IX) demonstrated that α1(IX) can self-trimerize to produce intact collagen molecules, suggesting that absence of either of the other two chains could still lead to synthesis of type IX collagen[100-102]. However, the results are inconsistent for α2(IX) and α3(IX). In Jäälinoja et al. 2008, full-length α2(IX) and α3(IX) were shown to be able to homotrimerize[101], but this finding was not replicated in the Pihlajaama et al. 1999 study[100]. Peptides from α2(IX) containing just the NC1 and COL1 domain were shown to homotrimerize[102], as were peptide fragments containing just the NC4-COL2 domains[101] but this did not occur with α3(IX) peptides. In order to determine whether α2(IX) is essential to the synthesis of functional type IX collagen, I constructed an *in vivo* knockout mouse model for *Col9a2* to assess the biochemical and phenotypic consequences of the loss of this subunit. Chapter 3 discusses the results of this study and resolves the different findings in the literature, demonstrating that α2(IX) is also essential to type IX collagen biosynthesis and showing that the *Col9a2* $^{-/-}$ mouse phenocopies Stickler syndrome.

Figures

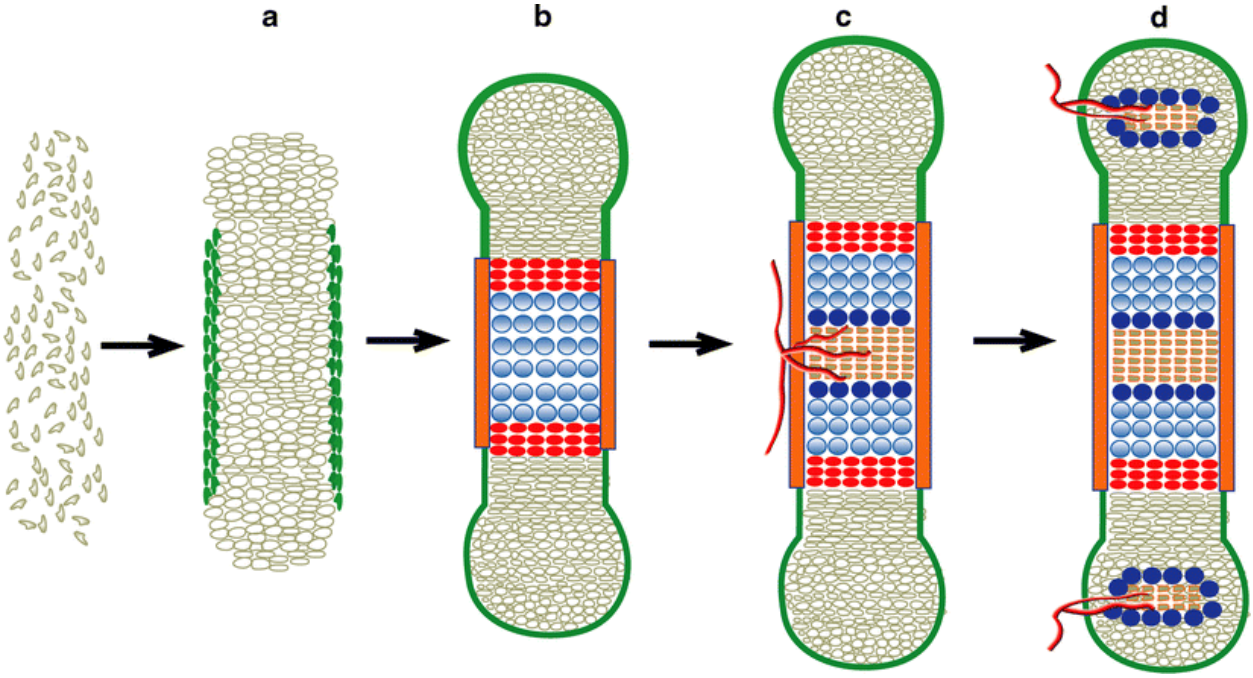

Figure 1.1: Endochondral Ossification. This figure is from Wuelling & Vortkamp 2010[37] a) The mesenchymal stem cells (MSCs) condense to form the early skeletal elements b) MSCs differentiate into chondrocytes, which form the endochondral growth plate. The reserve chondrocytes (grey) form columnar proliferative cells (red), which terminally differentiate into hypertrophic chondrocytes (blue). The cells are surrounded by the perichondrium (green) and the future periosteum (orange). c) The hypertrophic chondrocytes are replaced by osteoblasts (brown), and blood vessels have invaded the growth plate to vascularize the tissue. d) Secondary ossification centers form distal to the growth plate, and skeletal growth ceases when the primary and secondary ossification centers fuse together.

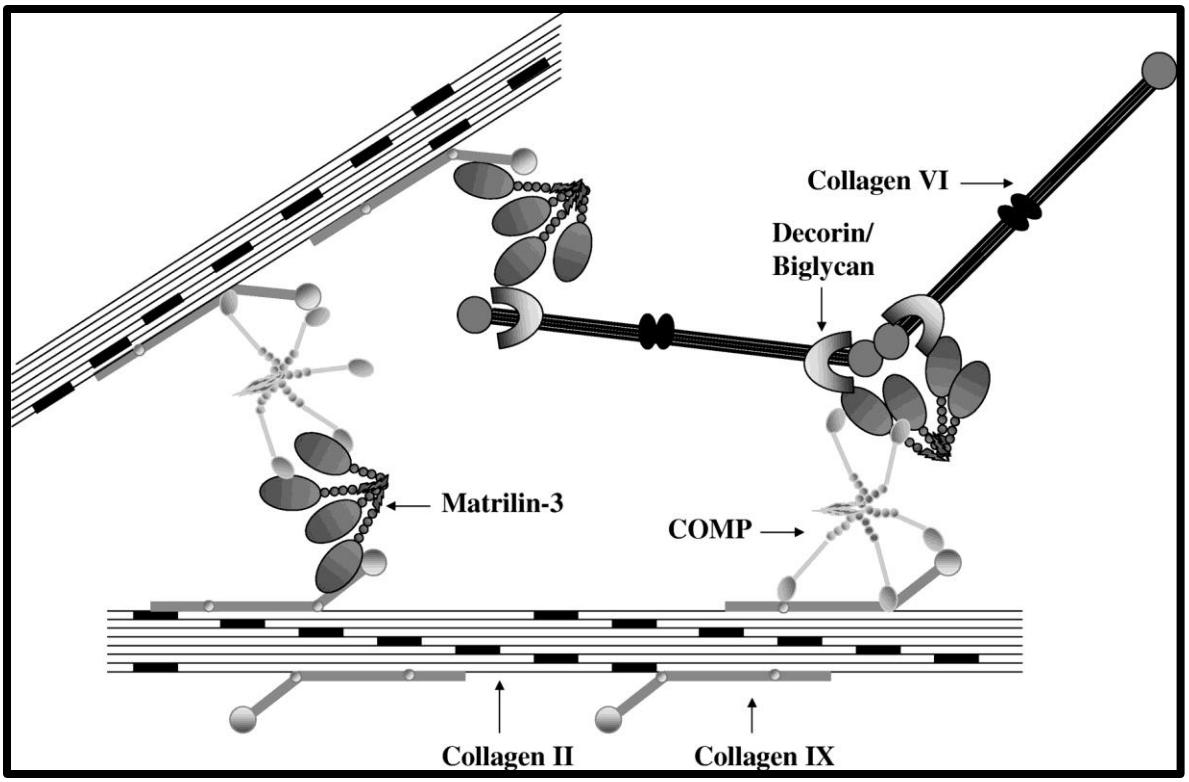

Figure 1.2: Structure of the Cartilage Extracellular Matrix. This figure is from Budde et al. 2005 [103]. The fibrillar type II and type XI collagens form the scaffolding of the extracellular matrix. Type IX collagen fibrils are covalently crosslinked to the collagen fibrils, connecting the fibrils to the adaptor proteins COMP pentamers and matrilin 1/3 tetramers. These adaptor proteins connect the collagen fibrils to other fibrils and proteoglycans such as aggrecan in the extrafibrillar matrix.

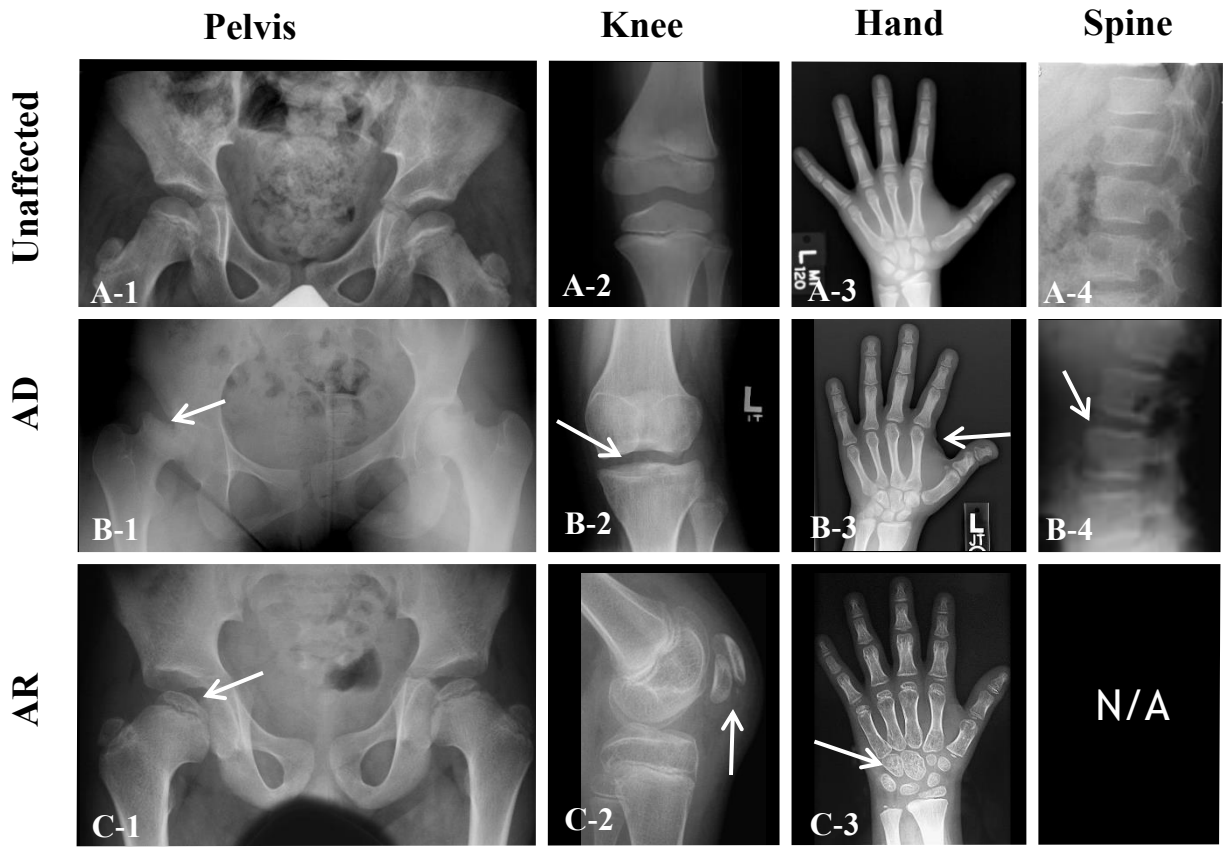

Figure 1.3: Radiographic Phenotype of Autosomal Dominant and Autosomal Recessive MED. A) Unaffected Adolescent films from an unaffected individual. A-1) AP Pelvis at age 9. A-2) AP knee (Figure for A-2 is is modified from Boeyer and Ousley 2016 [104]). A-3) Hand at age 12. A-4) Lateral spine at age 12. B) Autosomal dominant MED due to *COMP* mutations. B-1) Female pelvis at age 15 with flattened, irregularly shaped capital femoral epiphyses. B-2) Female knee at age 15 with flattened knee epiphyses. B-3) Female hand at age 15 with brachydactyly. B-4) Male spine at age 13 with irregularly shaped vertebral bodies and platyspondyly. C) Autosomal recessive MED due to mutations in *SLC26A2* (Figures for C are modified from Unger et al. 2008[59]). C-1) Pelvis with irregularly shaped capital femoral epiphyses. C-2) Knee depicting clinically distinctive double-layered patella. C-3) Advanced carpal ossification of the carpals.

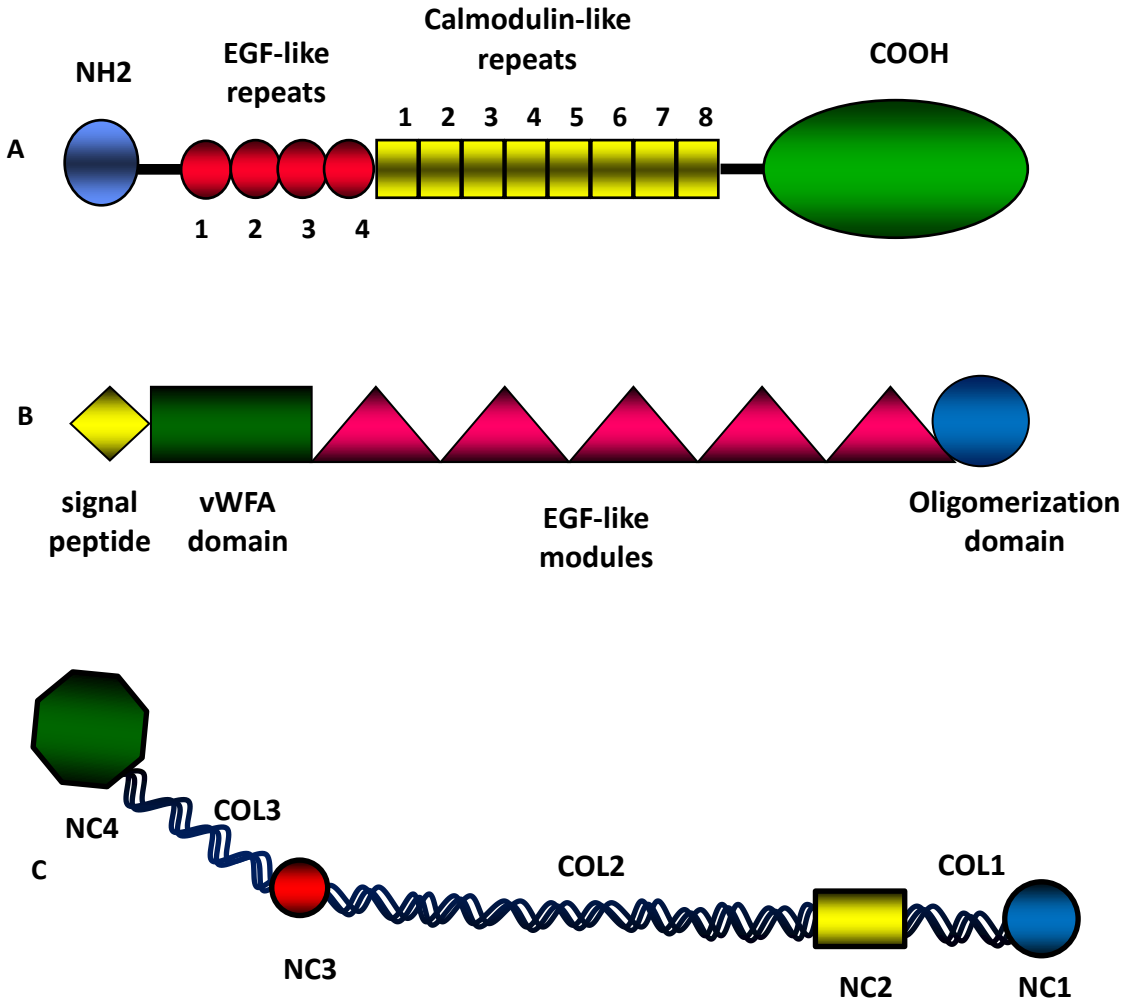

Figure 1.4: Mutations in Autosomal Dominant MED Loci A) COMP monomers contain four domains and all of the MED mutations are missense changes or small in-frame deletions/duplications clustered in the calmodulin-like repeats and the C-terminal domain, resulting in misfolded, structurally abnormal proteins. B) Matrilin-3 monomers contain 4 domains, and all of the MED mutations are clustered in the von Willebrand factor A domain and result in misfolded alpha and beta sheet domains. C) Type IX collagen is a heterotrimeric protein with 3 collagenous domains and 4 non-collagenous domains. All MED mutations are splicing mutations that lead to in-frame deletions in the COL3 domain.

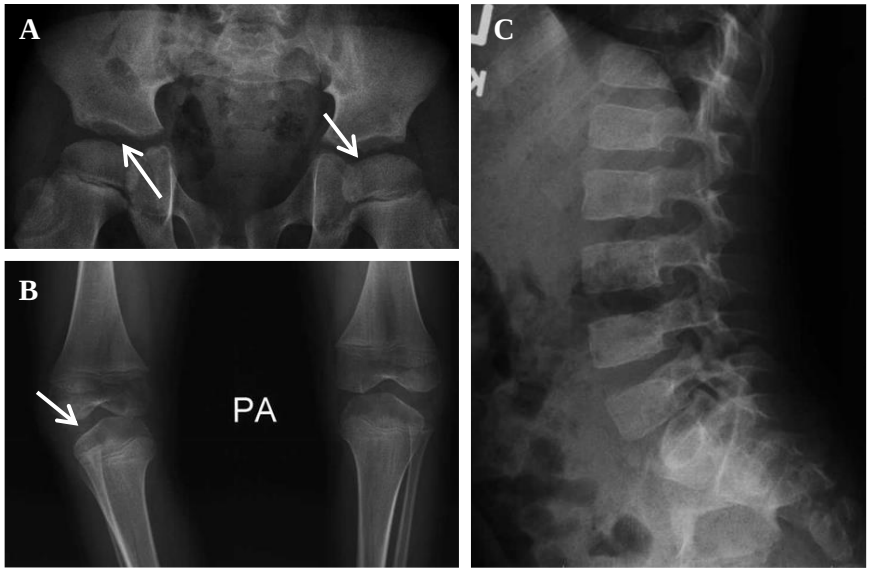

Figure 1.5: Radiographs of Patients Affected with Stickler Syndrome. Radiographs from a patient with a homozygous recessive mutation in *COL9A3*. A. AP hip showing mildly flat capital femoral epiphyses (left arrow) with irregularly-shaped acetabulae (right arrow). B) AP knee shows irregularly shaped proximal tibial epiphyses. C) No significant abnormalities observed in the lateral spine.

Table 1.1: Clinical Features of Patients with Stickler Syndrome

Table I. Clinical Finding in Autosomal Dominant and Recessive Stickler Syndrome

Clinical findings	STL1 and STL2 (*COL2A1* and *COL11A1*)	STL3 (*COL11A2*)	*COL9A1* Arg295*	*COL9A2* Asp281Glnfs*70	*COL9A3* Gln393Cysfs*25
Clinical findings in stickler syndrome					
High myopia	+	−	+	+	+
Vitreoretinal degeneration	+	−	+	+	−
Retinal detachment	+	−	−	+	−
Cataracts	+	−	−	−	−
Hearing loss	+	+	+	+	+
Mid-face hypoplasia	+	+	−	+	+
Cleft palate/Pierre Robin sequence	+	+	−	−	−
Anteverted nares	+	+	−	−	−
Small chin	+	+	−	+	−
Short stature	+/−	+/−	+	+	−
Spondyloepiphyseal dysplasia	+	+	+	?	−
Early-onset osteoarthritis	+	+	?	?	−
Other findings	−	−	Genua valga	−	Internal tibial rotation, pes planus, downslanted palpebral fissures

"−", absent; "+", present; "?", not known.

This table is from Faletra et al. 2014[90].

References

1. Bonafe L, Cormier-Daire V, Hall C, Lachman R, Mortier G, Mundlos S, Nishimura G, Sangiorgi L, Savarirayan R, Sillence D *et al*: **Nosology and classification of genetic skeletal disorders: 2015 revision**. *American Journal of Medical Genetics Part A* 2015, **167**(12):2869-2892.

2. Aggarwal S: **Skeletal dysplasias with increased bone density: Evolution of molecular pathogenesis in the last century**. *Gene* 2013, **528**(1):41-45.

3. Rimoin DL, Cohn D, Krakow D, Wilcox W, Lachman RS, Alanay Y: **The Skeletal Dysplasias**. *Annals of the New York Academy of Sciences* 2007, **1117**(1):302-309.

4. Krakow D, Rimoin DL: **The skeletal dysplasias**. *Genet Med* 2010, **12**(6):327-341.

5. Krakow D: **Skeletal Dysplasias**. *Clinics in Perinatology* 2015, **42**(2):301-319.

6. Barkova E, Mohan U, Chitayat D, Keating S, Toi A, Frank J, Frank R, Tomlinson G, Glanc P: **Fetal skeletal dysplasias in a tertiary care center: radiology, pathology, and molecular analysis of 112 cases**. *Clinical Genetics* 2015, **87**(4):330-337.

7. Mortier GR, Chapman K, Leroy JL, Briggs MD: **Clinical and radiographic features of multiple epiphyseal dysplasia not linked to the COMP or type IX collagen genes**. *European Journal of Human Genetics* 2001, **9**(8):606-612.

8. Rousseau F, Bonaventure J, Legeai-Mallet L, Pelet A, Rozet J-M, Maroteaux P, Merrer ML, Munnich A: **Mutations in the gene encoding fibroblast growth factor receptor-3 in achondroplasia**. *Nature* 1994, **371**(6494):252-254.

9. Huber C, Oulès B, Bertoli M, Chami M, Fradin M, Alanay Y, Al-Gazali LI, Ausems MGEM, Bitoun P, Cavalcanti DP *et al*: **Identification of CANT1 Mutations in Desbuquois Dysplasia**. *The American Journal of Human Genetics* 2009, **85**(5):706-710.

10. Krakow D, Alanay Y, Rimoin LP, Lin V, Wilcox WR, Lachman RS, Rimoin DL: **Evaluation of prenatal-onset osteochondrodysplasias by ultrasonography: A retrospective and prospective analysis**. *American Journal of Medical Genetics Part A* 2008, **146A**(15):1917-1924.

11. Offiah AC: **Skeletal Dysplasias: An Overview**. In: *Calcium and Bone Disorders in Children and Adolescents.* Edited by Allgrove J SN, vol. 28. Endocrine Development; 2015.

12. Alanay Y, Lachman RS: **A Review of the Principles of Radiological Assessment of Skeletal Dysplasias**. *Journal of Clinical Research in Pediatric Endocrinology* 2011, **3**(4):163-178.

13. Lachman RS, Krakow D, Cohn DH, Rimoin DL: **MED, COMP, multilayered and NEIN: an overview of multiple epiphyseal dysplasia**. *Pediatric Radiology* 2005, **35**(2):116-123.

14. Agochukwu NB, Solomon BD, Muenke M: **Impact of genetics on the diagnosis and clinical management of syndromic craniosynostoses**. *Child's Nervous System* 2012, **28**(9):1447-1463.

15. Lin AE, Traum AZ, Sahai I, Keppler-Noreuil K, Kukolich MK, Adam MP, Westra SJ, Arts HH: **Sensenbrenner syndrome (Cranioectodermal dysplasia): Clinical and molecular analyses of 39 patients including two new patients**. *American Journal of Medical Genetics Part A* 2013, **161**(11):2762-2776.

16. Bredrup C, Saunier S, Oud Machteld M, Fiskerstrand T, Hoischen A, Brackman D, Leh Sabine M, Midtbø M, Filhol E, Bole-Feysot C *et al*: **Ciliopathies with Skeletal Anomalies and Renal Insufficiency due to Mutations in the IFT-A Gene WDR19**. *The American Journal of Human Genetics*, **89**(5):634-643.

17. Loo CKC, Pereira TN, Ramsing M, Vogel I, Petersen OB, Ramm GA: **Mechanism of pancreatic and liver malformations in human fetuses with short-rib polydactyly syndrome**. *Birth Defects Research Part A: Clinical and Molecular Teratology* 2016, **106**(7):549-562.

18. Terhal PA, Nievelstein RJAJ, Verver EJJ, Topsakal V, van Dommelen P, Hoornaert K, Le Merrer M, Zankl A, Simon MEH, Smithson SF *et al*: **A study of the clinical and radiological features in a cohort of 93 patients with a COL2A1 mutation causing spondyloepiphyseal dysplasia congenita or a related phenotype**. *American Journal of Medical Genetics Part A* 2015, **167**(3):461-475.

19. Van Camp G, Snoeckx RL, Hilgert N, van den Ende J, Fukuoka H, Wagatsuma M, Suzuki H, Erica Smets RM, Vanhoenacker F, Declau F *et al*: **A New Autosomal Recessive Form of Stickler Syndrome Is Caused by a Mutation in the COL9A1 Gene**. *American Journal of Human Genetics* 2006, **79**(3):449-457.

20. Baker S, Booth C, Fillman C, Shapiro M, Blair MP, Hyland JC, Ala-Kokko L: **A loss of function mutation in the COL9A2 gene causes autosomal recessive Stickler syndrome**. *American Journal of Medical Genetics Part A* 2011, **155**(7):1668-1672.

21. Geister KA, Camper SA: **Advances in Skeletal Dysplasia Genetics**. *Annual Review of Genomics and Human Genetics* 2015, **16**(1):199-227.

22. Tompson SW, Merriman B, Funari VA, Fresquet M, Lachman RS, Rimoin DL, Nelson SF, Briggs MD, Cohn DH, Krakow D: **A Recessive Skeletal Dysplasia, SEMD Aggrecan Type, Results from a Missense Mutation Affecting the C-Type Lectin Domain of Aggrecan**. *The American Journal of Human Genetics* 2009, **84**(1):72-79.

23. Tompson SW, Bacino CA, Safina NP, Bober MB, Proud VK, Funari T, Wangler MF, Nevarez L, Ala-Kokko L, Wilcox WR *et al*: **Fibrochondrogenesis Results from Mutations in the COL11A1 Type XI Collagen Gene**. *The American Journal of Human Genetics* 2010, **87**(5):708-712.

24. Tompson SW, Faqeih EA, Ala-Kokko L, Hecht JT, Miki R, Funari T, Funari VA, Nevarez L, Krakow D, Cohn DH: **Dominant and recessive forms of**

fibrochondrogenesis resulting from mutations at a second locus, COL11A2. *American Journal of Medical Genetics Part A* 2012, **158A**(2):309-314.

25. Ornitz DM, Marie PJ: **FGF signaling pathways in endochondral and intramembranous bone development and human genetic disease**. *Genes & Development* 2002, **16**(12):1446-1465.

26. Corbani S, Chouery E, Eid B, Jalkh N, Abou Ghoch J, Mégarbané A: **Mild Campomelic Dysplasia: Report on a Case and Review**. *Molecular Syndromology* 2010, **1**(4):163-168.

27. Lee Y-H, Saint-Jeannet J-P: **Sox9 function in craniofacial development and disease**. *genesis* 2011, **49**(4):200-208.

28. Jaruga A, Hordyjewska E, Kandzierski G, Tylzanowski P: **Cleidocranial dysplasia and RUNX2-clinical phenotype–genotype correlation**. *Clinical Genetics* 2016:n/a-n/a.

29. Haila S, Hästbacka J, Böhling T, Karjalainen–Lindsberg M-L, Kere J, Saarialho–Kere U: **SLC26A2 (Diastrophic Dysplasia Sulfate Transporter) is Expressed in Developing and Mature Cartilage But Also in Other Tissues and Cell Types**. *Journal of Histochemistry & Cytochemistry* 2001, **49**(8):973-982.

30. Funari V, Day A, Krakow D, Cohn Z, Chen Z, Nelson S, Cohn D: **Cartilage-selective genes identified in genome-scale analysis of non-cartilage and cartilage gene expression**. *BMC Genomics* 2007, **8**(1):165.

31. Cameron T, Belluoccio D, Farlie P, Brachvogel B, Bateman J: **Global comparative transcriptome analysis of cartilage formation in vivo**. *BMC Developmental Biology* 2009, **9**(1):20.

32. Chau M, Lui JC, Landman EBM, Späth S-S, Vortkamp A, Baron J, Nilsson O: **Gene Expression Profiling Reveals Similarities between the Spatial Architectures of Postnatal Articular and Growth Plate Cartilage**. *PLoS ONE* 2014, **9**(7):e103061.

33. Mackie EJ, Ahmed YA, Tatarczuch L, Chen KS, Mirams M: **Endochondral ossification: How cartilage is converted into bone in the developing skeleton**. *The International Journal of Biochemistry & Cell Biology* 2008, **40**(1):46-62.

34. Kronenberg HM: **Developmental regulation of the growth plate**. *Nature* 2003, **423**.

35. Long F, Ornitz DM: **Development of the Endochondral Skeleton**. *Cold Spring Harbor Perspectives in Biology* 2013, **5**(1).

36. Wei X, Hu M, Mishina Y, Liu F: **Developmental Regulation of the Growth Plate and Cranial Synchondrosis**. *Journal of Dental Research* 2016.

37. Wuelling M, Vortkamp A: **Transcriptional networks controlling chondrocyte proliferation and differentiation during endochondral ossification**. *Pediatric Nephrology* 2010, **25**(4):625-631.

38. Lefebvre V, Smits P: **Transcriptional control of chondrocyte fate and differentiation**. *Birth Defects Research Part C: Embryo Today: Reviews* 2005, **75**(3):200-212.

39. Lefebvre V, Dvir-Ginzberg M: **SOX9 and the many facets of its regulation in the chondrocyte lineage**. *Connective Tissue Research* 2016:1-13.

40. Bernard P, Tang P, Liu S, Dewing P, Harley VR, Vilain E: **Dimerization of SOX9 is required for chondrogenesis, but not for sex determination**. *Human Molecular Genetics* 2003, **12**(14):1755-1765.

41. Lefebvre V, Huang W, Harley V, Goodfellow P, de Crombrugghe B: **SOX9 is a potent activator of the chondrocyte-specific enhancer of the pro alpha1(II) collagen gene**. *Mol Cell Biol* 1997, **17**(4):2336-2346.

42. Bridgewater LC, Walker MD, Miller GC, Ellison TA, Holsinger LD, Potter JL, Jackson TL, Chen RK, Winkel VL, Zhang Z *et al*: **Adjacent DNA sequences modulate Sox9 transcriptional activation at paired Sox sites in three chondrocyte-specific enhancer elements**. *Nucleic Acids Research* 2003, **31**(5):1541-1553.

43. Zhang P, Jimenez SA, Stokes DG: **Regulation of Human COL9A1 Gene Expression**. *Journal of Biological Chemistry* 2003, **278**(1):117-123.

44. Akiyama H, Chaboissier M-C, Martin JF, Schedl A, de Crombrugghe B: **The transcription factor Sox9 has essential roles in successive steps of the chondrocyte differentiation pathway and is required for expression of Sox5 and Sox6**. *Genes & Development* 2002, **16**(21):2813-2828.

45. Melrose J, Shu C, Whitelock JM, Lord MS: **The cartilage extracellular matrix as a transient developmental scaffold for growth plate maturation**. *Matrix Biology* 2016, **52–54**:363-383.

46. Patterson SE, Dealy CN: **Mechanisms and models of endoplasmic reticulum stress in chondrodysplasia**. *Developmental Dynamics* 2014, **243**(7):875-893.

47. Zaucke F GS: **Genetic mouse models for the functional analysis of the perifibrillar components collagen IX, COMP and matrilin-3: Implications for growth cartilage differentiation and endochondral ossification.** *Histology and Histopathology* 2009, **24**(8):13.

48. Myllyharju J: **Extracellular Matrix and Developing Growth Plate**. *Current Osteoporosis Reports* 2014, **12**(4):439-445.

49. Gibson BG, Briggs MD: **The aggrecanopathies; an evolving phenotypic spectrum of human genetic skeletal diseases**. *Orphanet Journal of Rare Diseases* 2016, **11**(1):1-8.

50. van der Rest M, Garrone R: **Collagen family of proteins**. *The FASEB Journal* 1991, **5**(13):2814-2823.

51. Olsen BR: **Collagen IX**. *The International Journal of Biochemistry & Cell Biology* 1997, **29**(4):555-558.

52. Wu JJ, Woods PE, Eyre DR: **Identification of cross-linking sites in bovine cartilage type IX collagen reveals an antiparallel type II-type IX molecular relationship and type IX to type IX bonding**. *Journal of Biological Chemistry* 1992, **267**(32):23007-23014.

53. Shaw LM, Olsen BR: **FACIT collagens: diverse molecular bridges in extracellular matrices**. *Trends in Biochemical Sciences* 1991, **16**:191-194.

54. Mayne R, Van Der Rest M, Ninomiya Y, Olsen BR: **The Structure of Type IX Collagena**. *Annals of the New York Academy of Sciences* 1985, **460**(1):38-46.

55. Muttigi M, Han I, Park H-K, Park H, Lee S-H: **Matrilin-3 Role in Cartilage Development and Osteoarthritis**. *International Journal of Molecular Sciences* 2016, **17**(4):590.

56. Svensson L, Aszódi A, Heinegård D, Hunziker EB, Reinholt FP, Fässler R, Oldberg Å: **Cartilage Oligomeric Matrix Protein-Deficient Mice Have Normal Skeletal Development**. *Molecular and Cellular Biology* 2002, **22**(12):4366-4371.

57. van der Weyden L, Wei L, Luo J, Yang X, Birk DE, Adams DJ, Bradley A, Chen Q: **Functional Knockout of the Matrilin-3 Gene Causes Premature Chondrocyte Maturation to Hypertrophy and Increases Bone Mineral Density and Osteoarthritis**. *The American Journal of Pathology*, **169**(2):515-527.

58. Ko Y, Kobbe B, Nicolae C, Miosge N, Paulsson M, Wagener R, Aszódi A: **Matrilin-3 Is Dispensable for Mouse Skeletal Growth and Development**. *Molecular and Cellular Biology* 2004, **24**(4):1691-1699.

59. Unger S, Bonafé L, Superti-Furga A: **Multiple epiphyseal dysplasia: clinical and radiographic features, differential diagnosis and molecular basis**. *Best Practice & Research Clinical Rheumatology* 2008, **22**(1):19-32.

60. Jackson GC, Mittaz-Crettol L, Taylor JA, Mortier GR, Spranger J, Zabel B, Le Merrer M, Cormier-Daire V, Hall CM, Offiah A *et al*: **Pseudoachondroplasia and multiple epiphyseal dysplasia: A 7-year comprehensive analysis of the known disease genes identify novel and recurrent mutations and provides an accurate assessment of their relative contribution**. *Human Mutation* 2012, **33**(1):144-157.

61. Kim O-H, Park H, Seong M-W, Cho T-J, Nishimura G, Superti-Furga A, Unger S, Ikegawa S, Choi IH, Song H-R *et al*: **Revisit of multiple epiphyseal dysplasia: Ethnic difference in genotypes and comparison of radiographic features linked to the COMP and MATN3 genes**. *American Journal of Medical Genetics Part A* 2011, **155**(11):2669-2680.

62. Cohn DH, Briggs MD, King LM, Rimoin DL, Wilcox WR, Lachman RS, Knowlton RG: **Mutations in the Cartilage Oligomeric Matrix Protein (COMP) Gene in Pseudoachondroplasia and Multiple Epiphyseal Dysplasiaa**. *Annals of the New York Academy of Sciences* 1996, **785**(1):188-194.

63. Briggs MD, Hoffman SMG, King LM, Olsen AS, Mohrenweiser H, Leroy JG, Mortier GR, Rimoin DL, Lachman RS, Gaines ES *et al*: **Pseudoachondroplasia and multiple epiphyseal dysplasia due to mutations in the cartilage oligomeric matrix protein gene**. *Nat Genet* 1995, **10**(3):330-336.

64. Chapman KL, Mortier GR, Chapman K, Loughlin J, Grant ME, Briggs MD: **Mutations in the region encoding the von Willebrand factor A domain of matrilin-3 are associated with multiple epiphyseal dysplasia**. *Nat Genet* 2001, **28**(4):393-396.

65. Czarny-Ratajczak M, Lohiniva J, Rogala P, Kozlowski K, Perälä M, Carter L, Spector TD, Kolodziej L, Seppänen U, Glazar R *et al*: **A Mutation in COL9A1 Causes Multiple Epiphyseal Dysplasia: Further Evidence for Locus Heterogeneity**. *The American Journal of Human Genetics* 2001, **69**(5):969-980.

66. Spayde EC, Joshi AP, Wilcox WR, Briggs M, Cohn DH, Olsen BR: **Exon skipping mutation in the COL9A2 gene in a family with multiple epiphyseal dysplasia**. *Matrix Biology* 2000, **19**(2):121-128.

67. P Paassilta JL, S Annunen, J Bonaventure, M Le Merrer, L Pai, and L Ala-Kokko: **COL9A3: A third locus for multiple epiphyseal dysplasia.** *American Journal of Human Genetics* 1999, **64**(4):9.

68. Superti-Furga A, Neumann L, Riebel T, Eich G, Steinmann B, Spranger J, Kunze J: **Recessively inherited multiple epiphyseal dysplasia with normal stature, club foot, and double layered patella caused by a DTDST mutation**. *Journal of Medical Genetics* 1999, **36**(8):621-624.

69. Bornstein P, Helene Sage E: **[4] Thrombospondins**. In: *Methods in Enzymology*. vol. Volume 245: Academic Press; 1994: 62-85.

70. Efimov VP, Lustig A, Engel J: **The thrombospondin-like chains of cartilage oligomeric matrix protein are assembled by a five-stranded α-helical bundle between residues 20 and 83**. *FEBS Letters* 1994, **341**(1):54-58.

71. Briggs MD, Brock J, Ramsden SC, Bell PA: **Genotype to phenotype correlations in cartilage oligomeric matrix protein associated chondrodysplasias**. *Eur J Hum Genet* 2014, **22**(11):1278-1282.

72. Posey KL, Hayes E, Haynes R, Hecht JT: **Role of TSP-5/COMP in Pseudoachondroplasia**. *The International Journal of Biochemistry & Cell Biology* 2004, **36**(6):1005-1012.

73. Wagener R, Kobbe B, Paulsson M: **Primary structure of matrilin-3, a new member of a family of extracellular matrix proteins related to cartilage matrix protein (matrilin-1) and von Willebrand factor**. *FEBS Letters* 1997, **413**(1):129-134.

74. Deák F, Wagener R, Kiss I, Paulsson M: **The matrilins: a novel family of oligomeric extracellular matrix proteins**. *Matrix Biology* 1999, **18**(1):55-64.

75. Fresquet M, Jackson GC, Loughlin J, Briggs MD: **Novel mutations in exon 2 of MATN3 affect residues within the α–helices of the A-domain and can result in the intracellular retention of mutant matrilin-3**. *Human Mutation* 2008, **29**(2):330-330.

76. Cotterill SL, Jackson GC, Leighton MP, Wagener R, Mäkitie O, Cole WG, Briggs MD: **Multiple epiphyseal dysplasia mutations in MATN3 cause misfolding of the A-domain and prevent secretion of mutant matrilin-3**. *Human Mutation* 2005, **26**(6):557-565.

77. Blumbach K, Niehoff A, Paulsson M, Zaucke F: **Ablation of collagen IX and COMP disrupts epiphyseal cartilage architecture**. *Matrix Biology* 2008, **27**(4):306-318.

78. Blumbach K, Bastiaansen-Jenniskens YM, DeGroot J, Paulsson M, van Osch GJVM, Zaucke F: **Combined role of type IX collagen and cartilage oligomeric matrix protein in cartilage matrix assembly: Cartilage oligomeric matrix protein counteracts type IX collagen–induced limitation of cartilage collagen fibril growth in mouse chondrocyte cultures**. *Arthritis & Rheumatism* 2009, **60**(12):3676-3685.

79. Chen T-LL, Posey KL, Hecht JT, Vertel BM: **COMP mutations: Domain-dependent relationship between abnormal chondrocyte trafficking and clinical PSACH and MED phenotypes**. *Journal of Cellular Biochemistry* 2008, **103**(3):778-787.

80. Nundlall S, Rajpar M, Bell P, Clowes C, Zeeff L, Gardner B, Thornton D, Boot-Handford R, Briggs M: **An unfolded protein response is the initial cellular response to the expression of mutant matrilin-3 in a mouse model of multiple epiphyseal dysplasia**. *Cell Stress and Chaperones* 2010, **15**(6):835-849.

81. Piróg-Garcia KA, Meadows RS, Knowles L, Heinegård D, Thornton DJ, Kadler KE, Boot-Handford RP, Briggs MD: **Reduced cell proliferation and increased apoptosis are significant pathological mechanisms in a murine model of mild pseudoachondroplasia resulting from a mutation in the C-terminal domain of COMP**. *Human Molecular Genetics* 2007, **16**(17):2072-2088.

82. Satoh H, Susaki M, Shukunami C, Iyama K-i, Negoro T, Hiraki Y: **Functional Analysis of Diastrophic Dysplasia Sulfate Transporter**. *Journal of Biological Chemistry* 1998, **273**(20):12307-12315.

83. Hastbacka J, Superti-Furga A, Wilcox WR, Rimoin DL, Cohn DH, Lander ES: **Sulfate Transport in Chondrodysplasia,a**. *Annals of the New York Academy of Sciences* 1996, **785**(1):131-136.

84. Rossi A, Kaitila I, Wilcox WR, Rimoin DL, Steinmann B, Cetta G, Superti-Furga A: **Proteoglycan sulfation in cartilage and cell cultures from patients with sulfate transporter chondrodysplasias: Relationship to clinical severity and indications on the role of intracellular sulfate production**. *Matrix Biology* 1998, **17**(5):361-369.

85. Briggs MD WM, Mortier GR. Multiple Epiphyseal Dysplasia, Dominant. 2003 Jan 8 [Updated 2011 Feb 1]. In: Pagon RA, Bird TD, Dolan CR, et al., editors. GeneReviews™ [Internet]. Seattle (WA): University of Washington, Seattle; 1993-. . In.

86. Robin NH MR, Ala-Kokko L. Stickler Syndrome. 2000 Jun 9 [Updated 2014 Nov 26]. In: Pagon RA, Adam MP, Ardinger HH, et al., editors. GeneReviews® [Internet]. Seattle (WA): University of Washington, Seattle; 1993-2015. Available from: http://www.ncbi.nlm.nih.gov/books/NBK1302/.

87. Ahmad NN, Ala-Kokko L, Knowlton RG, Jimenez SA, Weaver EJ, Maguire JI, Tasman W, Prockop DJ: **Stop codon in the procollagen II gene (COL2A1) in a family with the Stickler syndrome (arthro-ophthalmopathy)**. *Proceedings of the National Academy of Sciences of the United States of America* 1991, **88**(15):6624-6627.

88. Richards AJ, Yates JRW, Williams R, Payne SJ, Michael Pope F, Scott JD, Snead MP: **A Family with Stickler Syndrome Type 2 Has a Mutation in the COL11A1 Gene Resulting in the Substitution of Glycine 97 by Valine in a1(XI) Collagen**. *Human Molecular Genetics* 1996, **5**(9):1339-1343.

89. Vikkula M, Madman ECM, Lui VCH, Zhidkova NI, Tiller GE, Goldring MB, van Beersum SEC, de Waal Malefijt MC, van den Hoogen FHJ, Ropers H-H *et al*: **Autosomal dominant and recessive osteochondrodysplasias associated with the COL11A2 locus**. *Cell*, **80**(3):431-437.

90. Faletra F, D'Adamo AP, Bruno I, Athanasakis E, Biskup S, Esposito L, Gasparini P: **Autosomal recessive stickler syndrome due to a loss of function mutation in the COL9A3 gene**. *American Journal of Medical Genetics Part A* 2014, **164**(1):42-47.

91. Acke FR, Malfait F, Vanakker OM, Steyaert W, De Leeneer K, Mortier G, Dhooge I, De Paepe A, De Leenheer EMR, Coucke PJ: **Novel pathogenic COL11A1/COL11A2 variants in Stickler syndrome detected by targeted NGS and exome sequencing**. *Molecular Genetics and Metabolism*, **113**(3):230-235.

92. Sirko-Osadsa DA, Murray MA, Scott JA, Lavery MA, Warman ML, Robin NH: **Stickler syndrome without eye involvement is caused by mutations in COL11A2, the gene encoding the α2(XI) chain of type XI collagen**. *The Journal of Pediatrics*, **132**(2):368-371.

93. Exome Variant Server NGESPE, Seattle, WA (URL: http://evs.gs.washington.edu/EVS/) [(August, 2015) accessed].

94. Lek M, Karczewski K, Minikel E, Samocha K, Banks E, Fennell T, O'Donnell-Luria A, Ware J, Hill A, Cummings B *et al*: **Analysis of protein-coding genetic variation in 60,706 humans**. *bioRxiv* 2015.

95. Quintana-Murci L: **Understanding rare and common diseases in the context of human evolution**. *Genome Biology* 2016, **17**(1):225.

96. Hagg R, Hedbom E, Möllers U, Aszódi A, Fässler R, Bruckner P: **Absence of the α1(IX) Chain Leads to a Functional Knock-out of the Entire Collagen IX Protein in Mice**. *Journal of Biological Chemistry* 1997, **272**(33):20650-20654.

97. Dreier R, Opolka A, Grifka J, Bruckner P, Grässel S: **Collagen IX-deficiency seriously compromises growth cartilage development in mice**. *Matrix Biology* 2008, **27**(4):319-329.

98. Hu K, Xu L, Cao L, Flahiff CM, Brussiau J, Ho K, Setton LA, Youn I, Guilak F, Olsen BR *et al*: **Pathogenesis of osteoarthritis-like changes in the joints of mice deficient in type IX collagen**. *Arthritis & Rheumatism* 2006, **54**(9):2891-2900.

99. Asamura K, Abe S, Imamura Y, Aszodi A, Suzuki N, Hashimoto S, Takumi Y, Hayashi T, Fässler R, Nakamura Y *et al*: **Type IX collagen is crucial for normal hearing**. *Neuroscience* 2005, **132**(2):493-500.

100. Pihlajamaa T, Perälä M, Vuoristo MM, Nokelainen M, Bodo M, Schulthess T, Vuorio E, Timpl R, Engel J, Ala-Kokko L: **Characterization of Recombinant Human Type IX Collagen: ASSOCIATION OF α CHAINS INTO HOMOTRIMERIC AND HETEROTRIMERIC MOLECULES**. *Journal of Biological Chemistry* 1999, **274**(32):22464-22468.

101. Jäälinoja J, Ylöstalo J, Beckett W, Hulmes David JS, Ala-Kokko L: **Trimerization of collagen IX α-chains does not require the presence of the COL1 and NC1 domains**. *Biochemical Journal* 2008, **409**(2):545-554.

102. Labourdette L, van der Rest M: **Analysis of the role of the COL1 domain and its adjacent cysteine-containing sequence in the chain assembly of type IX collagen**. *FEBS Letters* 1993, **320**(3):211-214.

103. Budde B, Blumbach K, Ylöstalo J, Zaucke F, Ehlen HWA, Wagener R, Ala-Kokko L, Paulsson M, Bruckner P, Grässel S: **Altered Integration of Matrilin-3 into Cartilage Extracellular Matrix in the Absence of Collagen IX**. *Molecular and Cellular Biology* 2005, **25**(23):10465-10478.

104. Boeyer ME, Ousley SD: **Skeletal assessment and secular changes in knee development: a radiographic approach**. *American Journal of Physical Anthropology* 2016:n/a-n/a.

CHAPTER TWO

Exome Sequencing Identifies Locus Heterogeneity in Multiple Epiphyseal Dysplasia

Abstract

Multiple Epiphyseal Dysplasia (MED) is a relatively mild skeletal dysplasia that is characterized by mild short stature, joint pain, and early-onset osteoarthropathy. Dominant mutations in *COMP*, *MATN3, COL9A1, COL9A2,* and *COL9A3*, and recessive mutations in *SLC26A2* account for the molecular basis of disease in about 80-85% of the cases. The molecular basis of disease is unknown in about 15-20% of the cases. In this study, I used exome sequencing to determine the molecular basis of disease in a cohort of 15 MED families, identifying pathogenic mutations in 9 out of 15 cases. In addition, 18 additional families were analyzed by candidate gene mutation screening, yielding 2 additional mutations. Pathogenic mutations were identified in the known MED disease loci in six families: 3 previously observed mutations in *COMP*, 1 previously observed and 1 novel mutation in *MATN3,* and 1 previously observed mutation in *COL9A2.* Novel mutations were identified in other known skeletal dysplasia loci in 5 families: homozygosity for recessive mutations in *CANT1* was found in two families, compound heterozygosity for mutations in *GNPTAB* was found in one family, and heterozygosity for autosomal dominant mutations in *COL2A1* was found in two families. All of these cases had radiographic similarity to more severe diseases associated with their respective loci, i.e. Desbuquois dysplasia, mucolipidosis III, and spondyloepiphyseal dysplasia congenita. However, the phenotype associated with the recessive *CANT1* mutation is clinically distinct from Desbuquois dysplasia and more similar to MED, indicating that *CANT1* can be considered as another locus for recessive MED. Lastly, the causative mutation was not identified in the remaining six cases, emphasizing further locus heterogeneity in MED.

Introduction

Multiple Epiphyseal Dysplasia (MED) is a mild chondrodysplasia that is characterized by mild short stature, joint pain, and early-onset osteoarthropathy, frequently resulting in multiple

joint replacements in the third or fourth decade of life[1]. Radiographic features include epiphyseal dysplasia at the hips and knees, delayed carpal bone age and, in some cases, mild platyspondyly and irregularly-shaped vertebral bodies[2]. Autosomal dominant mutations in *COMP[3, 4]*, *MATN3[5]*, *COL9A1[6]*,*COL9A2[7]*, and *COL9A3[8]* account for the molecular basis of disease in approximately 70-75% of the cases. All of these genes encode structural proteins of the cartilage extracellular matrix that are selectively expressed in the tissue[9]. A clinically distinct recessive form of the disease, which is caused by homozygosity or compound heterozygosity for mutations in *SLC26A2*, is characterized by epiphyseal dysplasia at the hips, advanced carpal ossification, and a double-layered patella observed by lateral x-ray of the knee and accounts for an additional 10-15% of MED cases [10]. *SLC26A2* encodes a sulfate transporter that imports inorganic sulfate into the cell for posttranslational modification of proteoglycans and is a widely expressed gene [11, 12]. The molecular basis of disease remains unknown in approximately 15-20% of the cases.

Previously, MED patients were classified into three categories: "Fairbanks" type, "Ribbing" type, and "Unclassified"[2]. This classification system was based on the severity of the radiographic findings where the Fairbanks type represents more severe epiphyseal dysplasia with abnormalities at all of the major joints including severe abnormalities of the hips; the Ribbing type represents mild cases that typically only involve epiphyseal dysplasia at the hips; and the unclassified group represents an intermediate severity phenotype within the MED spectrum [2]. Among the dominant forms of the disease, it is challenging to determine the genotype of patients based on the observed phenotype, as there is a great deal of clinical and radiographic variability and there is no clinically distinct feature that reliably defines *COMP* vs *MATN3* vs type IX collagen MED. Typically *COMP* MED is more severe and results in very

small, irregular capital femoral epiphyses, flattened acetabulae, irregularly-shaped knee epiphyses with metaphyseal widening, brachydactyly, mild platspondyly, and mildly rounded vertebral bodies[2]. Type IX collagen MED is typically milder than *COMP* MED with defects primarily observed at the knee epiphyses[13]. An examination of patients with *MATN3* mutations demonstrates significant phenotypic variability. There are reports of patients with normal stature and very mild skeletal manifestations[14, 15], as well as cases presenting with small, dysplastic capital femoral epiphyses, irregular knee epiphyses, and platyspondyly with vertebral irregularities[16]. In addition to the variability in *MATN3* MED, there are also atypical cases of *COMP* MED that deviate from the aforementioned features, leading to radiographic overlap among cases with mutations in other genes[16]. More recently, mutations in *COL2A1* have been identified in patients with MED, indicating some difficulty in differentiating MED from related disorders with similar radiographic features, such as mild forms of spondyloepiphyseal dysplasia congenita (SEDC)[17].

All of the proteins encoded by the known MED associated genes are involved in maintaining the structural integrity of the cartilage extracellular matrix (ECM). For the autosomal dominant forms of the disease, the mutations exert their phenotypic effect through a dominant negative mechanism, leading to intracellular retention of structurally abnormal proteins within the rough endoplasmic reticulum (RER) [18-22]. In addition to disrupting the matrix, accumulation of abnormal proteins within the RER can induce an unfolded protein response and lead to secondary abnormalities, including chondrocyte apoptosis [23, 24]. The recessive mutations in *SLC26A2* result in reduced activity of the diastrophic dysplasia sulfate transporter, which ultimately leads to decreased sulfation of chondroitin sulfate proteoglycans, including ECM proteins[25, 26]. Considering that the molecular basis of disease is unknown in about 15%-

20% of the cases, I hypothesized that novel mutations in one or more genes involved in cartilage development and/or extracellular matrix biosynthesis might be the cause of MED. I used exome sequencing and candidate gene analysis to explore this possibility and have identified novel variants in *CANT1*, the gene encoding calcium-activated nucleotidase 1, that result in a form of recessively inherited MED that is clinically distinct from the allelic Desbuquois dysplasia phenotype. As the CANT1 enzyme is involved in the posttranslational modification of cartilage proteoglycans, this supports the proposed hypothesis and provides insight into the mechanism of pathogenesis in some cases with a previously unknown molecular basis of disease.

Materials and Methods

Patient Samples

All patient samples were obtained through the International Skeletal Dysplasia Registry at the University of California, Los Angeles. Informed consent was provided by all subjects under an approved Institutional Review Board (IRB) protocol.

DNA was obtained from whole blood, saliva, or cultured patient cells, which included Epstein Barr Virus transformed lymphoblastoid cell lines, fibroblasts, and/or chondrocytes and was isolated using a kit (Qiagen). All methods employed in this study were approved under a UCLA Biosafety protocol.

Exome Sequencing

Exome sequencing included affected individuals and selected unaffected family members from cases R95-334, R96-231, R74-111, R86-160, R92-280, R95-055, R97-290, R98-058, R89-205, R91-025, R93-046, R98-132, R98-306, R07-462, and R12-062.

To facilitate exome sequencing, DNA quality was assessed by two independent methods: agarose gel electrophoresis and the Agilent Bioanalyzer. All samples were separated by electrophoresis on 1 % agarose gels, stained with ethidium bromide, and assessed for the level of

DNA fragmentation. A broad, solid band indicated good DNA quality. Results were confirmed by interrogating samples on an Agilent DNA 1000 chip, again requiring that the DNA was not degraded. DNA samples that passed these two quality control measures were then quantified using the Qubit Broad Range DNA assay and 2-3 µg was used for exome library preparation.

Some exome libraries were prepared and exome sequences determined at UCLA. DNA was fragmented and sheared using the Covaris sonicator. Whole genome libraries were prepared using the Illumina Truseq DNA library preparation kit. Post library preparation, library quality was assessed using the Agilent DNA High Sensitivity Kit. Post quality assessment, libraries were quantified using the Qubit high sensitivity DNA assay. Samples were then pooled and exome capture was conducted using the Illumina Truseq Exome Enrichment kit. 100 bp paired-end sequences were obtained on three lanes of a high throughput sequencer at the UCLA Broad Stem Cell Sequencing Core. Additional exome libraries were prepared and sequences derived at the University of Washington Center for Mendelian Genomics. Other libraries were prepared and sequenced at the UCLA Clinical Microarray Core. All libraries were sequenced on the Illumina platform.

Data Analysis

Upon completion of sequencing, data were returned as either qseq or fastq files. All samples were aligned to the Human GRCh37 reference genome using the Burrows Wheelers Aligner (BWA) MEM algorithm[27, 28] followed by the removal of duplicate reads using Picard [29]. All further data processing was completed with the Genome Analysis Tool Kit (GATK)[30]. All libraries had a depth of coverage of >20X for at least 90% of the targeted bases. Bam files were then recalibrated and realigned around the insertions and deletions. Variant calling was conducted using Unified Genotyper. Variant quality was then assessed using

the Variant Quality Score Recalibration using a general linearized model for both SNPS and indels.

Upon completion of data processing, the final VCF was submitted to the SeattleSeq variant annotation server[31]. The returned annotation file was then converted to a SQL database and merged with the VCF. All variants not targeting the exome and splice junction consensus sequences were excluded. Initial screening for mutations in the known MED disease genes was conducted. Cases negative for mutations in the known MED loci were then filtered for mutations in all known skeletal dysplasia genes. Exclusion of the known MED genes and all skeletal dysplasia loci was followed by filtering for novel loci. Sporadic cases were initially filtered for novel *de novo* variants, recurrent cases for recessive variants, including homozygous and compound heterozygous variants, and small families with multiple affected individuals for heterozygous variants shared by the affected individuals. All candidate variants were confirmed by Sanger sequencing.

Sanger Sequencing

All Sanger sequencing was completed using the Qiagen Hotstart Taq polymerase and touchdown PCR. PCR primers were designed using Primer3 software[32, 33]. All primers were designed to include the exon and 20 bp flanking the intron-exon splice junction. In the case of exons producing PCR products larger than 700 bp, exons were amplified in 2 or more PCR products with overlapping regions covering approximately 30-40bp in the middle of the exon. Primers used can be found in Supplementary Tables 1 and 2.

For all trios, recurrent cases, and large families, DNA from both unaffected and affected individuals was PCR amplified. All PCR products were separated by electrophoresis on 1% agarose gels and stained with ethidium bromide to confirm completion and specificity of PCR.

Samples were then submitted for sequencing to third-party vendors. Sanger confirmation of the exome sequencing was verified by sequencing in both the forward and reverse directions. The sequencing results were then analyzed using Sequencher 2.0. All sequences were aligned to the GRCh37 reference sequences on the UC Santa Cruz Genome Browser[34].

Candidate Gene Mutation Screening

Candidate gene mutation screens of *CANT1, PRICKLE1,* and *PTH2R* (see below) were carried out in an additional cohort of MED patients with an unknown molecular basis of disease. Supplementary Table 2.3 summarizes all of the cases included in these mutation screens. Supplementary Table 2.4 summarizes all of the primers used for PCR and Sanger sequencing. All of the coding exons were amplified by PCR and sequenced in one or both directions.

Results

Mutations Identified in the Known MED Genes

Upon completion of exome sequencing, patients were first screened for mutations in the known MED loci. I identified 3 families with *COMP* mutations, 2 families with *MATN3* mutations, and 1 family with a *COL9A2* mutation (Tables 1 & 2). All of the *COMP* mutations, p.Asp317Asn in case R95-334A, p.Asn555Lys in case R98-306 and p.Thr585Met in case R07-462, which target the type III repeats (p.Asp317Asn) or the C-terminal domain (p.Asn555Lys and p.Thr585Met) , were previously determined to be pathogenic in Kim et al., 2011[16], Kennedy et al., 2005[35] and Briggs et al., 1998[36], respectively.

For the remaining families, the *MATN3* mutation identified in family R97-290, p.Ala173Asp, and the *COL9A2* mutation identified in patient R98-132A, c.186C>T resulting in the skipping of exon 3, have been previously described as pathogenic in Fresquet et al., 2008[21] and Holden et al., 1999[37], respectively. Radiographs of patient R98-132A in Figure 2.1D

illustrate that type IX collagen mutations can and generally do confer a much milder phenotype in comparison to the *COMP* and *MATN3* MED mutations. This patient had irregularly ossified epiphyses of the knees, but there were little to no radiographic abnormalities in the pelvis, hands and the vertebrae. Lastly, a novel *MATN3* mutation, p.Ile109Lys, was identified in family R95-055. This mutation targets the von Willebrand factor A domain and, as detailed below, I have concluded that this mutation is pathogenic.

Incomplete Penetrance of *MATN3* p.Ile109Lys Mutation

Family R95-055 is a multi-generation family affected with autosomal dominant MED, Fairbanks type, as depicted in Figure 2.2. An examination of the radiographs of patients R95-055A (IV-7) (Figure 2.1C) and R95-055B (III-7), led to the MED Fairbanks diagnosis as these patients presented with irregularly-shaped capital femoral epiphyses, short, small and flat proximal tibial epiphyses, and mildly rounded and flat vertebral bodies. Exome sequencing was carried out for patients R95-055A and R95-055J (III-1) and heterozygosity for the p.Ile109Lys variant in *MATN3* was identified in both affected individuals. The remaining family members were analyzed to determine the status for this allele (Table 2.3). The variant segregated with all clinically affected individuals in the family. Three individuals who phenotyped as unaffected, R95-055C (II-7), R95-055H (III-4) and R95-055I (III-2), also carried the variant, consistent with incomplete penetrance. This inference is supported by the observation that R95-055C is an obligate carrier as she has an affected parent and affected offspring. Furthermore, while she did not report joint pain, she was of short stature, similar to her clinically affected relatives who were heterozygous for the variant. Patients R95-055H and R95-055I inherited the variant from their clinically affected parents and R95-055H is of short stature. Although patient R95-055E (III-7) was self-diagnosed as affected, because his parents were clinically unaffected and negative for

the variant, it is unlikely that this individual was affected. Finally, all of the apparently incompletely penetrant individuals were female, raising the possibility that the sex of the affected individuals may be a contributing factor to penetrance in MED. The data are thus most consistent with the p.Ile109Lys variant being a pathogenic mutation.

CANT1 Mutations Result in Recessive Multiple Epiphyseal Dysplasia

Among the individuals for whom mutations at the known MED loci were excluded, filtering the exome sequences for variants in the known skeletal dysplasia disease loci identified homozygosity for a variant, p.Ile171Phe, in *CANT1*, the gene encoding calcium-activated nucleotidase 1, in affected individuals in a family with recurrence of MED Fairbanks type. Patient R92-280A presented with irregularly shaped capital femoral epiphyses and a short femoral neck, which resembles the Swedish key-appearance of the proximal femur that is characteristic of Desbuquois dysplasia (DBQD) patients with *CANT1* mutations (Figure 2.3A). Other notable defects included anterior wedging of the vertebral bodies, small epiphyses at the knees with metaphyseal flare, and advanced carpal ossification in the hands, which is also observed in DBQD patients. Patient R92-280B, sibling to patient R92-280A, also presented with the aforementioned radiographic features as well as midface hypoplasia. However, neither of the two affected siblings exhibited joint dislocations, scoliosis, coronal clefting, or any of the hand anomalies (accessory ossification centers and/or delta phalanx) consistent with a diagnosis of DBQD (Table 2.4). The observed radiographic phenotype is also distinct from the less severe DBQD Kim variant as the metacarpal and phalangeal lengths were also unaffected. The observed phenotype in family R92-280 thus represents a clinically distinct phenotype with the mildest severity known on the *CANT1* phenotypic spectrum.

Because of the identification of homozygosity for the variant, I tested whether there might be one or more regions of homozygosity, consistent with a recessive mutation inherited identically by descent, in the family. Homozygosity mapping identified two runs of homozygosity, a 34.5 Mb block at chromosome 3q12.1 that contained 22 variants in the homozygous state in 16 genes and a 22.1 Mb block at chromosome 17q25.3 that contained 58 variants in the homozygous state in 47 genes, including the identified variant in *CANT1*. After excluding all of the common variants (variants with high allele frequency), 4 variant-containing genes, *GPR128, MYH15, CASR,* and *PLXND1*, remained in the chromosome 3 block, and 10 variant-containing genes, including *CANT1*, remained in the chromosome 17 block. As family R92-280 is of Mexican ancestry, further filtering based on the Latino allele frequency in ExAC eliminated the variants in 4 genes and, with the exception of *CANT1* and *RHOT1* in the chromosome 17 block, the remaining variant-containing genes were either not expressed in cartilage or expressed at a very low level (FPKM $\leq$ 1.5). The variant in *RHOT1* was a 2 nucleotide deletion in an intron near a splice site and is of unknown functional consequence, while the *CANT1* variant was predicted "possibly damaging" by PolyPhen[38] with a CADD[39] score of 16.92. The *CANT1* variant was novel and was absent in dbSNP, the Exome Sequencing Project (ESP)[40], and the Exome Aggregation Consortium (ExAC)[41]. An examination of the functional consequence of this variant demonstrated that it lies in the middle of the second nucleotide conserved region and is adjacent to two mutations (p.Ser168Ala and p.Asp169Asn) identified by a mutagenesis study targeting the Ca^{2+} binding site that resulted in 96-99% diminished enzymatic activity[42]. Combining the molecular data with the "Swedish key" radiographic feature, I concluded that the variant is pathogenic. Under this hypothesis, I then identified and screened additional MED patients with the mild "Swedish key" proximal

femur/short femoral neck radiographic phenotype by Sanger sequencing. I identified a second patient (R01-152A) homozygous for a *CANT1* variant, p.Val226Met, a known pathogenic mutation that was predominantly observed in the heterozygous state [43] (Figure 2.4 and Table 2.5). This patient also presented with degenerative arthrosis of the spine and the hand at 25 years of age (Figure 2.3B). Although there was some mild radiographic overlap with Desbuquois dysplasia with the "Swedish key" proximal femur and advanced carpal ossification in the hands, the phenotype in both families is milder and clinically distinct from Desbuquois dysplasia, demonstrating that recessive mutations in *CANT1* can result in MED.

GNPTAB Mutations Identified in a Mild Case of Mucolipidosis III

During the screen of known skeletal disease loci, I identified compound heterozygosity for variants in *GNPTAB,* the gene encoding the alpha and beta subunit of the UDP-GlcNac phosphotransferase, in case R12-062A. The identified variants were a paternally inherited p.Asn593Ile missense change that targets the luminal domain of the alpha subunit and a maternally inherited p.Pro341CysfsX25 loss-of-function variant (Table 2.8). An examination of the clinical data demonstrated that this patient presented with a MED-like radiographic phenotype but with normal stature. Severe epiphyseal dysplasia was present at the hips with superiorly-notched capital femoral epiphyses. Additionally, there was mild involvement of the spine with mildly irregularly-shaped vertebral bodies and platyspondyly. Lastly, at the knee, there were irregularities present at the metaphyses of the distal femurs (Figure 2.5 and Table 2.7). Combining the molecular data and the clinical data, this patient is likely affected with mucolipidosis type III (ML III). Based on this study, I concluded that during the early stages of ML III, the radiographic phenotype can resemble a mild case of MED.

Novel Type II Collagen Mutation Resulting in MED

In a sporadic case of autosomal dominant MED, (R89-205), I identified heterozygosity for a p.Gly888Ser missense change in *COL2A1* (Table 2.10). The radiographic phenotype of this patient included bilateral avascular necrosis of the capital femoral epiphyses, small, irregularly shaped knee epiphyses, mild rounding of the vertebral bodies and slightly small carpal bones, consistent with the MED diagnosis and distinct from SEDC and related skeletal dysplasias that are usually associated with such non-lethal *COL2A1* mutations (Figure 2.6 and Table 2.9). Like most *COL2A1* structural mutations, as this variant targets the Glycine of the G-X-Y repeat in the triple helical domain, it is likely to be pathogenic. An additional case, R11-324A, was heterozygous for a p.Gly945Ser missense change in *COL2A1*. A generalized epiphyseal dysplasia with mild spinal abnormalities suggested a diagnosis closer to MED than SEDC. Furthermore, pathogenic mutations in *COL2A1* have been previously described in MED cases reported in Jackson et al. 2012[17], providing further evidence that MED can result from mutations in *COL2A1*.

Novel Variants Identified by Exome Sequencing

In the remaining 6 cases of this cohort, mutations in both the known MED disease loci and the known skeletal dysplasia loci were excluded. This would indicate that mutations in one or more novel loci exist that can result in MED. Filtering for novel *de novo* variants in cases with unaffected parents yielded the following results.

In a recurrent case of MED Ribbing type (R74-111) with two affected siblings, the patients presented with a very mild phenotype. R74-111A presented with irregular ossification of the capital femoral epiphyses and mild platyspondyly. The affected sibling, R74-111B presented

with malformed capital femoral epiphyses, subchondral sclerosis, degenerative arthrosis at age 28, Schmorl's nodes at vertebrae L3, T5, T7, & T8, and levoscoliosis. In neither individual was there radiographic evidence of involvement of the hands or the knees. DNA was not available on R74-111A, so exome sequencing was carried out for R74-111B and the unaffected parents.

Filtering under a dominant mode of inheritance, I identified heterozygosity for two *de novo* variants, p.Val291Phe in *PTH2R* and p.Pro152ProfsX44 in *PRICKLE1*. Both of these variants are novel, highly conserved amino acid changes, and absent in dbSNP, the Exome Variant Server, and the ExAC database. *PTH2R* is expressed in the endochondral growth plate and is involved in regulating chondrocyte proliferation[44, 45]. *PRICKLE1* is involved in regulating planar cell polarity, and loss-of-function mutations in a murine model result in severe chondrodysplasia[46]. Both of the genes are good candidates, but because of the lack of DNA for R74-111A, I was unable to determine whether either or both variants were present in this patient. Since MED was recurrent in the family, pathogenicity would have to be based on dominant inheritance with parental germline mosaicism. Additionally, 16 MED cases with an unknown molecular basis of disease were screened for mutations in both of these genes, and no causative mutations were identified. As both of these genes are involved in chondrocyte growth and cartilage development, it is challenging to determine if the variants identified in either gene is causative for MED. Additional genetic and biochemical data will be required to establish if either of these variants is pathogenic.

Discussion

Frequency of Mutations in Known MED Loci

In this study, I identified 3 dominant mutations in *COMP*, 2 in *MATN3*, and 1 in *COL9A2*. As described in the most recent GeneReview Update on MED, Briggs et al.[47] stated

that *COMP* mutations account for 50% of autosomal dominant MED mutations, *MATN3* accounts for 20%, and the three type IX collagen genes collectively account for 10% of the cases, leaving about 20% of patients with a yet unidentified molecular basis of disease[47]. Although the numbers are small, the proportions in which I identified mutations in the known loci thus correlate with what is observed in the literature.

Based on the results of this exome sequencing cohort, if I exclude the cases with phenotypic overlap with other skeletal diseases, I only identified mutations in the known disease loci in 50% of the cases. However, over half of the cases in the cohort were selected for exome sequencing because they were previously determined to be negative for mutations in the known loci by Sanger sequencing, therefore reducing the frequency of mutations at the known MED loci. I identified candidate variants in one of the unknown families, but this still leaves five families with an unknown molecular basis of disease. As the majority of these "unknown" cases presented with the milder Ribbing type, it is possible that patients with this radiographic phenotype are underdiagnosed and not generally included in MED research cohorts, resulting in a similar predicament to what is observed with patients with type IX collagen MED, where it is hypothesized that the observed 10% frequency of mutations in these genes is underestimated due to underdiagnosis of the mild phenotype.

Incomplete Penetrance in MED due to a *MATN3* Mutation

In family R95-055, I observed 3 individuals, all of whom were female, who carried a familial pathogenic *MATN3* mutation, but were clinically asymptomatic. Previous studies have also shown variable penetrance among other patients with *MATN3* mutations. Mortier et al. 2001 described a multi-generation family of MED with normal stature and radiographic features indicating moderate involvement of the hip and knees. In addition to the absence of short

stature, the female proband in this family was clinically asymptomatic[14]. In an additional study described in Makitie et al. 2004, clinically asymptomatic patients (the female proband in family 2 and a male parent in family 6) with radiographic evidence of MED were identified in 2 families with *MATN3* mutations[15]. The phenotype observed in family R95-055 provides further evidence of variable penetrance in MED due to *MATN3* mutations. The clinically affected patients in the family had normal to mild short stature in conjunction with joint pain, primarily at the hips and knees. Of the clinically asymptomatic individuals, radiographic data were only available for one patient, R95-055C (II-7). As this individual was 61 at the time of the skeletal survey, it cannot be conclusively determined whether the observed degenerative changes are simply age-related or due to her mutation status. The only evidence of possible affectation is her height at 61", which is mildly short for females but could be considered normal within the family as another unaffected individual negative for the mutation (III-4) was of the same height. Of the remaining two clinically asymptomatic individuals, patient R95-055H was also of mild short stature with an adult height of 61", which is consistent with R95-055C. I was unable to obtain height data on the third individual, R95-055I, but it would be reasonable to consider mild short stature as a defining feature of the clinically asymptomatic individuals. Since all of the patients with putative incomplete penetrance in family R95-055 and 2 out of the 3 non-penetrant patients described in the literature are females, it is possible that penetrance could vary due to sex-specific factors.

Clinically Distinct MED Phenotype Due to Recessive Mutations in *CANT1*

I identified recessive mutations in *CANT1* in two recurrent cases of MED, Fairbanks type. Recessive mutations in *CANT1* are known to cause Desbuquois dysplasia (DBQD), which is characterized by severe short stature, joint dislocations, scoliosis, advanced carpal and tarsal

ossification, accessory ossification centers in the hand, and a characteristic "Swedish key" appearance of the proximal femur on radiographs [48]. The phenotypic spectrum comprises three clinically distinct disorders, Type I DBQD, Type II DBQD, and the DBQD Kim Variant. Type I and Type II DBQD are distinguished based on the presence or absence of the accessory ossification centers distal to the second metacarpal or a delta phalanx[49] and the Kim variant is clinically distinguished by short metacarpals and elongated phalanges[50]. While the patients in our cohort presented with a mild "Swedish key" appearance of the proximal femurs, the hands were radiographically normal, with no evidence of the short metacarpals and elongated phalanges that are observed in the Kim variant. Thus the phenotype observed in MED due to *CANT1* mutations is clinically distinct from the DBQD Kim Variant and expands the phenotypic spectrum associated with mutations in the gene.

Despite the clinical and radiographic differences, one of the two *CANT1* MED mutations identified, p.Val226Met in R01-152A, was previously identified in patients with the Kim variant[43] and is a founder mutation within the Korean and Japanese population[51]. This mutation lies in the fourth nucleotide conserved region and Furuichi et al. 2011 demonstrated that CANT1 nucleotidase activity is diminished to 20% of the wild-type enzyme activity[43]. As this patient was not of Asian descent, it is likely that the same mutation has occurred independently among the ancestors of the patient. The mutation identified in the second family, p.Ile171Phe in family R92-280, is novel and lies in the second nucleotide conserved region, adjacent to the Ca^{2+} binding site. Because the observed radiographic phenotype is similar in families R92-280 and R01-152, the p.Ile171Phe mutation might also result in diminished enzyme activity similar to what is observed with the p.Val226Met mutation, and thus resulting in the MED phenotype.

From a mechanistic viewpoint, in the study by Nizon et al. 2012, CANT1 localizes to the Golgi and is involved in the synthesis of glycosaminoglycans (GAG) and the posttranslational modification of proteoglycans. This study demonstrated that missense mutations in DBQD patients positive for *CANT1* mutations have diminished GAG synthesis due to the inability of CANT1 to metabolize UDP to UMP. The UMP is normally exchanged for UDP-sugars, which are required for the synthesis and elongation of GAG chains [52]. Based on this function of CANT1, I have identified a novel MED locus that is indirectly involved in ECM biosynthesis as many of the ECM proteins, specifically proteins like type IX collagen, have GAG posttranslational modifications that may be altered by these mutations. It is not clear, however, whether the phenotype results from a general effect on multiple posttranslationally modified proteins or is due to defects in the mature form of one or a few proteins.

Radiographic Similarity of MED and Mucolipidosis III During Early Adolescence

In a single case (R12-062) with a radiographic diagnosis of MED, I identified compound heterozygosity for two novel mutations in *GNPTAB*, which suggested that this was actually a case of mucolipidosis alpha/beta III, a lysosomal storage disorder. Mutations in *GNPTAB* result in a spectrum of phenotypes ranging from severe ML II, in which affected individuals do not survive past early childhood, to the milder ML III, in which patients live into adulthood[53]. There is a great deal of variability in clinical presentation among ML III patients, and affected individuals may possess any or all of the following findings: coarsening of facial features, joint pain and/or stiffness, moderate to severe dysplasia of the hips and knees, mild generalized platyspondyly, mildly short metacarpals, mildly smaller carpal bones, and mild dysostosis multiplex[54, 55]. Elements of these clinical and radiographic features overlap with the MED phenotype, making a diagnosis without molecular data a challenge, especially in milder cases.

Recently, a mild case of ML III was hypothesized to be MED, and the mutations in *GNPTAB* were identified by exome sequencing[56]. A very mild ML III phenotype may be due to the effect of specific missense mutations on enzyme activity, as observed in the study by Velho et al. 2015 [57]. The clinical and radiographic overlap between MED and mild cases of ML III may be especially evident during childhood and early adolescence, before the full effects of storage become evident. As lysosomal storage diseases can be identified by elevated enzyme levels in the blood and urine[53], a comprehensive screen that includes these tests could be used to distinguish ML III from MED, even during the pediatric period.

Radiographic Overlap Between Mild Spondyloepiphyseal Dysplasia Congenita and MED

Two MED cases in the cohort, R89-205 and R11-324A, were heterozygous for missense mutations in the type II procollagen gene, a phenotype typically associated with the more severe SED congenita (SEDC) phenotype[58]. R89-205 presented with MED Fairbanks type and R11-324A presented with the MED Unclassified type, but there was little to no involvement of the spine in both patients. In R89-205, mild rounding of the vertebral bodies was observed, and in R11-324A there was neither significant platyspondyly nor other vertebral anomalies observed on x-ray. There are several published reports of patients that were initially diagnosed with either MED or Legg-Calve-Perthes Disease, but were subsequently reclassified as a mild SEDC based on mutations in *COL2A1* [17, 59, 60]. In Terhal et al. 2013, the p.Gly945Ser mutation also identified in our case R11-324A was also observed in another patient with an MED-like presentation of disease, but the defects in the spine were more pronounced in radiographs taken during early adulthood. These studies, and our data, provide evidence that a temporal component appears to be involved in the diagnosis of MED versus SEDC. The spinal abnormalities may not be apparent at a young age, so these patients may be diagnosed with MED Fairbanks during

childhood. As these individuals age, the defects in the spine may become more prominent, which would be more consistent with a diagnosis of SEDC. Because of this clinical evolution, *COL2A1* has been included on some gene panels that test for mutations in cases of autosomal dominant MED (e.g. CTGT: http://ctgt.net/panel/multiple-epiphyseal-dysplasia-med-ngs-panel#related-tests)[61].

Further Locus Heterogeneity in Cases Negative for Mutations MED and Skeletal Dysplasia Loci

Since the remaining six cases were negative for mutations in the MED loci and known skeletal dysplasia loci, and I only identified candidate variants in one case, this implies further locus heterogeneity in MED. Our analytical approach would have missed a molecular defect due to an intronic splicing variant outside the targeted regions of the exome, which might be present in a known MED locus or a novel locus. I also cannot rule out novel mechanisms that could produce MED, including regulatory mutations or copy number variations, neither of which would be detected by exome sequencing. Combining techniques such as RNA-sequencing to detect altered gene expression levels and whole genome sequencing to ensure complete coverage could aid in overcoming the shortcomings of capturing and sequencing just the exome. As these cases are all very mild, it is also possible that they may not represent MED but rather another skeletal dysplasia with a similar clinical phenotype such as Legg-Calve-Perthes, Beukes familial hip dysplasia, or Meyer's disease. I already observed this phenomenon in the patients with *GNPTAB* and *COL2A1* mutations. However, since a mutation in a known skeletal dysplasia locus would have been detected by our method, the data suggest that a novel locus might be involved in these cases. Ultimately, a study including more patients negative for mutations in the

known MED loci could aid in the discovery of the molecular basis of disease in these patients due to the increased chance of identifying patients with shared variants in a candidate gene.

Conclusion

In this study, I used exome sequencing to identify mutations in novel disease loci that result in the mild MED skeletal dysplasia phenotype. In a cohort of 15 cases, exome sequencing identified the causative mutations in 9 cases. Candidate sequencing of selected genes in an additional 18 cases identified mutations in 2 patients. Dominant mutations were identified in the known MED disease loci in 6 cases including a novel *MATN3* variant which displayed incomplete penetrance in a multi-generation family, further emphasizing the variable expressivity of mutations in *MATN3*.

Novel causative mutations were identified in known skeletal dysplasia loci in the rest of the positive cases. Homozygosity for a mutation in *CANT1* was identified in two cases, revealing a new type of recessive MED that is allelic with Desbuquois dysplasia. Two cases of MED due to defects in type II collagen were found, illustrating the age-dependent changes in the spine that can complicate distinguishing MED from SEDC. A similar age-dependent diagnostic issue was revealed with the identification of *GNPTAB* mutations in a case of mucolipidosis III, which is radiographically similar to MED during childhood. These examples address part of the reason that about 15-20% of MED cases are unsolved.

In the remaining 6 negative cases, causative mutations were not identified, but candidate variants in *PTH2R* and *PRICKLE1* were identified in one case. However, because the variants were identified in a single case, it is not possible at this point to conclude that they are causative. The negative cases further emphasize the locus heterogeneity in MED and account for the remaining unexplained etiology observed in this highly genetically heterogeneous disorder. In order to determine the molecular basis of disease in these cases, increasing the number of

samples being studied and modifying the protocol by using a technique such as whole genome sequencing should improve the chances of identifying the causative mutations.

Figures

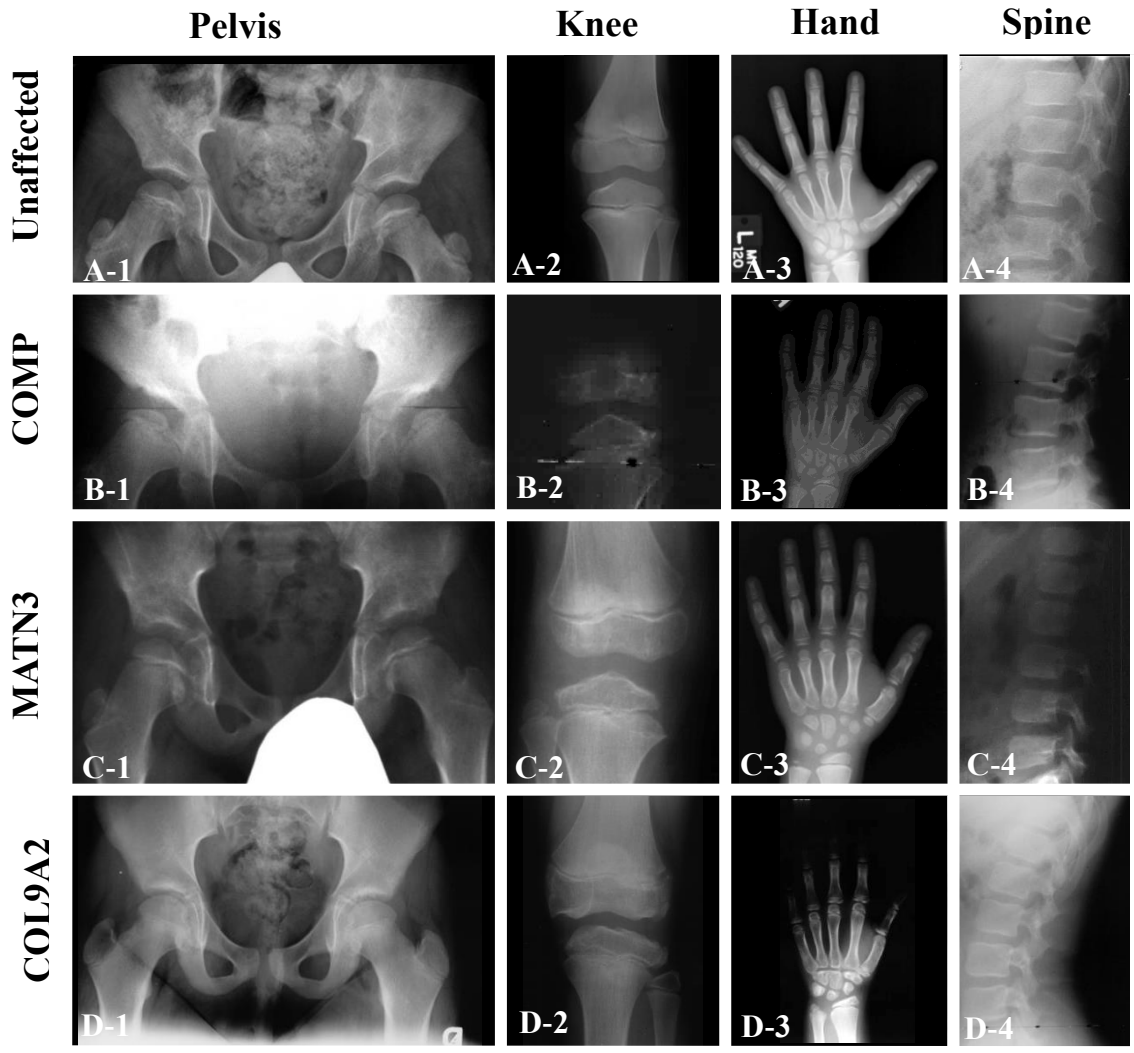

Figure 2.1: Radiographic Phenotype of MED Patients with Mutations in *COMP*, *MATN3*, and *COL9A2*. A) Adolescent films from an unaffected individual. A-1. AP pelvis at age 9. A-2. AP knee (Figure A-2 is modified from Boeyer and Ousley 2016 [62]). A-3. AP hand at age 12. A-4. Lateral spine at age 12. B) Patient R95-334A at age 13, positive for *COMP* p.Asp317Asn mutation B-1. Pelvis has small, irregularly-shaped capital femoral epiphyses with flat, under-modeled acetabulum and abnormal metaphyses of the proximal femurs. B-2. Knee epiphyses are flat and small B-3. Hand phenotype is severe with brachydactyly, irregularly-shaped carpal bones with a 2-4 year delay in ossification, and poorly ossified distal phalanges. B-4. Vertebral bodies are mildly anteriorly rounded. C) Patient R95-055A at age 8, positive for *MATN3* p.Ile109Lys mutation. C-1. AP pelvis showing that capital femoral epiphyses are irregularly-shaped with metaphyseal irregularities. Acetabular roof is relatively normal. C-2. AP knee showing that the proximal tibial knee epiphyses are small, short, and flat with abnormal metaphyses. C-3. AP hand is relatively normal with no brachydactyly but advanced carpal ossification was observed. C-4. Lateral spine showing that vertebral bodies that are mildly rounded and a little flat, but

otherwise normal. D) Patient R98-132A at age 10.5. D-1. AP pelvis with no significant abnormalities observed. D-2. AP knee showing femoral and tibial epiphyses that are hypoplastic with abnormal contouring. D-3. AP hand is relatively normal with no significant abnormalities. D-4. Lateral spine is relatively normal with no significant abnormalities.

Table 2.1: Mutations Identified in the Known MED Loci

ID	Gene	Exon	Domain	DNA Change	Protein Change	Inheritance	Previously Observed
R95-334A	COMP	9	Type III Repeats	c.949C>T	p.Asp317Asn	Sporadic	Kim et al. 2011
R98-306	COMP	14	C-Terminal Domain	c.1665G>C	p.Asn555Lys	Familial	Kennedy et al. 2005
R07-462	COMP	16	C-Terminal Domain	c.1754G>A	p.Thr585Met	Sporadic	Briggs et al. 1998
R97-290A	MATN3	2	vWFA	c.518G>T	p.Ala173Asp	Familial	Fresquet et al. 2008
R95-055A	MATN3	2	vWFA	c.326A>T	p.Ile109Lys	Familial	This Study
R98-132	COL9A2	3	COL3	c.186C>T	p.Gly63_Asp74del	Unknown	Holden et al. 1999

Table 2.2: Clinical and Radiographic Features of Patients with Mutations in the Known Loci

ID	Clinical Diagnosis	Locus	Pelvis	Knees	Vertebrae	Hand	Other Features
R95-334A	MED Fairbanks	COMP	Small CFE; Under-modeled acetabulum; irregular femoral metaphyses	Small, flat epiphyses	Mild anterior rounding of vertebral bodies; lumbar lordosis	Brachydactyly; delayed carpal ossification	Genu Varum
R98-306	MED Fairbanks	COMP	Small CFE	Small, irregularly-ossified knee epiphyses	--	Delayed carpal ossification	--
R07-462	MED Fairbanks	COMP	Dysplastic CFE	Flat knee epiphyses	Mild scoliosis	Brachydactyly of the distal phalanges	Genu Valgum
R95-055	MED Fairbanks	MATN3	Small CFE; Mild metaphyseal abnormality	Small and flat knee epiphyses with mild metaphyseal irregularities	Mildly anteriorly rounded and flat.	Advanced Carpal Ossification	--
R98-132	MED Ribbing	COL9A2	--	Hypoplastic, abnormal contouring of knee epiphyses	--	--	--

"--" indicates absence of a phenotype at this region.

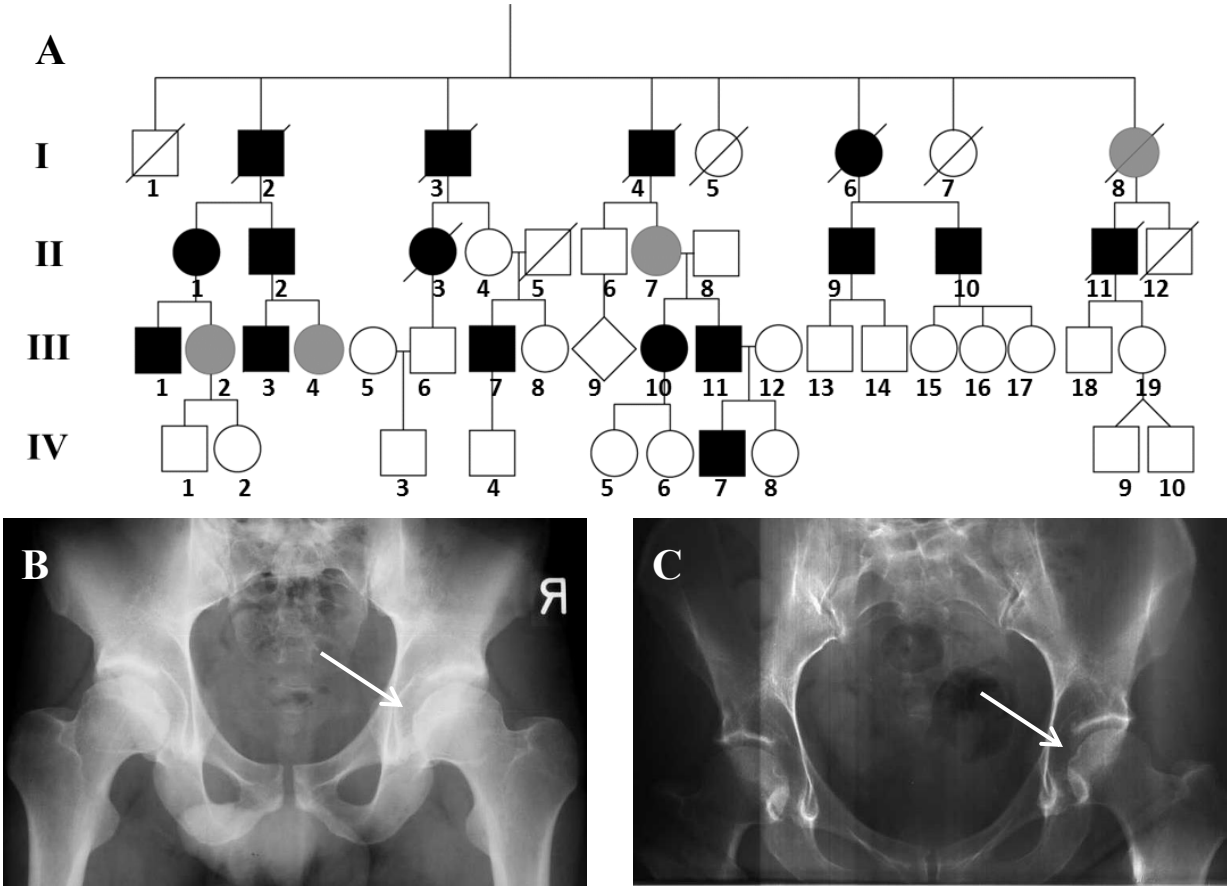

Figure 2.2: Radiographic Features of Adults in Family R95-055. A) Family R95-055 is a multi-generation family affected with autosomal dominant MED Fairbanks. The pedigree details all affected individuals (filled symbols), including incompletely penetrant family members (grey). **B)** Case R95-055B (III-7) at age 32, who is positive for the p.Ile109Lys mutation and radiographically presents with premature degenerative arthrosis of the hip joint. **C)** Case R95-055C (II-7) at age 61, who is positive for the p.Ile109Lys mutation but was clinically asymptomatic. Degenerative changes are present, but it is challenging to determine if these are age-related or due to her mutation status. **D)** Case R95-055D at age 30**,** who is positive for the p.Ile109Lys mutation but showed no signs of degenerative arthrosis.

Table 2.3: Clinical and Mutation Status of Family R95-055

R-Number	Pedigree	Clinical Features	Age of Symptoms	Adult Height	Sex	Clinical Status	Genotype
R95-055A	IV-7	Hip Pain	3	--	Male	Affected	Ile/Lys
R95-055B	III-11	Bilateral Hip Pain	Infancy	63”	Male	Affected	Ile/Lys
R95-055C	II-7	Back Pain		61”	Female	Unaffected	Ile/Lys
R95-055D	III-10	Hip Tightness/Knee Pain, genu valgum	27/12	62”	Female	Affected	Ile/Lys
R95-055E	III-7	--	--	66”	Male	Affected	Ile/Ile
R95-055F	III-8	Lower Back Pain	45	65”	Female	Unaffected	Ile/Ile
R95-055G	IV-4	--	--	71”	Male	Unaffected	Ile/Ile
R95-055H	III-4	None	--	61”	Female	Unaffected	Ile/Lys
R95-055I	III-2	None	--	--	Female	Unaffected	Ile/Lys
R95-055J	III-1	--	--	--	Male	Affected	Ile/Lys
R95-055K	II-1	Bilateral Hip Replacement	--	--	Female	Affected	Ile/Lys
R95-055L	II-2	Hip Pain, Bilateral Hip Replacement	18-20/55	--	Male	Affected	Ile/Lys
R95-055M	II-4	Shoulder/Knee Pain	68/75	62.5”	Female	Unaffected	Ile/Ile
R95-055N	II-10	Knee Problems	--	66”	Male	Affected	Ile/Lys
R95-055P	II-6	--	--	69”	Male	Unaffected	Ile/Ile
R95-055Q		--	--	--	Female	Unaffected	Ile/Ile

“--” indicates absence of a clinical data for this field.

Figure 2.3: Radiographs of Patients with *CANT1* Mutations. A) Radiographs of patient R92-280A at age 8. A-1. AP pelvis shows flat capital femoral epiphyses with flat acetabulae (left arrow) and mild Swedish key appearance of the proximal femur, as indicated by the right arrow. A-2. Lateral lumbar spine showing platyspondyly and anterior wedging of the vertebral bodies, as indicated by the arrow. A-3. AP hand shows no structural abnormality, but carpal age is advanced by 2 years. A-4. AP knee showing small epiphyses with metaphyseal flare. B) Radiographs of patient R01-152A at age 25. B-1. AP right upper leg film shows epiphyseal dysplasia of the capital femoral epiphysis (right arrow) and a mild Swedish key, as indicated by

the left arrow. B-2. Lateral spine shows degenerative arthrosis (arrow). B-3 AP hand showing degenerative arthrosis. B-4. AP knee revealing epiphyseal dysplasia.

Table 2.4: Clinical and Radiographic Features of Patients with *CANT1* Mutations

ID	Clinical Diagnosis	Pelvis	Knees	Vertebrae	Hand	Other Features
R92-280A	MED Fairbanks	Flat CFE; flat acetabular roof, short femoral neck	Mild Epiphyseal Dysplasia; metaphyseal flare	Anteriorly Wedged Vertebral Bodies; mild platyspondyly	Mild brachydactyly; Advanced Carpal Ossification	Genu varum
R92-280B	MED Fairbanks	Short femoral neck	Small, Dysplastic Epiphyses; Metaphyseal Flare	Mildly rounded vertebral bodies	Advanced Carpal Ossification	Midface Hypoplasia; Genu Varum
R01-152A	MED Fairbanks	Severe Epiphyseal Dysplasia; short femoral neck	Severe Epiphyseal Dysplasia	Degenerative Arthrosis	Degenerative Arthrosis	Epiphyseal hypoplasia of proximal humerus; Mild varus deformity.

Table 2.5: Mutations Identified in *CANT1*

ID	Gene	Exon	Domain	DNA Change	Protein Change	Inheritance	Ancestral Consanguinity
R92-280	CANT1	3	Topological	c.511T>A	p.Ile171Phe	Autosomal Recessive	Yes
R01-152	CANT1	4	Topological	c.676G>A	p.Val226Met	Autosomal Recessive	Unknown

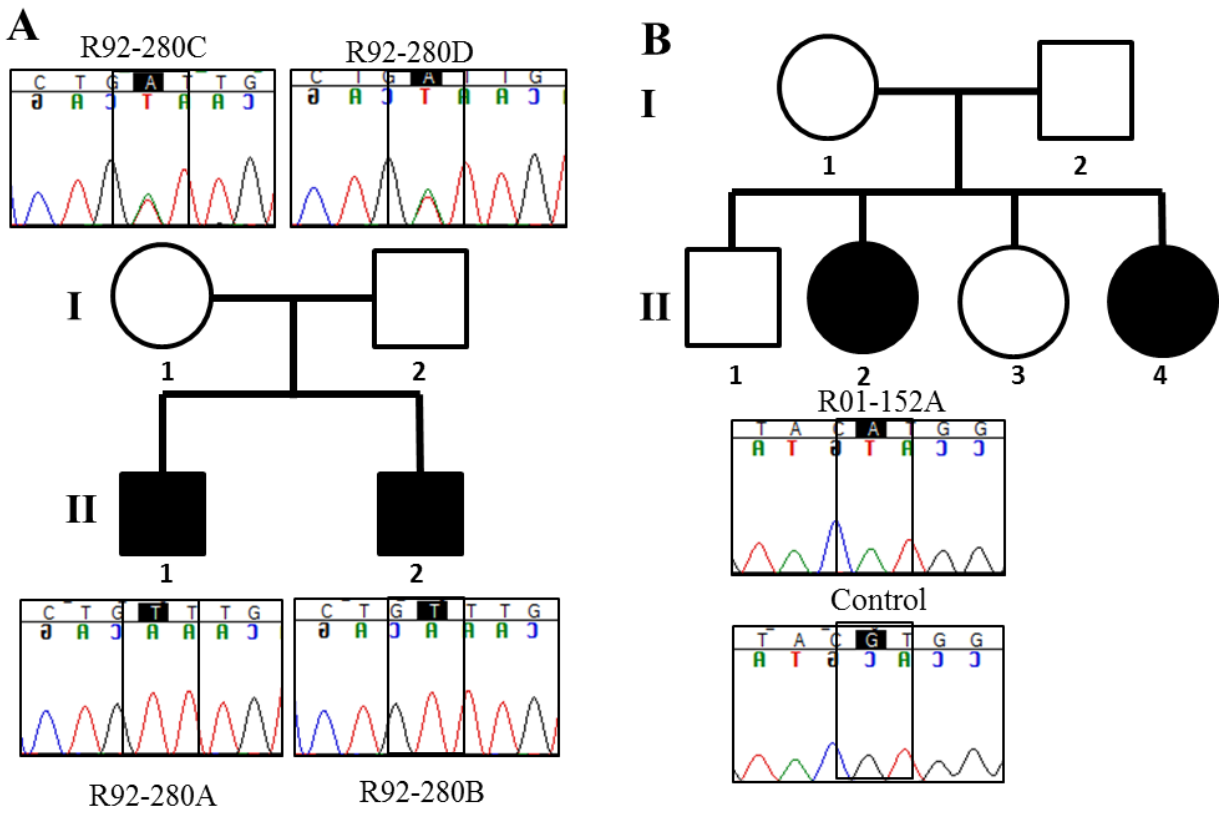

Figure 2.4: MED Families with *CANT1* Mutations. A) Family 1, R92-280, with recurrence of MED Fairbanks. Sanger sequencing confirmed that the two unaffected parents (R92-280C and R92-280D) are carriers of variant p.Ile171Phe and the affected probands (R92-280A and R92-280B) are homozygous for the variant. **B)** Family 2, R01-152, with recurrence of MED Fairbanks. Individual II-2 (R01-152A) was screened for *CANT1* variants and the p.Val226Met variant was identified in the patient and absent in the control sequence.

Table 2.6: Clinical and Radiographic Features of Disorders in the *CANT1* Phenotypic Spectrum

Feature	Type I Desbuquois	Type II Desbuquois	Desbuquois Kim Variant	R92-280	R01-152
"Swedish Key"	+	+	+	+	+
Hand Anomalies	+	_	_	_	_
Advance Carpal/Tarsal Bone Age	+	+	+	+	+
Elongated Phalanges	_	_	+	_	_
Coronal Clefting	+	+	_	_	_
Scoliosis	Severe	Severe	Severe	_	MIld
Joint Laxity/Dislocations	Multiple	Multiple	Multiple	_	Knee
Facial Anomalies	+	+	+	ND	_
Intelligence	ID	ID	Normal	ND	Normal
Club Foot	+	+	+	ND	+
Genu Varum	+	+	+	+	+

"ID" indicates Intellectual Disability. "ND" indicates No Data.

Figure 2.5: Radiographic Features of Mild Mucolipidosis III with MED-like Presentation. Radiographs of case R12-062 at age 9. The patient presented with MED with normal stature but is likely affected with mucolipidosis III. **A.** AP pelvis showing severe epiphyseal dysplasia with flat, superiorly notched capital femoral epiphyses. **B.** AP knee showing mild metaphyseal abnormalities at the distal femur. **C.** AP hand appears relatively normal. **D.** Lateral spine revealing some platyspondyly and mildly irregularly shaped vertebral bodies.

Table 2.7: Clinical and Radiographic Features of Patient with *GNPTAB* Mutations

ID	Clinical Diagnosis	Age	Pelvis	Knees	Vertebrae	Hand	Other Features
R12-062A	MED with Full Stature	9	Severe epiphyseal dysplasia; flat, superiorly notched CFE	Mild metaphyseal irregularity of distal femur.	Mildly irregularly-shaped vertebral bodies; mild platyspondyly	Mild pointing of first and fourth metacarpals.	Hip/Knee Pain, Waddling Gait

Table 2.8: Mutations Identified in *GNPTAB*

ID	Gene	Exon	Domain	DNA Change	Protein Change	Allele Inheritance
R12-062A	GNPTAB	9	--	c.1021_1025insTGCA	p.Pro341CysfsX25	Maternal
	GNPTAB	13	Luminal	c.1778T>A	p.Asn593Ile	Paternal

Figure 2.6: Radiographs of Patients with *COL2A1* Mutations. A) Radiographs of patient R89-205 at ages 5.5-6. A-1. AP pelvis showing small capital femoral epiphyses with bilateral avascular necrosis as indicated by the arrow on the right. A-2. AP knee showing small, irregularly shaped knee epiphyses as indicated by the arrow. A-3. AP hand showing slightly small carpal bones consistent with delayed ossification. A-4. Lateral spine showing slightly rounded vertebral bodies. B) Radiographs of patient R11-324 at ages 3-4. B-1. AP hip with virtually absent ossification of the capital femoral epiphyses. B-2. AP knee showing hypoplastic epiphyses. B-3. AP hand showing hypoplastic distal epiphyses of the radius and ulna and delayed carpal ossification. B-4. Lateral spine with vertebral body ossification appropriate for age.

Table 2.9: Clinical and Radiographic Features of Patient with *COL2A1* Mutations

ID	Clinical Diagnosis	Age	Pelvis	Knees	Vertebrae	Hand	Other Features
R89-205	MED Fairbanks	5	Bilateral avascular necrosis; small CFE	Small, irregularly-shaped epiphyses	Rounded lumbar vertebral bodies	Slightly small carpals	Bilateral Hearing Loss
R11-324A	MED Unclassified	3	Absent ossification of CFE	Hypoplastic epiphyses	--	Hypoplastic wrist epiphyses	--

Table 2.10: Mutations Identified in *COL2A1*

ID	Gene	Exon	Domain	DNA Change	Protein Change	Inheritance
R89-205	COL2A1	40	Triple Helical	c.2662C>T	p.Gly888Ser	Autosomal Dominant
R11-324A	COL2A1	42	Triple Helical	c.2833G>A	p.Gly945Ser	Autosomal Dominant

Supplementary Tables

Supplementary Table 2.1: Primers for Known MED Disease Genes

Gene	Exon	Forward Primer	Reverse Primer
COMP	9	5' ACACTGACCTAGACGGCTTCC 3'	5' TTTTTAGTAGAGGAGGGGTTTCAC 3'
COMP	14	5' CGGGCCCTGACTTTAGCC 3'	5' TCATTGTCTGCACGATCTCC 3'
COMP	16	5' GGCAGGTTTGGGTTCTGG 3'	5' GGGGCTCTAAGGGCTGTAAA 3'
COL9A2	3 & 4	5' TAGGGGACCTGGACAGAAGA 3'	5' GATCAGTGAAGATGCCAGAGC 3'
MATN3	2	5' GATGTTGGGGTCAGGAGATG 3'	5' ATCTTGAGGGACGCCATGT 3'

Supplementary Table 2.2: Primers for MED Candidate Genes

Gene	Exon	Forward Primer	Reverse Primer
CANT1	3	5' ATCGCAGTTATCGCAGACCT 3'	5' TACCATGTGCCTGTGTTTGC 3'
COL2A1	40	5' AGCTGCATCTTCGAAAACCTC 3'	5' GGCATCCCAGAACACCCC 3'
GNPTAB	9	5' GGCAGAAGGAAAGGACAAAG 3'	5' GGGAAGGCAATGAAGAGCTA 3'
GNPTAB	13	5' CACAAGGACGACATGCAAAT 3'	5' CGTAACCCTTCTGGGCTGTA 3'
PRICKLE1	5	5' GGAAAGCCTGAGAATCCTGTC 3'	5' TGCACACAGAACAAAATCCAG 3'
PTH2R	8	5' TCATGTCTATTTTTATCTCTGAACAGC 3'	5' TCATGTCTATTTTTATCTCTGAACAGC 3'

Supplementary Table 2.3: MED Patients Included in Candidate Mutation Screens

Patient ID	Genes Tested
R81-123A	*PTH2R*, *PRICKLE1*, *CANT1*
R83-023	*PTH2R*, *PRICKLE1*
R97-116	*PTH2R*, *PRICKLE1*
R90-222A	*PTH2R*, *PRICKLE1*
R90-222B	*PTH2R*, *PRICKLE1*
R90-222C	*PTH2R*, *PRICKLE1*
R97-214A	*PTH2R*, *PRICKLE1*
R97-214C	*PTH2R*, *PRICKLE1*
R86-008A	*PTH2R*, *PRICKLE1*
R97-015A	*PTH2R*, *PRICKLE1*
R97-108	*PTH2R*, *PRICKLE1*
R94-307A	*PTH2R*, *PRICKLE1*
R95-111A	*PTH2R*, *PRICKLE1*
R96-056A	*PTH2R*, *PRICKLE1*
R96-056B	*PTH2R*, *PRICKLE1*
R02-373	*PTH2R*, *PRICKLE1*
R93-062	*PTH2R*, *PRICKLE1*
R00-151A	*PTH2R*, *PRICKLE1*
R96-282A	*PTH2R*, *PRICKLE1*
R01-096A	*PTH2R*, *PRICKLE1*
R01-096D	*PTH2R*, *PRICKLE1*
R94-131	*CANT1*

Supplementary Table 2.4: Primers Used in Candidate Gene Mutation Screens

Gene	Exon	Forward Primer	Reverse Primer
CANT1	3-1	5' CTGGAAAAGTCAGCCTCCAG 3'	5' CATGGTCTTTGTCCCATTCC 3'
CANT1	3-2	5' ATCGCAGTTATCGCAGACCT 3'	5' TACCATGTGCCTGTGTTTGC 3'
CANT1	4	5' AGTCAGGTGCGGGGTCTAA 3'	5' AAACGGTTTTGGAGGCAAAT 3'
CANT1	5	5' AGCCCCTTGCCTGCTACT 3'	5' CCAGGCACAGTTCCAAAAAG 3'
PRICKLE1	2	5' ATAAAAGCTCTGGGTCGGGG 3'	5' AGGACTGAGGAGGGTGGTAT 3'
PRICKLE1	3	5' GGCTCAGCTGGTCTTCTCAT 3'	5' GGAAAGCTGTATTCTCTGGCC 3'
PRICKLE1	4	5' GTGACACAGGCGAGCTAAAC 3'	5' TTCTGGAGGCTTTCAGGACC 3'
PRICKLE1	5	5' GGAAAGCCTGAGAATCCTGTC 3'	5' TGCACACAGAACAAAATCCAG 3'
PRICKLE1	6	5' TCAGCACTGTCAATTTATGCTCT 3'	5' ACGTCACAGAACACAACTACT 3'
PRICKLE1	7-1	5' TGTCACCCACACAGCTCC 3'	5' ATCAGCCCATTCTTCAGGGT 3'
PRICKLE1	7-2	5' CCGGTCAGCAGATCAGTGTA 3'	5' CCTCAAATGATCTGCCCACC 3'
PRICKLE1	8-1	5' ACATGTTGGCTTTCCCTATGG 3'	5' GGATCTCCCGGGCACTTTTA 3'
PRICKLE1	8-2	5' TGACATTGAAATCCGGCAGC 3'	5' CATTTACATGGGCAAAGAAAGCA 3'
PTH2R	1	5' GAAGACAAGACCAACCTCGC 3'	5' CTCCACTAATTGCCTGCCAG 3'
PTH2R	2	5' ACCTTACACATTGATGGATTTTGAA 3'	5' CATGGAAATGTGGATTGACTGAT 3'
PTH2R	3-4	5' TTTTGCTACAGACAATGACCTAAAA 3'	5' TTATGATCCTTGTGTCGTGGAA 3'
PTH2R	5	5' GGGGCACAAATGAACTTGGT 3'	5' TGCATTTGAGGAAAACATTTGGA 3'
PTH2R	6	5' CAGATTTTGGAATTTGTGTGGAGT 3'	5' TGAAAGGACAGAATTGAGGGAGA 3'
PTH2R	7	5' TGTTTTGGCCTCTCAACAGT 3'	5' TCCTCTCAAGAATCTGGCCT 3'
PTH2R	8	5' TCATGTCTATTTTTATCTCTGAACAGC 3'	5' CCTTGTGGCATCCCTAAAAA 3'
PTH2R	9	5' CACTGGCTTGGGTGTTTTAAGA 3'	5' GTCCCAGACTCTCCCAATAGA 3'
PTH2R	10	5' GGTTCCCCTGTTCACATTTATGA 3'	5' GAATTGCTTGAACCCGGGAG 3'
PTH2R	11	5' GGAGGTCGACACTGCAGTAA 3'	5' TATTGACCTTTCTGCACCCC 3'
PTH2R	12	5' GCTGACACCAAGGAAAGACG 3'	5' GCTTCCTTCTCCTCACCCAT 3'
PTH2R	13	5' AGATAAAGTCCCTGGCACGT 3'	5' GTCGTTAGTATTTACAGGAGCCA 3'

References

1. Unger S, Bonafé L, Superti-Furga A: **Multiple epiphyseal dysplasia: clinical and radiographic features, differential diagnosis and molecular basis**. *Best Practice & Research Clinical Rheumatology* 2008, **22**(1):19-32.

2. Lachman RS, Krakow D, Cohn DH, Rimoin DL: **MED, COMP, multilayered and NEIN: an overview of multiple epiphyseal dysplasia**. *Pediatric Radiology* 2005, **35**(2):116-123.

3. Cohn DH, Briggs MD, King LM, Rimoin DL, Wilcox WR, Lachman RS, Knowlton RG: **Mutations in the Cartilage Oligomeric Matrix Protein (COMP) Gene in Pseudoachondroplasia and Multiple Epiphyseal Dysplasiaa**. *Annals of the New York Academy of Sciences* 1996, **785**(1):188-194.

4. Briggs MD, Hoffman SMG, King LM, Olsen AS, Mohrenweiser H, Leroy JG, Mortier GR, Rimoin DL, Lachman RS, Gaines ES *et al*: **Pseudoachondroplasia and multiple epiphyseal dysplasia due to mutations in the cartilage oligomeric matrix protein gene**. *Nat Genet* 1995, **10**(3):330-336.

5. Chapman KL, Mortier GR, Chapman K, Loughlin J, Grant ME, Briggs MD: **Mutations in the region encoding the von Willebrand factor A domain of matrilin-3 are associated with multiple epiphyseal dysplasia**. *Nat Genet* 2001, **28**(4):393-396.

6. Czarny-Ratajczak M, Lohiniva J, Rogala P, Kozlowski K, Perälä M, Carter L, Spector TD, Kolodziej L, Seppänen U, Glazar R *et al*: **A Mutation in COL9A1 Causes Multiple Epiphyseal Dysplasia: Further Evidence for Locus Heterogeneity**. *The American Journal of Human Genetics* 2001, **69**(5):969-980.

7. Spayde EC, Joshi AP, Wilcox WR, Briggs M, Cohn DH, Olsen BR: **Exon skipping mutation in the COL9A2 gene in a family with multiple epiphyseal dysplasia**. *Matrix Biology* 2000, **19**(2):121-128.

8. P Paassilta JL, S Annunen, J Bonaventure, M Le Merrer, L Pai, and L Ala-Kokko: **COL9A3: A third locus for multiple epiphyseal dysplasia.** *American Journal of Human Genetics* 1999, **64**(4):9.

9. Zaucke F GS: **Genetic mouse models for the functional analysis of the perifibrillar components collagen IX, COMP and matrilin-3: Implications for growth cartilage differentiation and endochondral ossification.** *Histology and Histopathology* 2009, **24**(8):13.

10. Superti-Furga A, Neumann L, Riebel T, Eich G, Steinmann B, Spranger J, Kunze J: **Recessively inherited multiple epiphyseal dysplasia with normal stature, club foot, and double layered patella caused by a DTDST mutation**. *Journal of Medical Genetics* 1999, **36**(8):621-624.

11. Haila S, Hästbacka J, Böhling T, Karjalainen–Lindsberg M-L, Kere J, Saarialho–Kere U: **SLC26A2 (Diastrophic Dysplasia Sulfate Transporter) is Expressed in Developing**

and Mature Cartilage But Also in Other Tissues and Cell Types. *Journal of Histochemistry & Cytochemistry* 2001, **49**(8):973-982.

12. Satoh H, Susaki M, Shukunami C, Iyama K-i, Negoro T, Hiraki Y: **Functional Analysis of Diastrophic Dysplasia Sulfate Transporter**. *Journal of Biological Chemistry* 1998, **273**(20):12307-12315.

13. Unger LS, Briggs DM, Holden P, Zabel B, Ala-Kokko L, Paassilta P, Lohiniva J, Rimoin LD, Lachman SR, Cohn HD: **Multiple epiphyseal dysplasia: radiographic abnormalities correlated with genotype**. *Pediatric Radiology* 2001, **31**(1):10-18.

14. Mortier GR, Chapman K, Leroy JL, Briggs MD: **Clinical and radiographic features of multiple epiphyseal dysplasia not linked to the COMP or type IX collagen genes**. *European Journal of Human Genetics* 2001, **9**(8):606-612.

15. Mäkitie O, Mortier GR, Czarny-Ratajczak M, Wright MJ, Suri M, Rogala P, Freund M, Jackson GC, Jakkula E, Ala-Kokko L *et al*: **Clinical and radiographic findings in multiple epiphyseal dysplasia caused by MATN3 mutations: Description of 12 patients**. *American Journal of Medical Genetics Part A* 2004, **125A**(3):278-284.

16. Kim O-H, Park H, Seong M-W, Cho T-J, Nishimura G, Superti-Furga A, Unger S, Ikegawa S, Choi IH, Song H-R *et al*: **Revisit of multiple epiphyseal dysplasia: Ethnic difference in genotypes and comparison of radiographic features linked to the COMP and MATN3 genes**. *American Journal of Medical Genetics Part A* 2011, **155**(11):2669-2680.

17. Jackson GC, Mittaz-Crettol L, Taylor JA, Mortier GR, Spranger J, Zabel B, Le Merrer M, Cormier-Daire V, Hall CM, Offiah A *et al*: **Pseudoachondroplasia and multiple epiphyseal dysplasia: A 7-year comprehensive analysis of the known disease genes identify novel and recurrent mutations and provides an accurate assessment of their relative contribution**. *Human Mutation* 2012, **33**(1):144-157.

18. Blumbach K, Niehoff A, Paulsson M, Zaucke F: **Ablation of collagen IX and COMP disrupts epiphyseal cartilage architecture**. *Matrix Biology* 2008, **27**(4):306-318.

19. Blumbach K, Bastiaansen-Jenniskens YM, DeGroot J, Paulsson M, van Osch GJVM, Zaucke F: **Combined role of type IX collagen and cartilage oligomeric matrix protein in cartilage matrix assembly: Cartilage oligomeric matrix protein counteracts type IX collagen–induced limitation of cartilage collagen fibril growth in mouse chondrocyte cultures**. *Arthritis & Rheumatism* 2009, **60**(12):3676-3685.

20. Cotterill SL, Jackson GC, Leighton MP, Wagener R, Mäkitie O, Cole WG, Briggs MD: **Multiple epiphyseal dysplasia mutations in MATN3 cause misfolding of the A-domain and prevent secretion of mutant matrilin-3**. *Human Mutation* 2005, **26**(6):557-565.

21. Fresquet M, Jackson GC, Loughlin J, Briggs MD: **Novel mutations in exon 2 of MATN3 affect residues within the α–helices of the A-domain and can result in the intracellular retention of mutant matrilin-3**. *Human Mutation* 2008, **29**(2):330-330.

22. Chen T-LL, Posey KL, Hecht JT, Vertel BM: **COMP mutations: Domain-dependent relationship between abnormal chondrocyte trafficking and clinical PSACH and MED phenotypes**. *Journal of Cellular Biochemistry* 2008, **103**(3):778-787.

23. Nundlall S, Rajpar M, Bell P, Clowes C, Zeeff L, Gardner B, Thornton D, Boot-Handford R, Briggs M: **An unfolded protein response is the initial cellular response to the expression of mutant matrilin-3 in a mouse model of multiple epiphyseal dysplasia**. *Cell Stress and Chaperones* 2010, **15**(6):835-849.

24. Piróg-Garcia KA, Meadows RS, Knowles L, Heinegård D, Thornton DJ, Kadler KE, Boot-Handford RP, Briggs MD: **Reduced cell proliferation and increased apoptosis are significant pathological mechanisms in a murine model of mild pseudoachondroplasia resulting from a mutation in the C-terminal domain of COMP**. *Human Molecular Genetics* 2007, **16**(17):2072-2088.

25. Hastbacka J, Superti-Furga A, Wilcox WR, Rimoin DL, Cohn DH, Lander ES: **Sulfate Transport in Chondrodysplasia,a**. *Annals of the New York Academy of Sciences* 1996, **785**(1):131-136.

26. Rossi A, Kaitila I, Wilcox WR, Rimoin DL, Steinmann B, Cetta G, Superti-Furga A: **Proteoglycan sulfation in cartilage and cell cultures from patients with sulfate transporter chondrodysplasias: Relationship to clinical severity and indications on the role of intracellular sulfate production**. *Matrix Biology* 1998, **17**(5):361-369.

27. Li H: **Exploring single-sample SNP and INDEL calling with whole-genome de novo assembly**. *Bioinformatics* 2012, **28**(14):1838-1844.

28. **http://bio-bwa.sourceforge.net/bwa.shtml#12**

29. **http://picard.sourceforge.net**

30. McKenna A, Hanna M, Banks E, Sivachenko A, Cibulskis K, Kernytsky A, Garimella K, Altshuler D, Gabriel S, Daly M *et al*: **The Genome Analysis Toolkit: A MapReduce framework for analyzing next-generation DNA sequencing data**. *Genome Research* 2010, **20**(9):1297-1303.

31. Ng SB, Turner EH, Robertson PD, Flygare SD, Bigham AW, Lee C, Shaffer T, Wong M, Bhattacharjee A, Eichler EE *et al*: **Targeted capture and massively parallel sequencing of 12 human exomes**. *Nature* 2009, **461**(7261):272-276.

32. Koressaar T, Remm M: **Enhancements and modifications of primer design program Primer3**. *Bioinformatics* 2007, **23**(10):1289-1291.

33. Untergasser A, Cutcutache I, Koressaar T, Ye J, Faircloth BC, Remm M, Rozen SG: **Primer3—new capabilities and interfaces**. *Nucleic Acids Research* 2012, **40**(15):e115.

34. Kent WJ, Sugnet CW, Furey TS, Roskin KM, Pringle TH, Zahler AM, Haussler D: **The human genome browser at UCSC**. *Genome Res* 2002, **12**.

35. Kennedy J, Jackson GC, Barker FS, Nundlall S, Bella J, Wright MJ, Mortier GR, Neas K, Thompson E, Elles R *et al*: **Novel and recurrent mutations in the C-terminal domain of COMP cluster in two distinct regions and result in a spectrum of phenotypes within the pseudoachondroplasia – multiple epiphyseal dysplasia disease group**. *Human Mutation* 2005, **25**(6):593-594.

36. Briggs MD, Mortier GR, Cole WG, King LM, Golik SS, Bonaventure J, Nuytinck L, De Paepe A, Leroy JG, Biesecker L *et al*: **Diverse Mutations in the Gene for Cartilage Oligomeric Matrix Protein in the Pseudoachondroplasia–Multiple Epiphyseal Dysplasia Disease Spectrum**. *The American Journal of Human Genetics* 1998, **62**(2):311-319.

37. Yap P, Savarirayan R: **Emerging targeted drug therapies in skeletal dysplasias**. *American Journal of Medical Genetics Part A* 2016:n/a-n/a.

38. Adzhubei IA, Schmidt S, Peshkin L, Ramensky VE, Gerasimova A, Bork P, Kondrashov AS, Sunyaev SR: **A method and server for predicting damaging missense mutations**. *Nat Meth* 2010, **7**(4):248-249.

39. Kircher M, Witten DM, Jain P, O'Roak BJ, Cooper GM, Shendure J: **A general framework for estimating the relative pathogenicity of human genetic variants**. *Nat Genet* 2014, **46**(3):310-315.

40. Exome Variant Server NGESPE, Seattle, WA (URL: http://evs.gs.washington.edu/EVS/) [(August, 2015) accessed].

41. Lek M, Karczewski K, Minikel E, Samocha K, Banks E, Fennell T, O'Donnell-Luria A, Ware J, Hill A, Cummings B *et al*: **Analysis of protein-coding genetic variation in 60,706 humans**. *bioRxiv* 2015.

42. Dai J, Liu J, Deng Y, Smith TM, Lu M: **Structure and Protein Design of a Human Platelet Function Inhibitor**. *Cell*, **117**(3):413.

43. Furuichi T, Dai J, Cho T-J, Sakazume S, Ikema M, Matsui Y, Baynam G, Nagai T, Miyake N, Matsumoto N *et al*: **CANT1 mutation is also responsible for Desbuquois dysplasia, type 2 and Kim variant**. *Journal of Medical Genetics* 2011, **48**(1):32-37.

44. Panda D, Goltzman D, Jüppner H, Karaplis AC: **TIP39/parathyroid hormone type 2 receptor signaling is a potent inhibitor of chondrocyte proliferation and differentiation**. *American Journal of Physiology - Endocrinology and Metabolism* 2009, **297**(5):E1125-E1136.

45. Panda DK, Goltzman D, Karaplis AC: **Defective postnatal endochondral bone development by chondrocyte-specific targeted expression of parathyroid hormone type 2 receptor**. *American Journal of Physiology - Endocrinology and Metabolism* 2012, **303**(12):E1489-E1501.

46. Yang T, Bassuk AG, Fritzsch B: **Prickle1 stunts limb growth through alteration of cell polarity and gene expression**. *Developmental Dynamics* 2013, **242**(11):1293-1306.

47. Briggs MD WM, Mortier GR. Multiple Epiphyseal Dysplasia, Dominant. 2003 Jan 8 [Updated 2011 Feb 1]. In: Pagon RA, Bird TD, Dolan CR, et al., editors. GeneReviews™ [Internet]. Seattle (WA): University of Washington, Seattle; 1993-. . In.

48. Huber C, Oulès B, Bertoli M, Chami M, Fradin M, Alanay Y, Al-Gazali LI, Ausems MGEM, Bitoun P, Cavalcanti DP *et al*: **Identification of CANT1 Mutations in Desbuquois Dysplasia**. *The American Journal of Human Genetics* 2009, **85**(5):706-710.

49. Faivre L, Cormier-Daire V, Eliott AM, Field F, Munnich A, Maroteaux P, Merrer ML, Lachman R: **Desbuquois dysplasia, a reevaluation with abnormal and "normal" hands: Radiographic manifestations**. *American Journal of Medical Genetics Part A* 2004, **124A**(1):48-53.

50. Kim O-H, Nishimura G, Song H-R, Matsui Y, Sakazume S, Yamada M, Narumi Y, Alanay Y, Unger S, Cho T-J *et al*: **A variant of Desbuquois dysplasia characterized by advanced carpal bone age, short metacarpals, and elongated phalanges: Report of seven cases**. *American Journal of Medical Genetics Part A* 2010, **152A**(4):875-885.

51. Dai J, Kim O-H, Cho T-J, Miyake N, Song H-R, Karasugi T, Sakazume S, Ikema M, Matsui Y, Nagai T *et al*: **A founder mutation of CANT1 common in Korean and Japanese Desbuquois dysplasia**. *J Hum Genet* 2011, **56**(5):398-400.

52. Nizon M, Huber C, De Leonardis F, Merrina R, Forlino A, Fradin M, Tuysuz B, Abu-Libdeh BY, Alanay Y, Albrecht B *et al*: **Further delineation of CANT1 phenotypic spectrum and demonstration of its role in proteoglycan synthesis**. *Human Mutation* 2012, **33**(8):1261-1266.

53. David-Vizcarra G, Briody J, Ault J, Fietz M, Fletcher J, Savarirayan R, Wilson M, McGill J, Edwards M, Munns C *et al*: **The natural history and osteodystrophy of mucolipidosis types II and III**. *Journal of Paediatrics and Child Health* 2010, **46**(6):316-322.

54. Leroy JG CS, Friez MJ. Mucolipidosis III Alpha/Beta. 2008 Aug 26 [Updated 2012 May 10]. In: Pagon RA, Adam MP, Ardinger HH, et al., editors. GeneReviews® [Internet]. Seattle (WA): University of Washington, Seattle; 1993-2016. Available from: http://www.ncbi.nlm.nih.gov/books/NBK1875/.

55. Cathey SS, Leroy JG, Wood T, Eaves K, Simensen RJ, Kudo M, Stevenson RE, Friez MJ: **Phenotype and genotype in mucolipidoses II and III alpha/beta: a study of 61 probands**. *Journal of Medical Genetics* 2010, **47**(1):38-48.

56. Sperb-Ludwig F, Alegra T, Velho RV, Ludwig N, Kim CA, Kok F, Kitajima JP, van Meel E, Kornfeld S, Burin MG *et al*: **Exome sequencing for mucolipidosis III: Detection of a novel GNPTAB gene mutation in a patient with a very mild phenotype**. *Molecular Genetics and Metabolism Reports* 2015, **2**:34-37.

57. Velho RV, De Pace R, Klünder S, Sperb-Ludwig F, Lourenço CM, Schwartz IVD, Braulke T, Pohl S: **Analyses of disease-related GNPTAB mutations define a novel**

GlcNAc-1-phosphotransferase interaction domain and an alternative site-1 protease cleavage site. *Human Molecular Genetics* 2015, **24**(12):3497-3505.

58. Anderson IJ, Goldberg RB, Marion RW, Upholt WB, Tsipouras P: **Spondyloepiphyseal dysplasia congenita: genetic linkage to type II collagen (COL2AI)**. *American Journal of Human Genetics* 1990, **46**(5):896-901.

59. Kannu P, Irving M, Aftimos S, Savarirayan R: **Two Novel COL2A1 Mutations Associated with a Legg-Calvé-Perthes Disease-like Presentation**. *Clinical Orthopaedics and Related Research®* 2011, **469**(6):1785-1790.

60. Terhal PA, Nievelstein RJAJ, Verver EJJ, Topsakal V, van Dommelen P, Hoornaert K, Le Merrer M, Zankl A, Simon MEH, Smithson SF *et al*: **A study of the clinical and radiological features in a cohort of 93 patients with a COL2A1 mutation causing spondyloepiphyseal dysplasia congenita or a related phenotype**. *American Journal of Medical Genetics Part A* 2015, **167**(3):461-475.

61. **http://ctgt.net/panel/multiple-epiphyseal-dysplasia-med-ngs-panel#related-tests**

62. Boeyer ME, Ousley SD: **Skeletal assessment and secular changes in knee development: a radiographic approach**. *American Journal of Physical Anthropology* 2016:n/a-n/a.

CHAPTER THREE

The Alpha-2 Chain of Type IX Collagen is Essential for Trimerization

Abstract

Type IX collagen is a heterotrimeric structural protein of the cartilage extracellular matrix (ECM) that is composed of three procollagen chains, α1(IX), α2(IX) and α3(IX), which are encoded by the genes *COL9A1*, *COL9A2*, and *COL9A3*, respectively. Dominant splice site mutations in each of these genes result in the mild chondrodysplasia Multiple Epiphyseal Dysplasia (MED), and recessive loss-of-function mutations in these genes result in Stickler Syndrome (STL), a mild skeletal dysplasia with craniofacial, ocular, and auditory abnormalities. Biochemical studies in the *Col9a1* $^{-/-}$ mouse demonstrated that the loss of α1(IX) results in a functional knockout of type IX collagen and is therefore required for trimerization *in vivo*. Previous *in vitro* biochemical studies assessing the trimerization of recombinant type IX collagen have also shown that the α1(IX) chain is essential to trimerization, but it is unclear whether this is the case for the α2(IX) and α3(IX) chains. To answer this question for the α2(IX) chain, I generated a *Col9a2* $^{-/-}$ mouse. I found that the absence of α2(IX) also produced a functional knockout of type IX collagen. Additional phenotypic characterization of the knockout mice demonstrated that the loss of type IX collagen results in mild short stature, craniofacial defects, short-limbs, and hearing loss. These phenotypes overlap with the clinical features of STL, confirming that the mechanism of *COL9A2* STL is the result of the loss of type IX collagen. Additional analysis of the growth plate demonstrated altered growth plate architecture with disorganized proliferation of growth plate chondrocytes. Unexpectedly, ultrastructural analysis identified endoplasmic reticulum distension in reserve and proliferating chondrocytes, suggesting that an unfolded protein response may contribute to the observed phenotype.

Introduction

Type IX collagen is a heterotrimeric structural protein of the cartilage extracellular matrix (ECM) that is comprised of three procollagen chains, α1(IX), α2(IX) and α3(IX), which are encoded by the genes *COL9A1*, *COL9A2*, and *COL9A3*, respectively[1]. As a bridging molecule, type IX collagen maintains the long-term integrity of hyaline cartilage through two distinct functions: regulating the diameter of the heterotypic cartilage collagen fibril, which is composed of type II and type IX collagens, and mediating interactions between the fibrillar and extrafibrillar matrix[2-4].

Type IX collagen is a FACIT (Fibril-Associated Collagens with Interrupted Triple Helices) collagen, with a protein structure of three collagenous domains (COL 1-3) flanked by four non-collagenous domains (NC1-4)[3, 5, 6]. Each domain serves a specific function in ECM maintenance. The COL1 and COL2 domains are responsible for crosslinking with collagen fibrils at conserved lysine residues to maintain the diameter of collagen fibrils[2, 7-9]. The NC3 domain functions as a hinge for the protein, allowing for interactions between the COL3 and NC4 type IX collagen domains and non-collagenous ECM proteins, including the proteoglycans COMP and Matrilin-3 [3, 10-12]. The remaining domains, NC1, COL1, and NC2, have integral roles in directing type IX collagen trimerization [13-16].

Both dominant and recessive mutations in the type IX procollagen genes are associated with mild skeletal dysplasias. Dominant splice site mutations in *COL9A1[17]*, *COL9A2[18]*, and *COL9A3[19]* that result in exon skipping leading to in-frame deletions within the COL3 domain result in Multiple Epiphyseal Dysplasia (MED)[20, 21]. MED is characterized by mild short stature, joint pain, and early onset osteoarthropathy[22], and the mutations likely exert their effect in part by disruption of interactions between type IX collagen and other matrix proteins via the secretion of mutant protein into the matrix [21]. Recessive loss-of-function mutations in any

of the three type IX procollagen genes result in Stickler syndrome (STL) [23-25], which is characterized by mild short stature, craniofacial defects, myopia, and sensorineural hearing loss[26]. Based on studies in the mouse, for the α1(IX) chain the STL phenotype is due to a functional knockout of type IX collagen[23]. Additional case-control studies have also identified associations with the *COL9A2* Gln326Trp and *COL9A3* Arg103Trp missense substitutions and Intervertebral Disc Disease (IVDD), with these alleles contributing to the development and severity of IVDD by an as yet unknown mechanism [27-30].

Previously, several studies have been conducted to determine the stoichiometry of α1(IX), α2(IX), and α3(IX) that is required for type IX collagen trimerization. *In vitro* expression of various combinations of α1(IX), α2(IX) and α3(IX) demonstrated that α1(IX) can self-trimerize to produce intact collagen molecules, suggesting that absence of either of the other two chains could still lead to synthesis of type IX collagen trimers[13, 15, 31]. However, the results have been inconsistent for α2(IX) and α3(IX). In Jäälinoja et al. 2008, full-length α2(IX) and α3(IX) were shown to be able to homotrimerize[15], but this finding was not replicated in the Pihlajaama et al. 1999 study[31]. In Labourdette et al. 1993, peptides from α2(IX) containing just the NC1 and COL1 domain were shown to homotrimerize [13], as were peptide fragments containing just the NC4-COL2 domains in Jäälinoja et al. 2008[15] but this did not occur with α3(IX) peptides. This suggests that α1(IX) is essential to producing a functional protein, but this may not be true for α2(IX) and α3(IX). The α1(IX) biochemical data were consistent with *in vivo* biochemical studies of the *Col9a1* $^{-/-}$ mouse, demonstrating that the loss of α1(IX) results in a functional knockout of type IX collagen[32]. The loss of type IX collagen resulted in dysregulated chondrocyte proliferation and differentiation in the endochondral growth plate, leading to shortened and thickened long bones[33]. These mice also exhibited impaired auditory

function [34, 35] and early-onset osteoarthritis of the knee joints and intervertebral discs [36, 37]. Collectively, these traits demonstrated that the *Col9a1* $^{-/-}$ mouse phenocopies STL, and this phenotype resulted from the total loss of type IX collagen[32].

While it has been established that α1(IX) is essential to trimerization, it has been assumed that a similar phenomenon occurs with α2(IX) and α3(IX), an inference supported by the fact that loss of function mutations in *COL9A2* or *COL9A3* each result in STL in single cases, but no *in vivo* biochemical studies have been completed to determine the validity of this assumption[24, 25]. To determine whether α2(IX) is essential to the synthesis of functional type IX collagen, I constructed an *in vivo* knockout mouse model for *Col9a2* to assess the biochemical and phenotypic consequences of the loss of this subunit. This study resolves the different findings in the literature, demonstrating that α2(IX) is also essential to type IX collagen biosynthesis and showing that the *Col9a2* $^{-/-}$ mouse has a phenotype similar to Stickler syndrome.

Materials and Methods

Generation of Transgenic Mice

Transgenic mice were obtained from MRC Harwell through the International Mouse Phenotyping Consortium[38-40]. The targeting construct for this allele was a knockout first conditional ready allele with the ability to revert back to wild-type or to be used as a conditional knockout allele. This allele is labeled as *tm1a* (Figure 3.1A). The transgenic line was generated on a C57Bl/6NTac background. Mice heterozygous for the *Col9a2* null allele were crossed to the CMV-*Cre* line to create a global floxed allele lacking the neo selection cassette. This allele is labeled as *tm1b* (Figure 3.1B). The *tm1b* mice were then bred to homozygosity and used for the subsequent experiments.

Mouse Genotyping

Biopsies were collected from either the ear or tail of postnatal mice and DNA was isolated using the KAPA Mouse Genotyping Kit (KK7352). Genotypes for the *Col9a2 tm1a* and *tm1b* null alleles were obtained using the following primers: *Tm1a* Allele- Col9a2-5arm-WTF-5'GGTACTCAGTGAACTGGGAGCTA 3'; Col9a2-Crit-WTR-5' CTGGGGACCATACCTTCCTC 3'; 5mut-R1- 5'GAACTTCGGAATAGGAACTTCG 3'; and *Tm1b* Allele- LacZ-F-5' CCAGTTGGTCTGGTGTCA3'; Crit-WTF-5'TATATGTGCTTGTCAGTCTGGATG 3'; 3arm-WTR-5'CACCACAGACCATGAGAACACCC 3'

Radiography of Mouse Skeletons

Radiographs of mice were captured postmortem using the Faxitron laboratory x-ray machine. Post-euthanasia, whole-body anterior, posterior, and lateral x-rays were obtained without magnification.

Mouse Growth Measurements

Starting at postnatal day 7, mice were measured on a weekly basis every seven days until postnatal day 168 (wild-type males: n=3, wild-type females: n=3, heterozygous males: n=5, heterozygous females: n=8, knockout males: n=3, and knockout females: n=3). For mice with partial measurements starting at p7 through p70-p112, growth data was imputed to p168 based on the recorded growth rate (wild-type males: n=3, wild-type females: n=6, heterozygous males: n=5, heterozygous females: n=3, knockout males: n=2, and knockout females: n=2). All data were combined per genotype for growth rate analysis. Measurements of body weight (g) were obtained with a scale. Measurements of trunk length (mm) and tail length (mm) were obtained

using a digital caliper. Trunk length was defined as the length from the snout to the base of the tail. Tail length was defined as the length from the base to the tip of the tail.

Statistical Analysis of Mouse Growth Measurements

Statistical analysis of the mouse growth measurements was done in collaboration with the UCLA Department of Medicine Statistics Core. Linear mixed models were used to analyze mouse weight, trunk length, and tail length data. Random mouse effects were used to cluster repeated measurements on the same mouse, and a three-way interaction between genotype (wild-type, heterozygous, and knockout), sex (male and female), and log transformed postnatal time (days) was included to estimate differential growth curves in strata defined by sex and genotype. Differences in growth rates were evaluated using model contrasts of wild-type versus heterozygote and wild-type versus knockout in males and females independently. Growth rates were defined as the change in weight, trunk length, or tail length associated with a doubling of postnatal time in a particular sex by genotype strata. Model results were summarized in terms of estimates and standard errors of differences in growth rates, and p-values derived from testing for equal growth rates. P-values less than 0.05 were considered statistically significant. All analyses were performed using SAS v .9.4 (SAS Institute Inc., Cary NC).

Tissue Isolation for Biochemistry

Cartilage was isolated from the knee joints and the rib cages of p6-p8 mice. Knee cartilage was dissected from the distal femur and the proximal tibia and sternal and rib cartilage was dissected from the rib cage. Tissue was snap frozen in liquid nitrogen and stored at –80ºC for use in later experiments.

RNA Isolation and cDNA Synthesis for qRT-PCR

RNA was isolated from the knee joint cartilage of p6-p8 mice. Frozen tissue was homogenized in liquid nitrogen using a metal/titanium mortar and pestle, and RNA was isolated using TriZol. cDNA was synthesized using the Invitrogen Superscript III Reverse Transcriptase Super Mix kit. Random hexamers were used to initiate reverse transcription. Gene expression was then quantitated using the Roche FastStart Universal SYBR Green Master Mix with ROX reference dye on a Stratagene MX3000 thermalcycler. Relative expression was quantified through a comparison of the expression of the target genes to the expression of *Gapdh* using the delta-delta CT method to quantify the relative expression based on genotype. Primer sequences are as follows: *Col9a1*F- 5'GTATCCGCAACTCTTAAGCGTC 3', *Col9a1*R- 5'TGCAGCCTTCTCAATTTGGAAC 3', *Col9a2*F- 5'CATTCCTGGCATCGTGGGAG 3', *Col9a2*R- 5'GGCCACGACCCATTTCTCCT 3', *Col9a3*F- 5'TGACAGAGGGGACAAGGGAG 3', and *Col9a3*R- 5'GAGCACCATCTCGACCATCTTT 3'.

Preparation of Mouse Collagen Samples for Protein Biochemistry

Preparation of mouse collagen samples was done in collaboration with the laboratory of Dr. David Eyre at the University of Washington. Mouse cartilage from the rib cages of p6-p8 mice was processed in modification of the previously described protocol in Eyre, et al 2004[7]. Briefly, tissue was minced and collagen fibrils were extracted in 4M guanidine HCL, 0.05M Tris, pH 7.4, containing protease inhibitors (2mM EDTA, 5mM benzamidine, 2 mM phenylmethylsulfonyl fluoride, and 5 mM phenanthroline) at 4ºC for 48 hours. Tissue pellets were washed with water and resuspended in 3% acetic acid followed by an overnight pepsin digestion at 4ºC. Solubilized type IX collagen was precipitated with 2.2 M NaCl and prepared for western blotting.

Western Blotting

Western blotting was done in collaboration with the laboratory of Dr. David Eyre at the University of Washington as previously described in Ichimura et al. 2000[41]. Briefly, pepsin-digested fragments were resolved on a 12.5% SDS-PAGE with DTT or on a 7.5% SDS-PAGE without DTT and transferred to a PVDF membrane. Type IX collagen fragments were detected using an antibody raised against bovine type IX collagen and recognizes epitopes in all three mouse type IX collagen chains. No cross-reactivity with other collagen chains has been observed.

Whole-Mount Skeletal Staining

Whole-mount skeletal staining of newborn (p1 mice) and was conducted as previously described in Rigueur, et al 2014[42]. Briefly, newborn mice were euthanized and immersed in water heated to 55ºC-60ºC for 30-40s to soften the tissue. Following the removal of skin, organs, and adipose tissue, skeletons were fixed overnight in 95% ethanol. Tissue was further fixed overnight in acetone. Cartilage was stained with 0.03% Alcian blue (w/v) 80% Ethanol and 20% glacial acetic acid, followed by two 70% ethanol washes to destain the surrounding soft tissue and overnight incubation in 95% ethanol to fix the stain. Tissues were then pre-cleared for 1 hour in 1% potassium hydroxide and mineralized bone was stained with 0.005% Alizarin red (w/v) 1% potassium hydroxide overnight at 4ºC. Tissue was further cleared using a 50:50 glycerol: 1% potassium hydroxide solution. All incubations were conducted at room temperature unless otherwise specified. Stained skeletons were imaged under a Leica dissecting microscope using bright-field microscopy and images were stitched using Adobe Photoshop.

Limb Segment Measurements

Individual limb segments (femur, tibia, humerus, and ulna) were dissected from the newborn skeletal preparations and imaged at 4.0X magnification on the Leica dissecting microscope. The mineralized diaphysis of each limb segment, as defined by the Alizarin red stain, was measured using a 1 mm pinwheel reticle (Swift Microscope World, Carlsbad, CA, USA) in Adobe Photoshop.

Tissue Processing for Immunohistochemistry

Tissue for immunohistochemistry was isolated from the hind limbs of newborn, p42, p90, and p180 mice. The intact femur and tibia, joined at the knee, was isolated from all right hind limbs. The left knee joint, including the distal femur and the proximal tibia, were isolated from all left hind limbs. Tissue was fixed in 10% buffered formalin overnight at 4ºC, followed by decalcification in Immunocal for 3 days at 4ºC. Tissues were then dehydrated in varying concentrations of ethanol and cleared using 100% xylene. Samples were then paraffin-embedded in a vacuum oven.

Growth Plate Histology

7 µm sagittal sections of intact newborn (p0-p1) mouse hind limbs, including the femur and tibia, were prepared using a Leica microtome. Hematoxylin and Eosin stains were used to determine growth plate morphology and chondrocyte organization. Stained sections were imaged on a Zeiss upright microscope at 20X magnification using bright-field microscopy. Histomorphometric measurements of the growth plate were conducted using the Zeis AxioVision v.4.9.1 software.

Assessment of Osteoarthritis Joint Pathology

Osteoarthritis-like degenerative changes were assessed in the cartilage of the knee joint. 7 µM sagittal sections of the knee joint from p42, p90, and p180 mice were obtained, and 25-30 sections, one every 70 µm, was stained with safranin-O/Fast-Green FCF to determine the integrity of the articular cartilage. Stained sections were imaged on a Zeiss upright microscope at 20X magnification using bright-field microscopy.

Auditory Brainstem Response Testing

Auditory brainstem response testing was done in collaboration with the laboratory of Dr. Rick Friedman at the University of Southern California as previously described in Myint, et al., 2016[43]. Briefly, all ABRs were performed in a sound proof chamber where auditory stimuli were delivered to anesthetized mice using an Intelligent Hearing Systems speaker that was inserted into the right ear canal. Stainless steel electrodes were placed subcutaneously at the vertex of the head and the right mastoid with a ground electrode at the base of the tail. Tone pips were delivered to the right ear at frequencies of 4, 8, 12, 16, 24, and 32 kHz and were delivered below threshold and increased in 5 dB increments up to 100 dB SPL. Hearing thresholds were determined by visual inspection of ABR waveforms and defined as the minimum intensity at which a wave 1 complex could be distinguished.

Preparation of Tissue for Transmission Electron Microscopy (EM)

Immediately post-euthanasia, cartilage from the right knee joint was dissected from the distal femur and proximal tibia and chopped into discs 1 mm thick. Tissue was fixed in 1.5% glutaraldehyde/1.5% paraformaldehyde/10% PBS overnight at 4ºC. Tissue was processed and embedded for EM at the UCLA Brain Research Institute Microscopy Core.

Statistical Analysis

All data, with the exception of the mouse growth measurements, was analyzed using a student's t-test. Data with a p-value < 0.05 was considered significant.

Results

Col9a2 is Ablated in Knockout Mice

To test whether the *Col9a2* targeting construct truly ablated the gene, I used quantitative real-time PCR (qRT-PCR) to assess the levels of *Col9a2* expression in wild-type, heterozygous, and homozygous mutant mice. Expression levels correlated with the mouse genotypes. Heterozygous mice produce *Col9a2* mRNA transcripts at levels approximately 50% reduced as compared with wild-type mice, and transcripts were at undetectable levels in the homozygous knockouts, confirming that *Col9a2* was ablated (Figure 3.2).

An examination of the mRNA expression of the remaining type IX procollagen genes, *Col9a1* and *Col9a3,* by qRT-PCR indicated that both transcripts were expressed in the wild-type, heterozygous, and knockout mice. Expression levels of both of these genes were not significantly different in the heterozygous and knockout mice, indicating that the absence of *Col9a2* did not alter the gene expression of *Col9a1* and *Col9a3*.

Loss of α2(IX) Results in a Total Protein Knockout of Type IX Collagen

To assess the trimerization of type IX collagen in the absence of the α2(IX) chain, I isolated protein from sternal and rib cartilage of p6-p8 wild-type, heterozygous and knockout mice. Protein extractions post pepsin-digestion were separated on a 12.5% SDS-PAGE under reducing conditions and 7.5% SDS-PAGE under non-reducing conditions and probed with an anti-type IX collagen antibody that detects all three procollagen chains. I detected type IX collagen in both the wild-type and heterozygotes, but no type IX collagen was detectable in the knockouts, consistent with dependence of type IX collagen assembly on presence of the α2(IX)

chain (Figure 3.3). The type IX collagen protein levels were diminished in the heterozygous mice, consistent with the expected effects of haploinsufficiency for the α2(IX) chain.

Col9a2 $^{-/-}$ Mice Exhibit Mild Short Stature

To determine the phenotype of the *Col9a2* $^{-/-}$ mice, I examined the external appearance of adult mice and radiographs of the skeleton in comparison to the wild-type littermates at 6 weeks of age. Mice homozygous for the *Col9a2* null allele presented with a skeletal phenotype primarily consisting of mild short stature with shortened limbs and mild midface hypoplasia (Figure 3.4A). The phenotype was observed in both males and females, with the midface hypoplasia more pronounced in the male mice. Both the trunk and tail lengths of male and female mice were shorter than their wild-type littermates, a finding also observed in the radiographs (Figure 3.4B). No overt phenotypic differences were observed in the heterozygous adult littermates.

I next assessed whether the knockout mice possessed any developmental growth delays by measuring the body weight, trunk length, and tail length of the wild-type, heterozygous and knockout male and female mice on a weekly basis for 24 weeks, starting at p7. Analysis of the growth rate using all three parameters demonstrated that the *Col9a2* $^{-/-}$ mice grew at a significantly reduced rate (Figure 3.5 and Table 3.1). Interestingly, a mild growth delay in the trunk and tail length was also observed in the female heterozygous mice, which grew at a significantly slower rate than the wild-type females, suggesting that heterozygous mice with haploinsufficiency for *Col9a2* exhibit a mild phenotype of growth delay in a sex-dependent manner which resolves by adulthood.

Absence of Type IX Collagen Results in Short-Limb Phenotype

To determine whether the loss of type IX collagen affects endochondral ossification and skeletal development, I used whole-mount skeletal staining of newborn (p1) mice to assess the phenotype. Similar to the findings generated by growth measurements and radiographic analyses, comparison of the wild-type, heterozygous, and knockout mice demonstrated that knockouts were smaller than their wild-type littermates. The heterozygous mice also exhibited mild short stature, but this difference in stature was resolved by adulthood, as indicated previously (Figure 3.6). A comparison of the lengths of the upper and lower extremities, including the humerus, ulna, femur and tibia, indicated that all limb segments were shorter in the knockout mice at p1. Quantitative analysis of the mineralized diaphysis length of all limb segments confirmed that all of the limb segments were significantly shorter in the knockouts, with the most significant length difference observed at the tibia ($p<0.001$). No significant differences in the limb segment length was observed between the wild-type and heterozygous mice. Thus as a consequence of the loss of type IX collagen, the *Col9a2* $^{-/-}$ mice exhibited mild short stature and shortened limbs.

I also examined the endochondral growth plates of the knockout mice to determine whether there were observable defects in chondrocyte proliferation, growth plate length and morphology. Hematoxylin and Eosin staining of the proximal tibia in newborn mice (p1) indicated that the growth plates of the knockout mice were significantly wider than the wild-type mice across all growth plate zones with a large hypocellular region in the center of the proliferative zone (Figure 3.7). This was also observed in growth plates of the distal femur (data not included). Significant widening of the growth plates was not observed in the heterozygous mice. A closer examination of the chondrocytes in the reserve, proliferative, and hypertrophic zones indicated that with the exception of the widened growth plate no defects were observed in

the reserve zone, but chondrocyte column formation was lost in the proliferative zone. Cells were irregularly shaped and proliferating in all directions, resulting in disorganized growth plate architecture. Hypertrophic chondrocytes continued to differentiate irrespective of polarity of the growth plate, likely contributing to the mild short stature and limb segment shortening observed in the skeletal preparations.

Absence of α2(IX) Results in an Alterations in Chondrocyte Morphology and ER Distention

To assess the cellular phenotype in the knockout mice, I used transmission electron microscopy to examine the cellular morphology, collagen content and endoplasmic reticulum (ER) of growth plate cartilage in newborn mice (p1). As ER stress can be a consequence of the synthesis of mutant ECM proteins in chondrodysplasias such as MED, I hypothesized that a similar phenomenon may be occurring in the knockout chondrocytes [44, 45]. First, an examination of the growth plate chondrocytes in the reserve and proliferative zone highlighted irregularities in the chondrocyte morphology in the proliferative zone (Figure 3.8A-F). The cells were rounded and shaped like a semi-circle instead of the flattened ellipse that was observed in both the wild-type and heterozygous cells. A consistent cellular phenotype of ER distention was also detected in the knockout chondrocytes in both the reserve and proliferative zones, while an examination of the wild-type cartilage depicted normal ER (arrows in Figure 3.8). However, mild ER distention was observed in the cartilage of heterozygous animals. At higher magnifications, the collagen content of the extracellular matrix also appeared thinner and less dense (Figure 3.8G-I) in the knockout relative to the wild-type and heterozygous mice. While I observed the altered chondrocyte morphology and ER distention in the knockout chondrocytes, additional tests are required to determine if the observed phenotype is due to ER stress.

Col9a2 -/- Exhibit Impaired Auditory Function

Because *Col9a2* is also expressed in the cochlea of the ear and patients affected with STL exhibit hearing loss, I also tested the auditory function of *Col9a2* knockout mice to identify any hearing-related defects. I used auditory brainstem response (ABR) testing at 6 weeks of age to determine the baseline decibels at which tone pips at frequencies ranging from 4-32 KHz could be detected. Our data show the null mice detected tone pips at thresholds 30-40 decibels higher than both the wild-type and heterozygous mice, indicating that the auditory function of the null mice is significantly compromised ($p<0.001$) (Figure 3.9). The heterozygous mice did not exhibit any auditory impairment in comparison to the wild-type littermates. Due to the loss of type IX collagen, the knockout mice exhibit severe hearing loss.

Early Onset Joint Degeneration Observed in *Col9a2* $^{-/-}$ Mice

Since type IX collagen is integral to the long-term maintenance of articular cartilage, as demonstrated by the development of early-onset osteoarthritis in the *Col9a1* $^{-/-}$ mouse[36, 46] and type IX collagen is present in the weight-bearing articular cartilage of the knee joint[47], I sought to determine the effect of the loss of type IX collagen on the cartilage in the knee joint. I collected the knee joints from 6 month old wild-type and knockout mice and stained serial sagittal sections every 70 µ with safranin-o and examined the tibial plateau for osteoarthritic-related joint degeneration. I observed a decrease in the intensity of the safranin-o stain in the knockouts, indicating a decrease in proteoglycan content. The articular cartilage of the distal femur and proximal tibia was also thinner with a reduced cellular density in comparison to the the wild-type littermates (Figure 3.10). I also compared male and female mice and observed more severe degenerative changes in the male mice. Combined, I determined that the loss of type IX collagen leads to the development of early-onset joint degeneration.

Discussion

In this study, I used the *in vivo* genetic model of the *Col9a2* knockout mouse to test whether the α2(IX) chain is dispensable for the trimerization of type IX collagen. Previous *in vitro* trimerization studies yielded inconsistent results suggesting that the α2(IX) chain might not be required to produce functional type IX collagen[31]. Although a single case of Stickler syndrome resulting from a homozygous loss-of-function mutation in *COL9A2* indicated that loss of the gene product has a similar phenotype as compared with loss of the *COL9A1* gene product, biochemical data to prove this were lacking [24]. Biochemical assessment of type IX collagen in the *Col9a2* $^{-/-}$ mouse demonstrated that the loss of α2(IX) results in a functional knockout of the entire type IX collagen trimer. Based on these data, I can say with certainty that α2(IX) is essential to protein trimerization, resolving the inconsistent results observed in the *in vitro* biochemical experiments. As the loss of α1(IX) also resulted in a total protein knockout in the *Col9a1* $^{-/-}$ mouse[32] and recessive loss of function mutations for *COL9A3* also results in Stickler syndrome in humans [25], it seems more likely than not that the loss of α3(IX) will also result in a functional knockout of type IX collagen.

While I determined that α2(IX) is essential to trimerization, I also sought to understand the consequences on α1(IX) and α3(IX) in the absence of α2(IX). Using a combination of qRT-PCR and TEM, I attempted to resolve this question. Using qRT-PCR, I assessed the transcript levels of both of these chains, and observed no significant difference in the mRNA levels of *Col9a1* and *Col9a3* in both the heterozygous and homozygous transgenic mice, similar to the observed mRNA levels of *Col9a2* and *Col9a3* in the *Col9a1* $^{-/-}$ mouse [32]. This suggests that gene-regulation does not occur at the RNA level, and the unincorporated procollagen chains are likely regulated at the protein level. Using TEM, I observed in the knockout mice severely enlarged and distended rough endoplasmic reticulum in the reserve and proliferative zones, data

suggesting the possibility of an unfolded protein response (UPR). The cells also appeared unhealthy with abnormal-appearing nuclei. While I did not conduct proliferation assays in the newborn growth plate, such experiments were conducted in the *Col9a1* $^{-/-}$ mouse in the study by Dreier et al. 2008 [33]. These experiments demonstrated that knockout growth plate chondrocytes exhibited a significant decrease in proliferation, based on a proliferative cell nuclear antigen (PCNA) stain, in both the reserve and the proliferative zones[33]. As the outcome of a functional knockout of type IX collagen is the same in both the *Col9a1* and the *Col9a2* null mice, I hypothesize a similar decrease in cell proliferation would be observed in the *Col9a2* $^{-/-}$ mouse. Based on this evidence, it is likely that the α1(IX) and α3(IX) chains in the ER trigger a UPR, which may be the underlying mechanism that results in the large hypocellular region that is observed in both the *Col9a1* $^{-/-}$ and the *Col9a2* $^{-/-}$ growth plate chondrocytes[33]. To be certain that this is the underlying mechanism, further ultrastructural analysis of growth plate cartilage using a type IX collagen antibody stain may aid in determining the identity of the proteins resulting in the ER dystrophy.

In our effort to ascertain the functional consequence of the loss of type IX collagen, I determined that the *Col9a2* null mouse phenocopies the human disease STL. Patients affected with this arthroopthalmopathy clinically present with mild craniofacial defects, mild short stature, sensorineural hearing loss, and myopia[26]. All of the known type IX collagen mutations are homozygous recessive loss-of-function mutations [23-25, 48]. Since the *Col9a2* $^{-/-}$ mouse also exhibited mild short stature, mild midface hypoplasia, and impaired auditory function, I can now conclude that the phenotype observed in the *COL9A2* STL patients is due to a total loss of the type IX collagen trimer.

As previously mentioned, since STL patients with type IX collagen mutations present with severe myopia and vitreoretinal degeneration[23-25, 48] and because *Col9a2* is expressed in the vitreous of the eye[49], I endeavored to also assess whether these mice inherited any vision abnormalities due to the defect in type IX collagen biosynthesis. However, I was unable to characterize this phenotype due to homozygosity for the Rd8 mutation at the *Crb1* locus, which is known to confer congenic eye defects in inbred mouse strains, specifically C57Bl/6N mice, and can confound the results of any detected ocular phenotype[50]. As a part of the International Mouse Phenotyping Consortium (IMPC) pipeline, the eye morphology of the *Col9a2* $^{-/-}$ mice was assessed by optical coherence tomography (OCT)/fundus imaging, and no gross abnormalities were detected [51, 52]. This is surprising considering that the *COL9A2* STL family exhibited significant myopia, vitreoretinal degeneration, and retinal detachment[24]. It is possible, as in the case of myopia, that the eye phenotype may not be detectable by this method, so I cannot rule out the possibility that the *Col9a2* $^{-/-}$ mice have a mild eye phenotype. Once the Rd8 mutation has been bred out of this mouse, I will be able to determine if these mice exhibit any ocular abnormalities.

During our investigation of the skeletal phenotype in the *Col9a2* $^{-/-}$, I also observed a mild phenotype in the heterozygous mice. Newborn males and females were shorter than their wild-type littermates, and adult female mice exhibited mild growth delays. A close examination of the type IX collagen STL cases identified several carriers of the loss-of-function mutations that presented with mild short stature and a mild skeletal phenotype [23, 48]. Both Van Camp et al. 2006 and Nikopoulos et al. 2011 suggested that haploinsufficiency for type IX collagen likely produces this mild skeletal phenotype, and our study supports this hypothesis [23, 48]. While there were no significant differences in the mRNA transcript levels of *Col9a1* and *Col9a3* in the

heterozygous animals, I did observe a mild decrease in the total amount of type IX collagen, consistent with haploinsufficiency. I also observed some mildly distended RER in some chondrocytes of the heterozygous growth plate cartilage, which may contribute to the possible mild STL carrier phenotype.

Conclusion

In this study, I used the *in vivo* genetic model of the *Col9a2* $^{-/-}$ mouse to resolve the ambiguity regarding the necessity of the α2(IX) chain of type IX collagen during protein trimerization. Biochemical analysis of type IX collagen in wild-type, heterozygous, and knockout mice demonstrated that the loss of α2(IX) resulted in a total protein knockout of type IX collagen, a phenomenon that was also observed in the *Col9a1* $^{-/-}$ mouse. While there was no significant reduction in the transcript level of *Col9a1* and *Col9a3*, I did not detect any other type IX collagen products by Western blotting, leaving some doubt about the fate of the remaining type IX procollagen chains. To address this question, I used ultrastructural analysis of growth plate cartilage to examine the cellular morphology of the chondrocytes, and observed severely distended endoplasmic reticulum, suggesting that the unincorporated chains accumulate and may trigger an unfolded protein response. Based on this evidence, it is likely that the α1(IX) and α3(IX) chains are regulated at the protein level, but further analysis is required to determine the exact mechanism.

In addition to assessing the biochemistry of trimerization, I also conducted phenotypic characterization experiments to determine the effects of the loss of type IX collagen on the development of the skeleton. I discovered that the knockout mice grew at a significantly reduced rate; they exhibited mild short stature, mid-face hypoplasia, and shorter limbs; and the auditory function was significantly diminished. Human patients with STL also exhibit these clinical

features and severe ocular defects including myopia, vitreoretinal degeneration, and retinal detachment. Based on the overlapping skeletal and auditory phenotype observed in the *Col9a2* $^{-/-}$ mouse and the human family affected with STL due to a homozygous null mutation in *COL9A2,* I have demonstrated that this knockout mouse phenocopies recessive STL.

Among the type IX collagen STL cases, 2 families have been identified with *COL9A1* mutations, 1 family with a *COL9A2,* and 1 family with a *COL9A3* mutation. Including the data from this study, there is now functional evidence that the resulting phenotype in *COL9A1* and *COL9A2* STL is due to a functional knockout of type IX collagen, as demonstrated by the *Col9a1* $^{-/-}$ and the *Col9a2* $^{-/-}$ mice. While a knockout mouse of *Col9a3* has not been studied, it is likely that the phenotypic consequence will be the same. However, further studies are required to determine whether this will be the case.

Figures

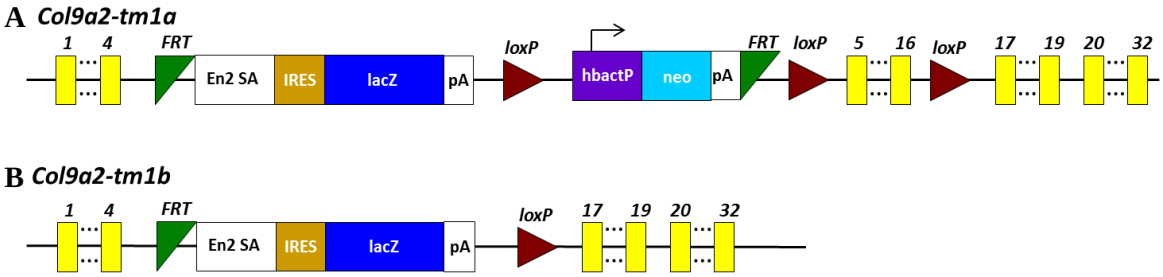

Figure 3.1: *Col9a2* Targeting Construct. A. *Col9a2 tm1a* allele knockout first conditional ready allele in transgenic mice generated at MRC Harwell. The targeting construct, flanked by FRT sites, is inserted after exon 4. Insertion of splice acceptor (En2 SA) and internal ribosomal entry site (IRES) lead to a poly adenylation signal (pA) to terminate transcription. Flanked by *Cre-loxP* sites, a neo selection cassette follows. B. Post Cre-recombinase, the neo selection cassette is removed, producing the *tm1b* allele that was used in all experiments.

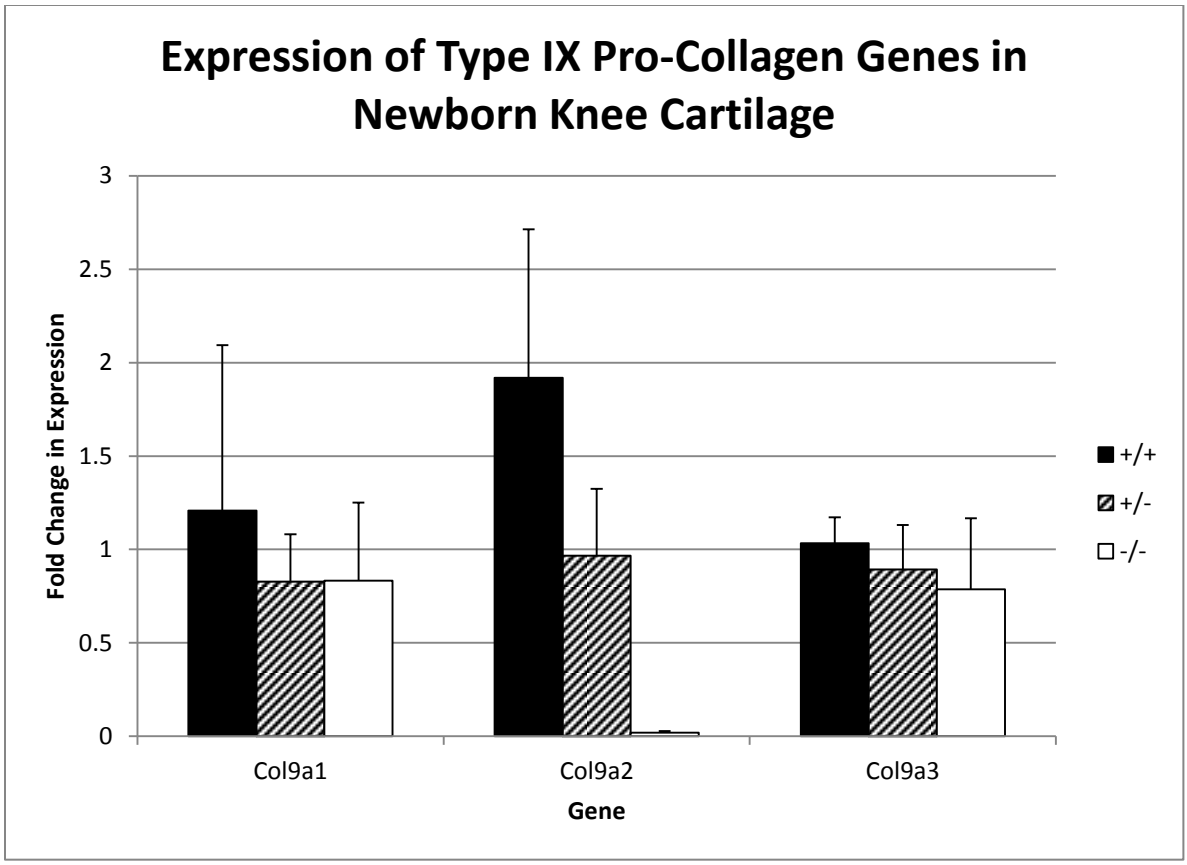

Figure 3.2: Expression of Type IX Pro-Collagen Genes in p6-p8 Epiphyseal Knee Cartilage. Using epiphyseal cartilage from newborn mice and qRT-PCR, the gene expression levels of *Col9a1*, *Col9a2*, and *Col9a3* were assessed. Data are representative of two experiments with n=5 biological replicates and n=3 technical replicates per biological replicate. No significant difference was observed in the expression levels of *Col9a1* and *Col9a3*.

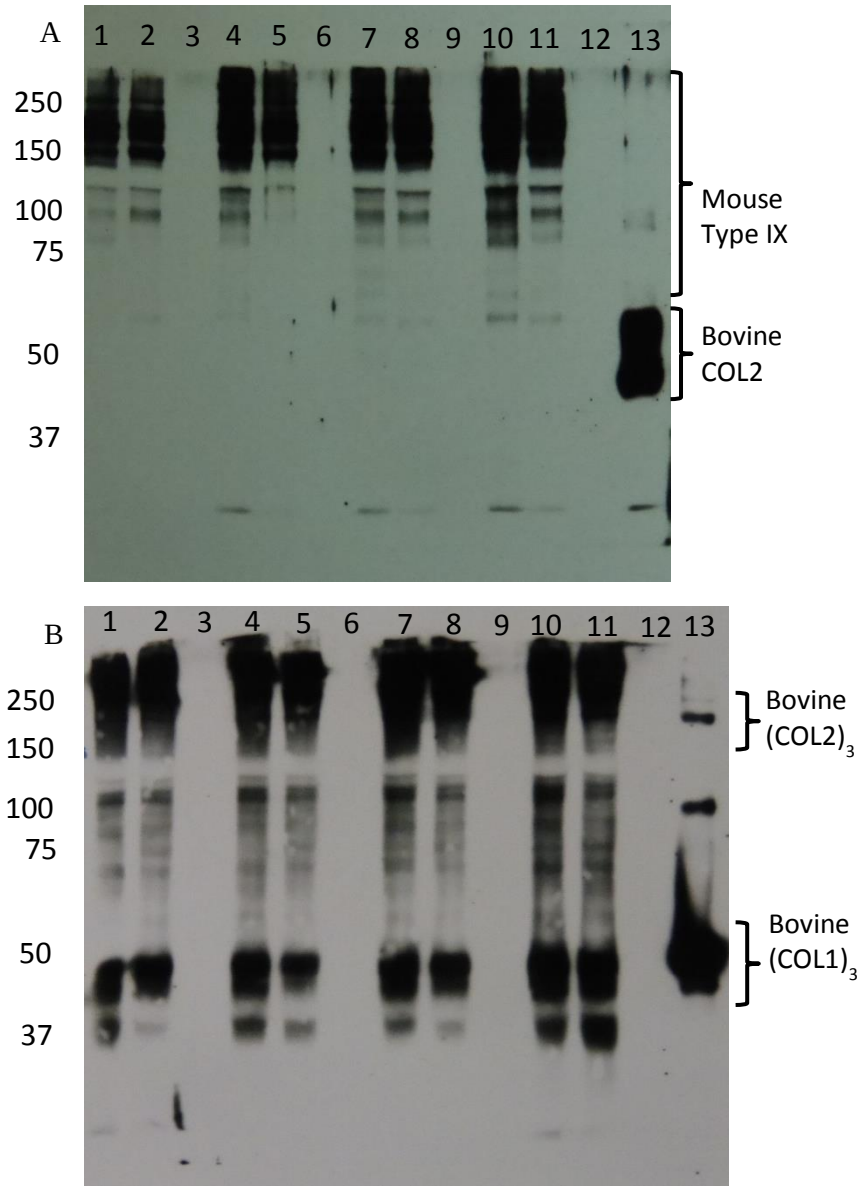

Figure 3.3: Type IX Collagen Immunoblot of p6-p8 Rib Cartilage. Immunoblot of pepsin-digested fragments of type IX collagen from rib and sternal cartilage of p6-p8 mice. Wild-type (lanes 1, 4, 7 and 10), heterozygous (lanes 2, 5, 8 and 11), and knockout (lanes 3, 6, 9 and 12) samples were separated by 12.5% SDS-PAGE with DTT (A) and 7.5% SDS-PAGE without DTT (B) and detected with an antibody against bovine type IX collagen. Bovine type IX collagen was used as a positive control in lane 13.

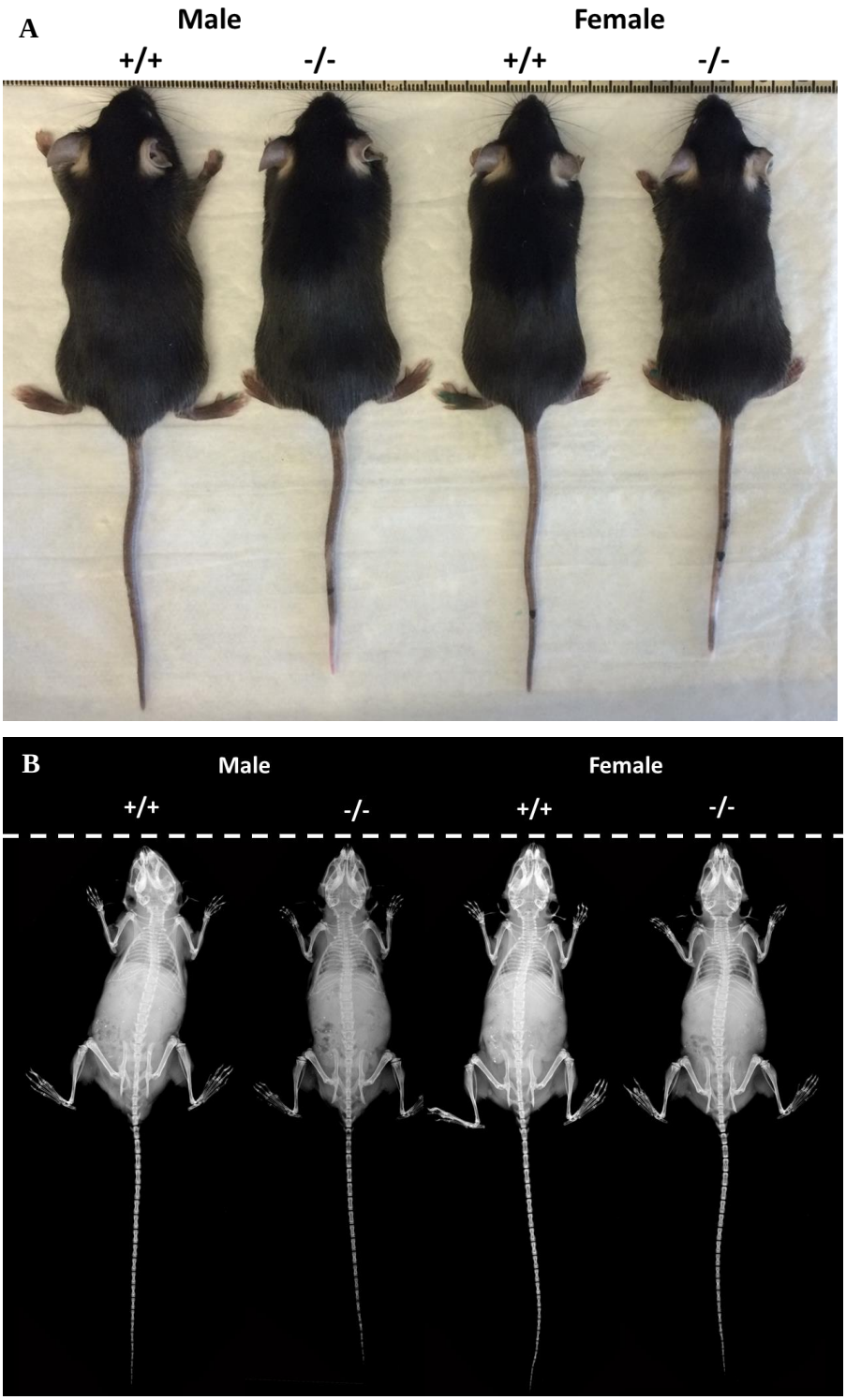

Figure 3.4: Phenotype of Adult *Col9a2* -/- Mice. External appearance (A) and radiographs (B) of wild-type and knockout male and female mice at 6 weeks of age. Knockout mice exhibited shorter trunk and tail lengths and shorter limbs.

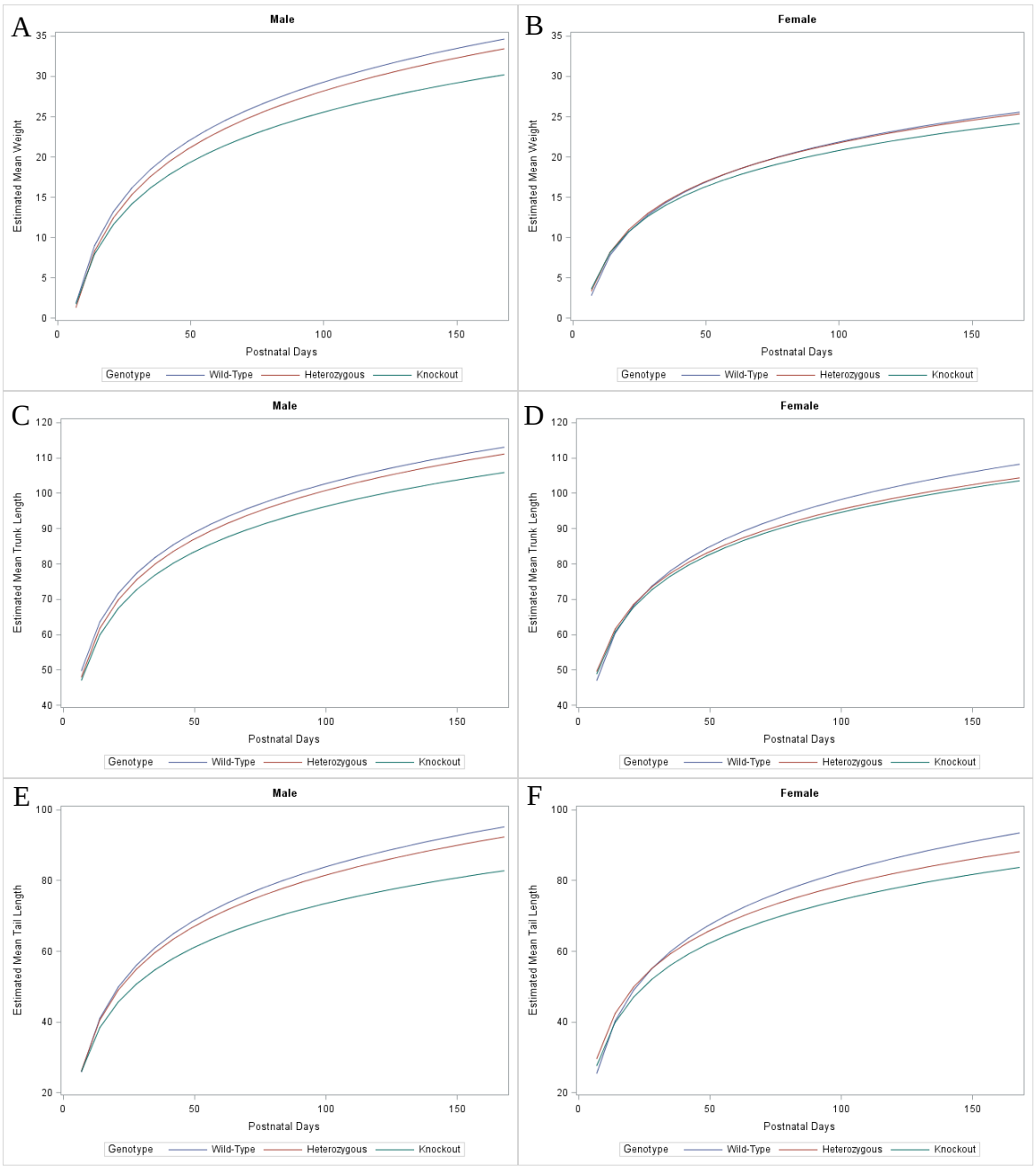

Figure 3.5: Growth Differences in Wild-Type, Heterozygous and Knockout Mice with respect to Body Weight, Trunk Length, and Tail Length. Estimated growth rates of the body weight (A-B), trunk lengths (C-D), and tail lengths (E-F) of male and female mice were computed using weekly measurements starting at p7 and ending at p168. Differences in growth rates between wild-type and heterozygotes and wild-type and knockouts was calculated (see Table 3.1).

Table 3.1: Estimated Difference in the Growth Rate Traits for Wild-type, Heterozygous, and Knockout Mice

Contrast	Weight		Trunk Length		Tail Length	
	Estimated Difference (SE)	p-value	Estimated Difference (SE)	p-value	Estimated Difference (SE)	p-value
Male WT (n=5) vs Het (n=12)	0.14 (0.21)	0.501	0.03 (0.55)	0.950	0.67 (0.67)	0.315
Male WT (n=5) vs KO (n=4)	0.95 (0.26)	**<0.001**	0.98 (0.65)	0.134	2.73 (0.79)	**<0.001**
Female WT (n=8) vs Het (n=9)	0.17 (0.19)	0.376	1.41 (0.49)	**0.004**	2.06 (0.60)	**<0.001**
Female WT (n=8) vs KO (n=5)	0.49 (0.22)	**0.031**	1.43 (0.57)	**0.013**	2.60 (0.70)	**<0.001**

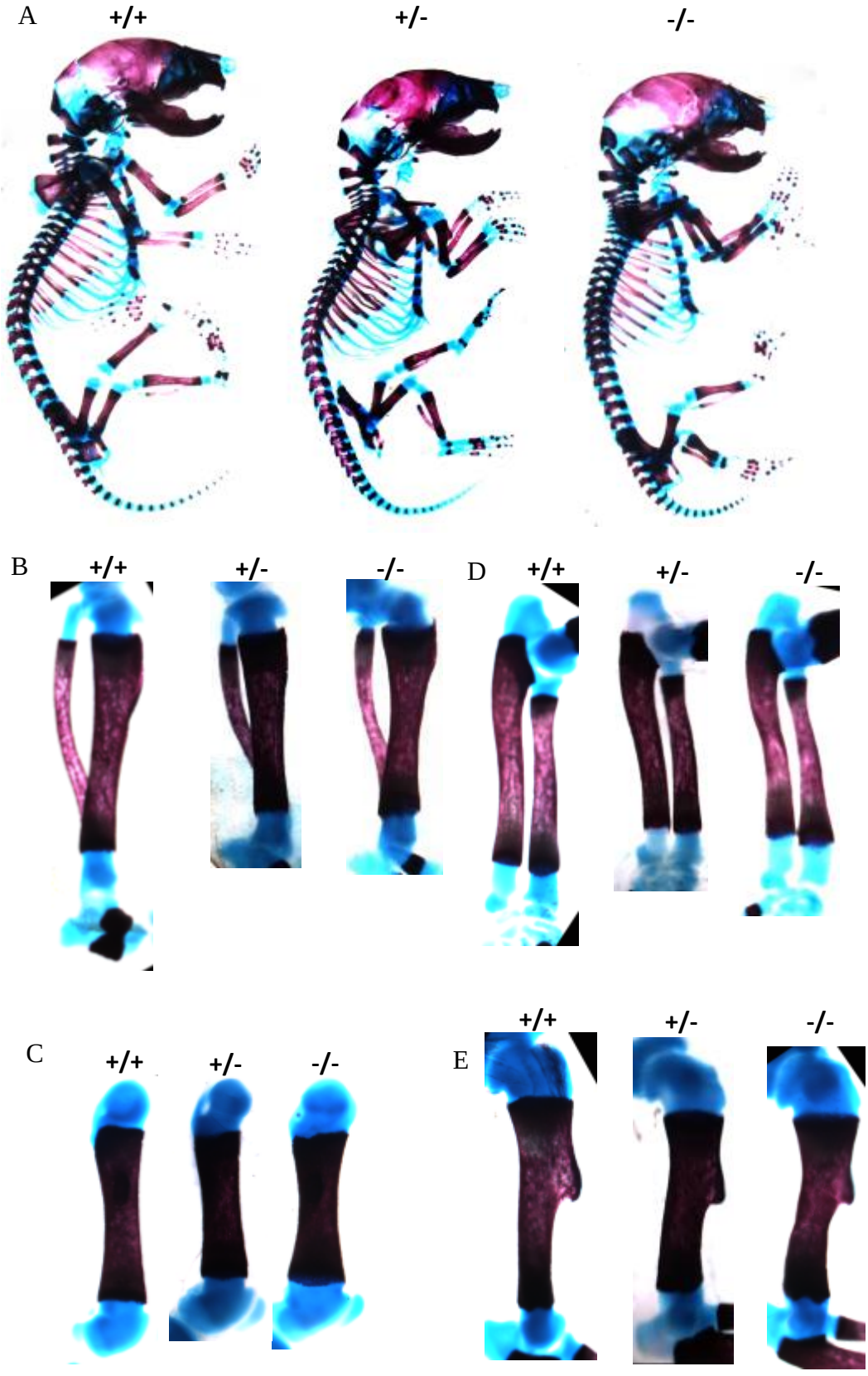
A
+/+
+/-
-/-
B
+/+
+/-
-/-
D
+/+
+/-
-/-
C
+/+
+/-
-/-
E
+/+
+/-
-/-

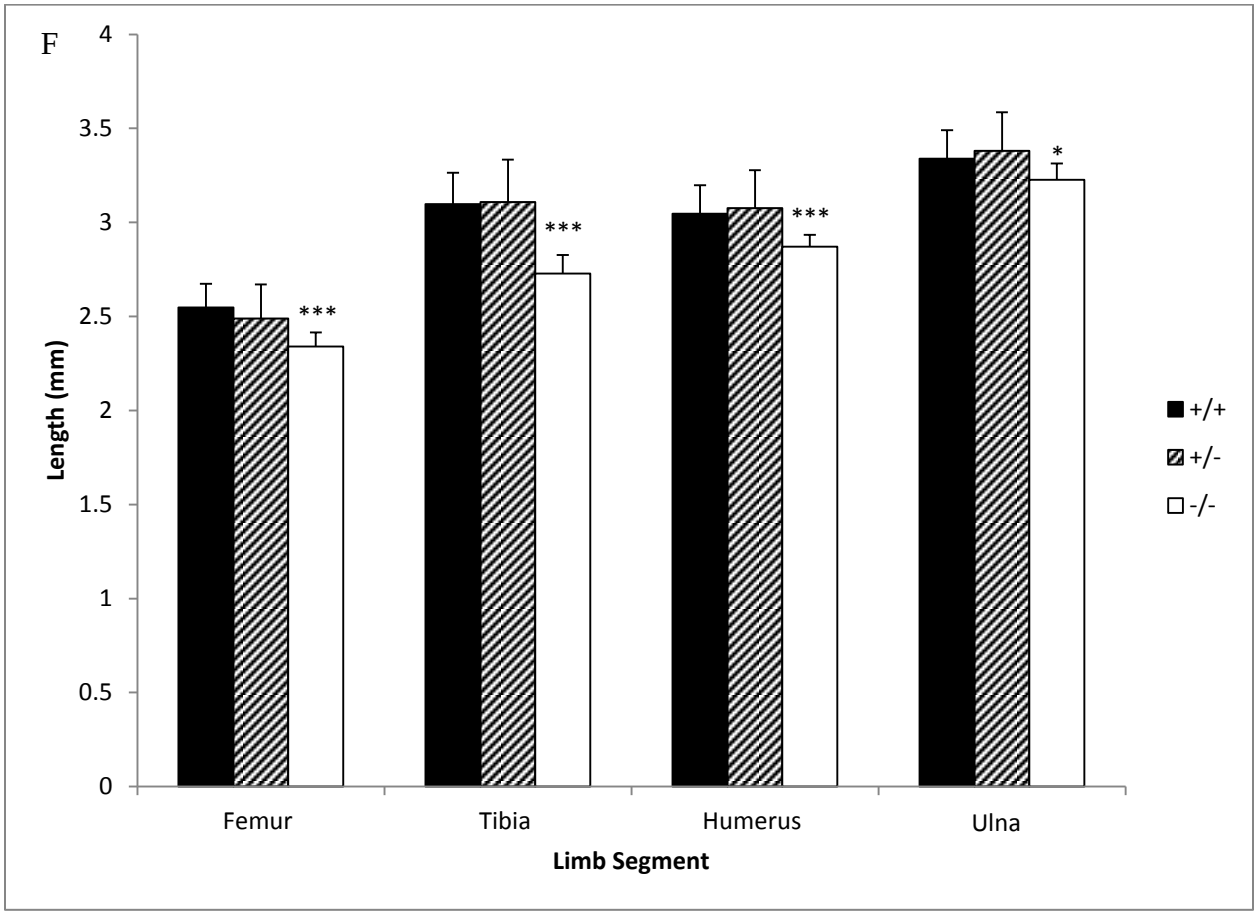

Figure 3.6. Newborn *Col9a2* -/- Mice Exhibit Shorter Limbs. Whole-mount skeletal staining of the newborn mice (p1) indicated that the heterozygous and knockout mice were smaller than their wild-type littermates (A). Limb segments, including the tibia (B), femur (C), ulna (D) and humerus (F) were also shorter. Quantification of the diaphysis length of the limb segments in wild-type (n=16), heterozygous (n=20) and knockout (n=14) mice indicated that the limb segments in the knockout mice were significantly shorter. *=$p<0.05$ and ***=$p<0.001$.

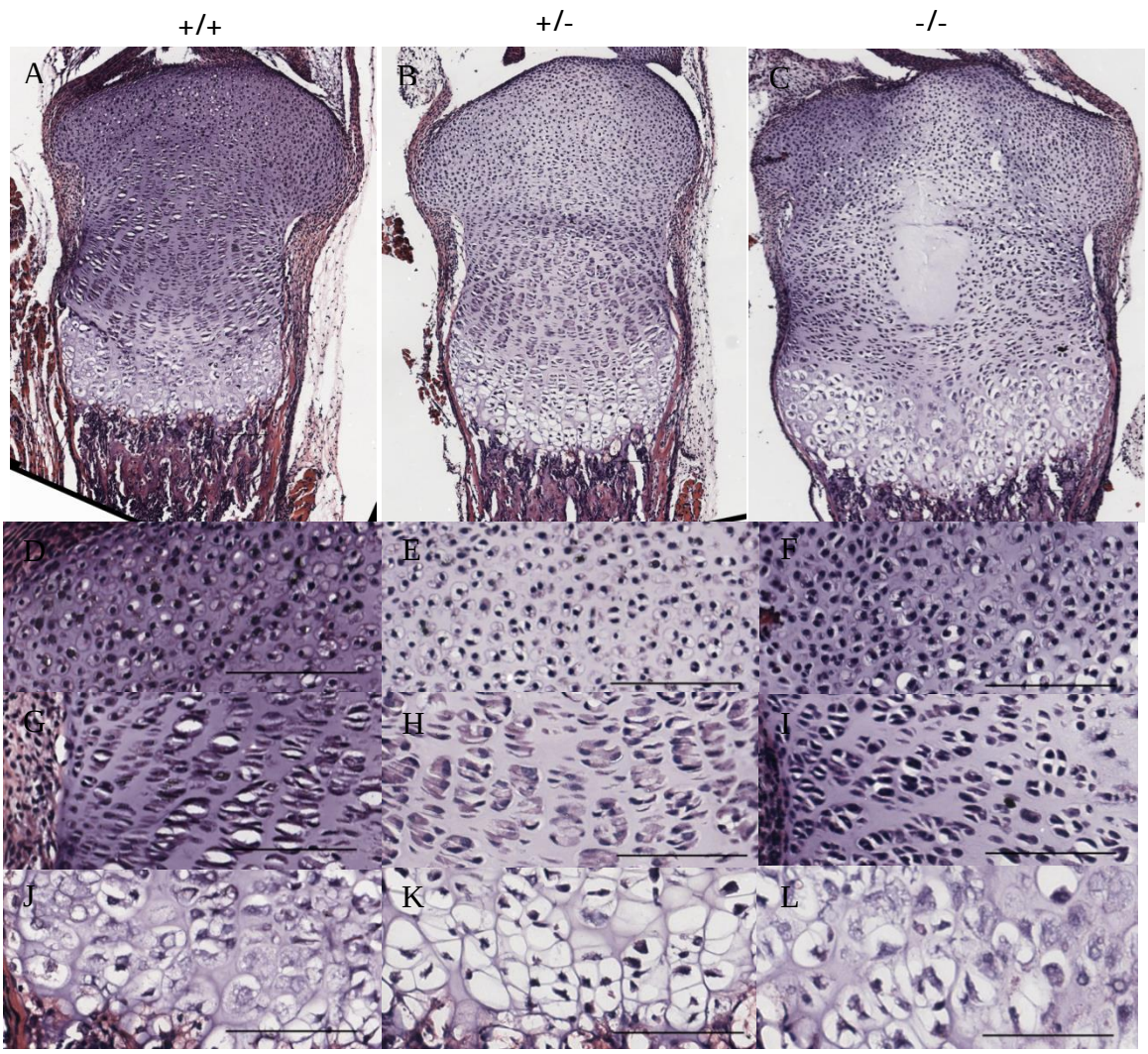
+/+
+/-
-/-
A
B
C
D
E
F
G
H
I
J
K
L

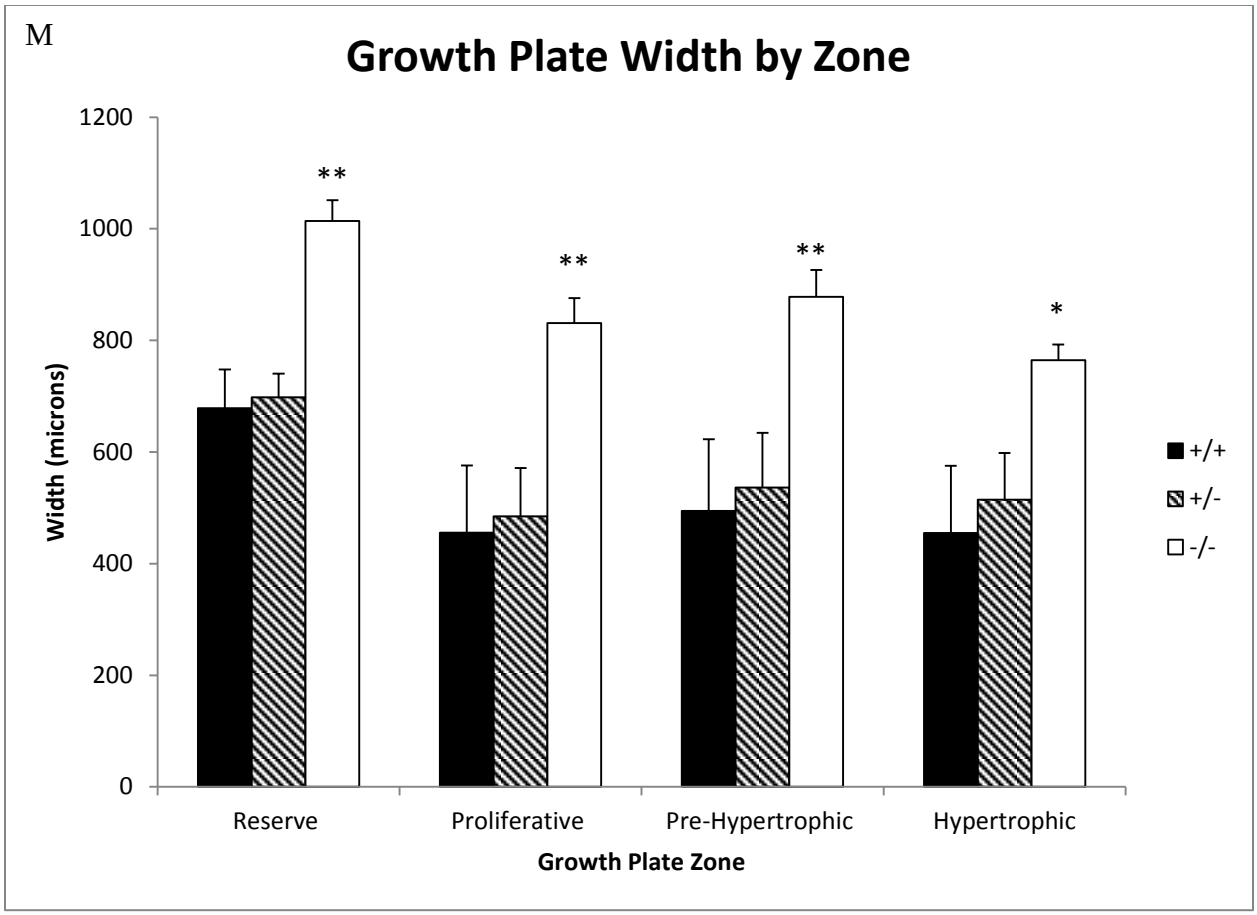

Figure 3.7. Altered Growth Plate Architecture Observed in Knockout Mice. H&E staining of the newborn (p1) proximal tibial growth plates in the wild-type (A), heterozygous (B), and knockout (C) mice. Magnified images of the reserve (D-F), proliferative (G-I) and hypertrophic (J-L) zones highlight altered chondrocyte morphology and polarity in the knockout growth plate. Histomorphometric analysis of the growth plate with p0-p1 wild-type (n=3), heterozygous (n=6) and knockout (n=3) mice demonstrate that the growth plate was significantly wider in the knockout mice. Scale bars are representative of 100 μm. *=$p<0.05$ and **=$p<0.01$.

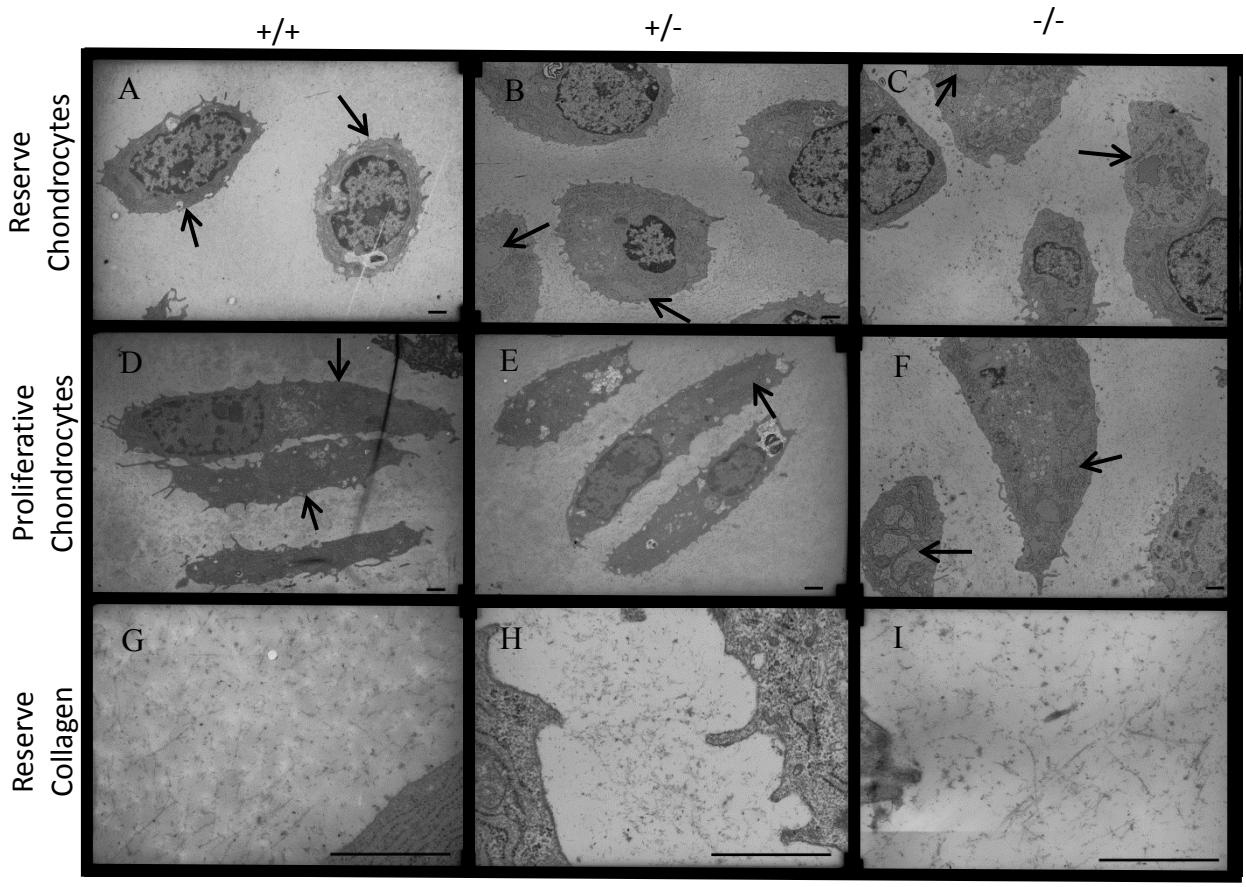

Figure 3.8. Altered Chondrocyte Morphology and ER Distention Observed in Newborn Growth Plate Cartilage. Ultrastructural analysis of newborn (p1) growth plate cartilage from the proximal tibia of wild-type, heterozygous and knockout mice. An examination of the reserve chondrocytes (A-C) and the proliferative chondrocytes (D-F) identified dilated endoplasmic reticulum in the knockout and heterozygotes (see arrows) in comparison to the normal ER in the wild-type (see arrows). Thinning of reserve zone collagen (G-I) was also observed in the knockout in comparison to the wild-type. Scale bars equal 1 µm.

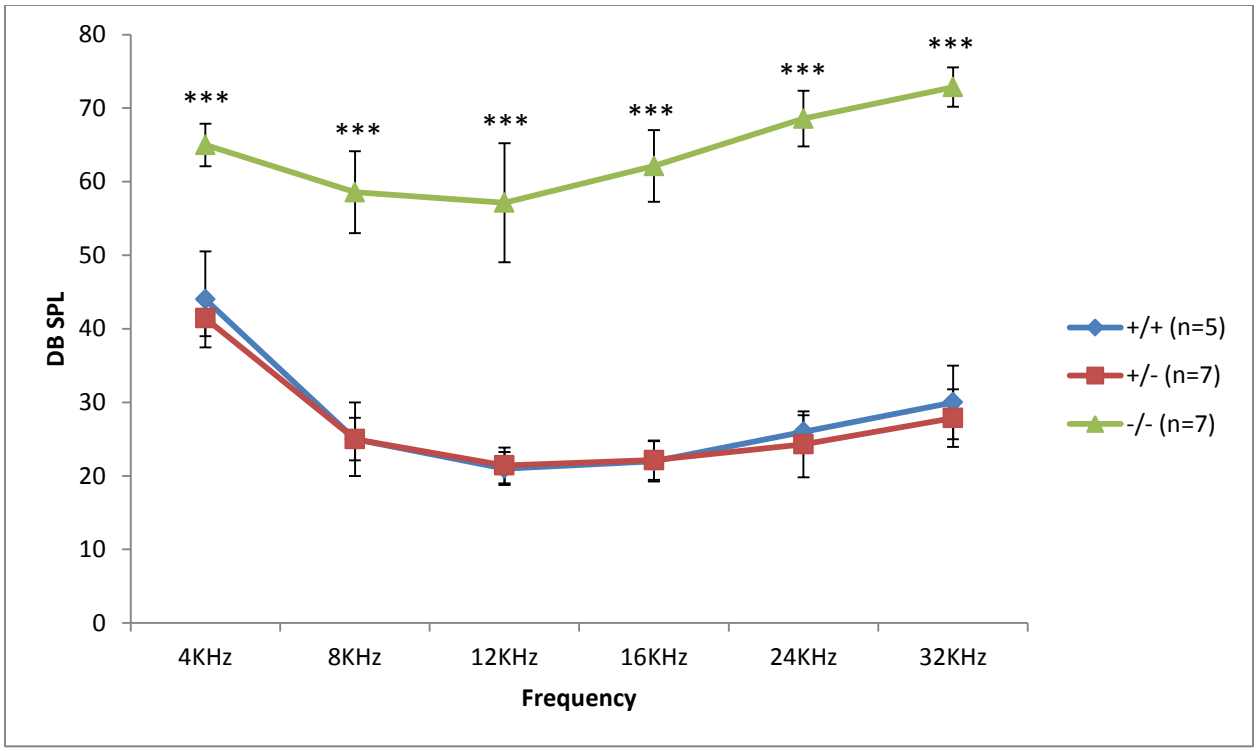

Figure 3.9: *Col9a2* -/- Mice Exhibit Severe Hearing Loss. ABR testing of wild-type, heterozygous and knockout mice at 6 weeks of age indicate that the auditory function was severely compromised and the mice exhibited hearing loss. ***=p<0.001.

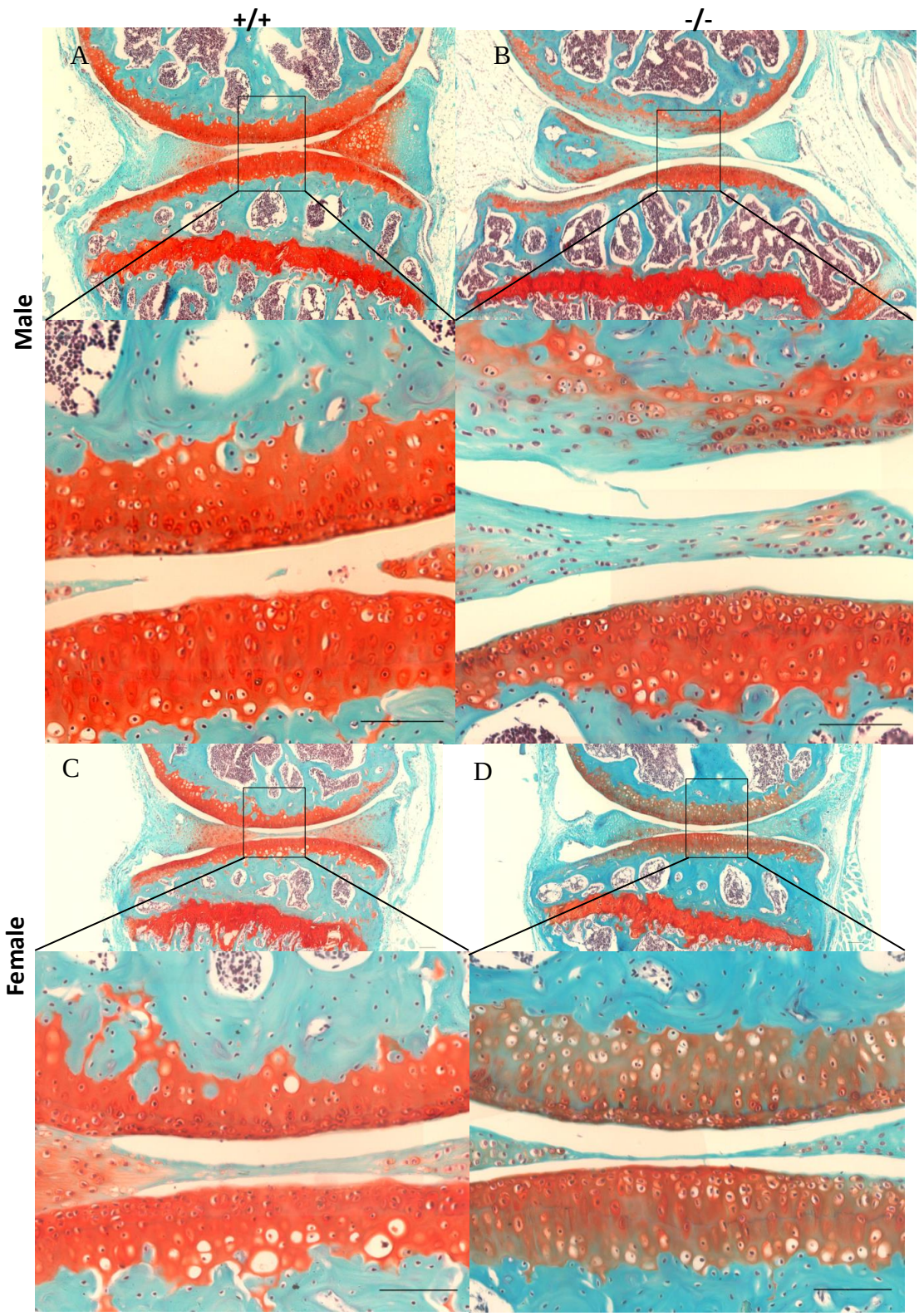

Figure 3.10. Osteoarthritic Degenerative Changes Observed in *Col9a2* -/- Mice. Knee Joints from 6 month old wild-type male (A) and female (C) and knockout male (B) and female (C)

mice (n=6 per group) were assessed for osteoarthritic changes using safranin-o. A decreased proteoglycan content was observed in the knockouts, with some thinning of the articular cartilage. Scale bars represent 100 μm.

References

1. Olsen BR: **Collagen IX**. *The International Journal of Biochemistry & Cell Biology* 1997, **29**(4):555-558.

2. Wu JJ, Woods PE, Eyre DR: **Identification of cross-linking sites in bovine cartilage type IX collagen reveals an antiparallel type II-type IX molecular relationship and type IX to type IX bonding**. *Journal of Biological Chemistry* 1992, **267**(32):23007-23014.

3. Shaw LM, Olsen BR: **FACIT collagens: diverse molecular bridges in extracellular matrices**. *Trends in Biochemical Sciences* 1991, **16**:191-194.

4. Zaucke F GS: **Genetic mouse models for the functional analysis of the perifibrillar components collagen IX, COMP and matrilin-3: Implications for growth cartilage differentiation and endochondral ossification.** *Histology and Histopathology* 2009, **24**(8):13.

5. Wu J-j, Eyre DR: **Cartilage type IX collagen is cross-linked by hydroxypyridinium residues**. *Biochemical and Biophysical Research Communications* 1984, **123**(3):1033-1039.

6. Mayne R, Van Der Rest M, Ninomiya Y, Olsen BR: **The Structure of Type IX Collagena**. *Annals of the New York Academy of Sciences* 1985, **460**(1):38-46.

7. Eyre DR, Pietka T, Weis MA, Wu J-J: **Covalent Cross-linking of the NC1 Domain of Collagen Type IX to Collagen Type II in Cartilage**. *Journal of Biological Chemistry* 2004, **279**(4):2568-2574.

8. van der Rest M, Mayne R: **Type IX collagen proteoglycan from cartilage is covalently cross-linked to type II collagen**. *Journal of Biological Chemistry* 1988, **263**(4):1615-1618.

9. Vaughan L, Mendler M, Huber S, Bruckner P, Winterhalter KH, Irwin MI, Mayne R: **D-periodic distribution of collagen type IX along cartilage fibrils**. *The Journal of Cell Biology* 1988, **106**(3):991-997.

10. Holden P, Meadows RS, Chapman KL, Grant ME, Kadler KE, Briggs MD: **Cartilage Oligomeric Matrix Protein Interacts with Type IX Collagen, and Disruptions to These Interactions Identify a Pathogenetic Mechanism in a Bone Dysplasia Family**. *Journal of Biological Chemistry* 2001, **276**(8):6046-6055.

11. Budde B, Blumbach K, Ylöstalo J, Zaucke F, Ehlen HWA, Wagener R, Ala-Kokko L, Paulsson M, Bruckner P, Grässel S: **Altered Integration of Matrilin-3 into Cartilage Extracellular Matrix in the Absence of Collagen IX**. *Molecular and Cellular Biology* 2005, **25**(23):10465-10478.

12. Pihlajamaa T, Lankinen H, Ylöstalo J, Valmu L, Jäälinoja J, Zaucke F, Spitznagel L, Gösling S, Puustinen A, Mörgelin M *et al*: **Characterization of Recombinant Amino-**

terminal NC4 Domain of Human Collagen IX. *Journal of Biological Chemistry* 2004, **279**(23):24265-24273.

13. Labourdette L, van der Rest M: **Analysis of the role of the COL1 domain and its adjacent cysteine-containing sequence in the chain assembly of type IX collagen**. *FEBS Letters* 1993, **320**(3):211-214.

14. Mechling DE, Gambee JE, Morris NP, Sakai LY, Keene DR, Mayne R, Bächinger HP: **Type IX Collagen NC1 Domain Peptides Can Trimerize in Vitro without Forming a Triple Helix**. *Journal of Biological Chemistry* 1996, **271**(23):13781-13785.

15. Jäälinoja J, Ylöstalo J, Beckett W, Hulmes David JS, Ala-Kokko L: **Trimerization of collagen IX α-chains does not require the presence of the COL1 and NC1 domains**. *Biochemical Journal* 2008, **409**(2):545-554.

16. Boudko SP, Zientek KD, Vance J, Hacker JL, Engel J, Bächinger HP: **The NC2 Domain of Collagen IX Provides Chain Selection and Heterotrimerization**. *Journal of Biological Chemistry* 2010, **285**(31):23721-23731.

17. Czarny-Ratajczak M, Lohiniva J, Rogala P, Kozlowski K, Perälä M, Carter L, Spector TD, Kolodziej L, Seppänen U, Glazar R *et al*: **A Mutation in COL9A1 Causes Multiple Epiphyseal Dysplasia: Further Evidence for Locus Heterogeneity**. *The American Journal of Human Genetics* 2001, **69**(5):969-980.

18. Muragaki Y, Mariman ECM, van Beersum SEC, Perala M, van Mourik JBA, Warman ML, Olsen BR, Hamel BCJ: **A mutation in the gene encoding the [alpha]2 chain of the fibril-associated collagen IX, COL9A2, causes multiple epiphyseal dysplasia (EDM2)**. *Nat Genet* 1996, **12**(1):103-105.

19. P Paassilta JL, S Annunen, J Bonaventure, M Le Merrer, L Pai, and L Ala-Kokko: **COL9A3: A third locus for multiple epiphyseal dysplasia.** *American Journal of Human Genetics* 1999, **64**(4):9.

20. Holden P, Canty EG, Mortier GR, Zabel B, Spranger J, Carr A, Grant ME, Loughlin JA, Briggs MD: **Identification of Novel pro-2(IX) Collagen Gene Mutations in Two Families with Distinctive Oligo-Epiphyseal Forms of Multiple Epiphyseal Dysplasia**. *The American Journal of Human Genetics*, **65**(1):31-38.

21. Spayde EC, Joshi AP, Wilcox WR, Briggs M, Cohn DH, Olsen BR: **Exon skipping mutation in the COL9A2 gene in a family with multiple epiphyseal dysplasia**. *Matrix Biology* 2000, **19**(2):121-128.

22. Unger S, Bonafé L, Superti-Furga A: **Multiple epiphyseal dysplasia: clinical and radiographic features, differential diagnosis and molecular basis**. *Best Practice & Research Clinical Rheumatology* 2008, **22**(1):19-32.

23. Van Camp G, Snoeckx RL, Hilgert N, van den Ende J, Fukuoka H, Wagatsuma M, Suzuki H, Erica Smets RM, Vanhoenacker F, Declau F *et al*: **A New Autosomal**

Recessive Form of Stickler Syndrome Is Caused by a Mutation in the COL9A1 Gene. *American Journal of Human Genetics* 2006, **79**(3):449-457.

24. Baker S, Booth C, Fillman C, Shapiro M, Blair MP, Hyland JC, Ala-Kokko L: **A loss of function mutation in the COL9A2 gene causes autosomal recessive Stickler syndrome**. *American Journal of Medical Genetics Part A* 2011, **155**(7):1668-1672.

25. Faletra F, D'Adamo AP, Bruno I, Athanasakis E, Biskup S, Esposito L, Gasparini P: **Autosomal recessive stickler syndrome due to a loss of function mutation in the COL9A3 gene**. *American Journal of Medical Genetics Part A* 2014, **164**(1):42-47.

26. Robin NH MR, Ala-Kokko L. Stickler Syndrome. 2000 Jun 9 [Updated 2014 Nov 26]. In: Pagon RA, Adam MP, Ardinger HH, et al., editors. GeneReviews® [Internet]. Seattle (WA): University of Washington, Seattle; 1993-2015. Available from: http://www.ncbi.nlm.nih.gov/books/NBK1302/.

27. Annunen S, Paassilta P, Lohiniva J, Perälä M, Pihlajamaa T, Karppinen J, Tervonen O, Kröger H, Lähde S, Vanharanta H *et al*: **An Allele of COL9A2 Associated with Intervertebral Disc Disease**. *Science* 1999, **285**(5426):409-412.

28. Paassilta P, Lohiniva J, Göring HH, et al.: **IDentification of a novel common genetic risk factor for lumbar disk disease**. *JAMA* 2001, **285**(14):1843-1849.

29. Kales SNMDMPH, Linos AMDMPH, Chatzis CMD, Sai YP, Halla MBM, Nasioulas GP, Christiani DCMDMPHMS: **The Role of Collagen IX Tryptophan Polymorphisms in Symptomatic Intervertebral Disc Disease in Southern European Patients**. *Spine* 2004, **29**(11):1266-1270.

30. Jim JJTP, Noponen-Hietala NMDP, Cheung KMCF, Ott JP, Karppinen JMDP, Sahraravand A, Luk KDKF, Yip S-PP, Sham PCMD, Song Y-QP *et al*: **The TRP2 Allele of COL9A2 is an Age-Dependent Risk Factor for the Development and Severity of Intervertebral Disc Degeneration**. *Spine* 2005, **30**(24):2735-2742.

31. Pihlajamaa T, Perälä M, Vuoristo MM, Nokelainen M, Bodo M, Schulthess T, Vuorio E, Timpl R, Engel J, Ala-Kokko L: **Characterization of Recombinant Human Type IX Collagen: ASSOCIATION OF α CHAINS INTO HOMOTRIMERIC AND HETEROTRIMERIC MOLECULES**. *Journal of Biological Chemistry* 1999, **274**(32):22464-22468.

32. Hagg R, Hedbom E, Möllers U, Aszódi A, Fässler R, Bruckner P: **Absence of the α1(IX) Chain Leads to a Functional Knock-out of the Entire Collagen IX Protein in Mice**. *Journal of Biological Chemistry* 1997, **272**(33):20650-20654.

33. Dreier R, Opolka A, Grifka J, Bruckner P, Grässel S: **Collagen IX-deficiency seriously compromises growth cartilage development in mice**. *Matrix Biology* 2008, **27**(4):319-329.

34. Asamura K, Abe S, Imamura Y, Aszodi A, Suzuki N, Hashimoto S, Takumi Y, Hayashi T, Fässler R, Nakamura Y *et al*: **Type IX collagen is crucial for normal hearing**. *Neuroscience* 2005, **132**(2):493-500.

35. Suzuki N, Asamura K, Kikuchi Y, Takumi Y, Abe S, Imamura Y, Hayashi T, Aszodi A, Fässler R, Usami S-i: **Type IX collagen knock-out mouse shows progressive hearing loss**. *Neuroscience Research* 2005, **51**(3):293-298.

36. Hu K, Xu L, Cao L, Flahiff CM, Brussiau J, Ho K, Setton LA, Youn I, Guilak F, Olsen BR *et al*: **Pathogenesis of osteoarthritis-like changes in the joints of mice deficient in type IX collagen**. *Arthritis & Rheumatism* 2006, **54**(9):2891-2900.

37. Boyd LM, Richardson WJ, Allen KD, Flahiff C, Jing L, Li Y, Chen J, Setton LA: **Early-onset degeneration of the intervertebral disc and vertebral end plate in mice deficient in type IX collagen**. *Arthritis & Rheumatism* 2008, **58**(1):164-171.

38. Pettitt SJ, Liang Q, Rairdan XY, Moran JL, Prosser HM, Beier DR, Lloyd KC, Bradley A, Skarnes WC: **Agouti C57BL/6N embryonic stem cells for mouse genetic resources**. *Nat Meth* 2009, **6**(7):493-495.

39. Skarnes WC, Rosen B, West AP, Koutsourakis M, Bushell W, Iyer V, Mujica AO, Thomas M, Harrow J, Cox T *et al*: **A conditional knockout resource for the genome-wide study of mouse gene function**. *Nature* 2011, **474**(7351):337-342.

40. Bradley A, Anastassiadis K, Ayadi A, Battey JF, Bell C, Birling M-C, Bottomley J, Brown SD, Bürger A, Bult CJ *et al*: **The mammalian gene function resource: the international knockout mouse consortium**. *Mammalian Genome* 2012, **23**(9):580-586.

41. Ichimura S, Wu J-J, Eyre DR: **Two-Dimensional Peptide Mapping of Cross-Linked Type IX Collagen in Human Cartilage**. *Archives of Biochemistry and Biophysics* 2000, **378**(1):33-39.

42. Rigueur D, Lyons KM: **Whole-Mount Skeletal Staining**. In: *Skeletal Development and Repair: Methods and Protocols.* Edited by Hilton JM. Totowa, NJ: Humana Press; 2014: 113-121.

43. Myint A, White CH, Ohmen JD, Li X, Wang J, Lavinsky J, Salehi P, Crow AL, Ohyama T, Friedman RA: **Large-scale phenotyping of noise-induced hearing loss in 100 strains of mice**. *Hearing Research* 2016, **332**:113-120.

44. Holden P, Keene DR, Lunstrum GP, Bächinger HP, Horton WA: **Secretion of Cartilage Oligomeric Matrix Protein Is Affected by the Signal Peptide**. *Journal of Biological Chemistry* 2005, **280**(17):17172-17179.

45. Fresquet M, Jackson GC, Loughlin J, Briggs MD: **Novel mutations in exon 2 of MATN3 affect residues within the α–helices of the A-domain and can result in the intracellular retention of mutant matrilin-3**. *Human Mutation* 2008, **29**(2):330-330.

46. Costello KE, Guilak F, Setton LA, Griffin TM: **Locomotor activity and gait in aged mice deficient for type IX collagen**. *Journal of Applied Physiology* 2010, **109**(1):211-218.

47. Koelling S, Kruegel J, Klinger M, Schultz W, Miosge N: **Collagen IX in weight-bearing areas of human articular cartilage in late stages of osteoarthritis**. *Archives of Orthopaedic and Trauma Surgery* 2008, **128**(12):1453-1459.

48. Nikopoulos K, Schrauwen I, Simon M, Collin RWJ, Veckeneer M, Keymolen K, Van Camp G, Cremers FPM, van den Born LI: **Autosomal Recessive Stickler Syndrome in Two Families Is Caused by Mutations in the COL9A1 Gene**. *Investigative Ophthalmology & Visual Science* 2011, **52**(7):4774-4779.

49. Theocharis DA, Skandalis SS, Noulas AV, Papageorgakopoulou N, Theocharis AD, Karamanos NK: **Hyaluronan and Chondroitin Sulfate Proteoglycans in the Supramolecular Organization of the Mammalian Vitreous Body**. *Connective Tissue Research* 2008, **49**(3-4):124-128.

50. Mattapallil MJ, Wawrousek EF, Chan C-C, Zhao H, Roychoudhury J, Ferguson TA, Caspi RR: **The Rd8 Mutation of the Crb1 Gene Is Present in Vendor Lines of C57BL/6N Mice and Embryonic Stem Cells, and Confounds Ocular Induced Mutant Phenotypes rd8 Mutation in Vendor B6 Mice and ES Cells**. *Investigative Ophthalmology & Visual Science* 2012, **53**(6):2921-2927.

51. Koscielny G, Yaikhom G, Iyer V, Meehan TF, Morgan H, Atienza-Herrero J, Blake A, Chen C-K, Easty R, Di Fenza A *et al*: **The International Mouse Phenotyping Consortium Web Portal, a unified point of access for knockout mice and related phenotyping data**. *Nucleic Acids Research* 2014, **42**(D1):D802-D809.

52. Brown SD, Moore MW: **Towards an encyclopaedia of mammalian gene function: the International Mouse Phenotyping Consortium**. *Dis Model Mech* 2012, **5**.

CHAPTER FOUR

Future Directions

Locus Heterogeneity in Multiple Epiphyseal Dysplasia

In this study, I used exome sequencing (15 cases) in tandem with Sanger sequencing (18 cases) to identify the molecular basis of disease in a cohort of 33 patients diagnosed with Multiple Epiphyseal Dysplasia (MED). Based on my data analysis, I identified the following mutations:

- 6 dominant mutations in the known MED disease loci—3 *COMP*, 2 *MATN3*, and 1 *COL9A2*.
- Heterozygosity for pathogenic mutations in *COL2A1* in 2 cases.
- Compound heterozygosity for pathogenic mutations in *GNPTAB* in one case.
- Homozygosity for pathogenic mutations in *CANT1* in two cases of a recessive form of MED clinically distinct from Desbuquois Dysplasia (DBQD).

Based on the exome sequencing, the pathogenic mutations were identified in 9 cases and excluded in 6 cases, suggesting that further locus heterogeneity exists. I identified candidate variants in *PTH2R* and *PRICKLE1* in one case, but no pathogenic variants were identified among the cases analyzed by Sanger sequencing of candidate genes.

While overall I identified the molecular basis of disease in 11 cases, the causative mutation(s) still remains unknown in the remaining cases. As previously mentioned, one of the pitfalls of exome sequencing is the uneven depth of coverage which can arise during exome capture. To aid in the identification of the pathogenic mutations in the remaining cases, whole-genome sequencing could be used in future sequencing studies to avoid this potential technical issue. For the cases only studied by Sanger sequencing of candidate genes, exome sequencing could be used in an attempt to identify the causative variants. By increasing the sample number

and improving the sequencing methodology, I may be able to identify the molecular basis of disease in additional patients in the MED cohort.

Of the mutations that I identified, the most notable finding was the identification of the novel mutations in *CANT1.* As discussed in Chapter 2, *CANT1* is the locus for DBQD, and recessive mutations result in DBQD type I, type II, and the Kim variant. Functional analysis of mutations that result in DBQD phenotypes have indicated that the severe type I and II DBQD typically result from loss-of-function mutations, either via nonsense mutations or missense mutations that result in loss of enzymatic activity[1, 2]. All reported cases of the milder Kim variant indicate that this phenotype results from the inheritance of one loss-of-function mutation and the p.Val226Met mutation, which prior to this study has only been identified in individuals of Japanese and Korean ethnicity [2, 3]. Homozygosity for the p.Val226Met mutation was observed in one family, but insufficient radiographic data were available for a full comparison of the phenotype in this family to the phenotype observed in the case I studied[4]. Examination of the enzymatic activity of the p.Val226Met mutation indicated that this mutation results in CANT1 activity that is 20% of that of the wild-type protein[2]. As the observed phenotype in the MED patients in our study is the mildest phenotype on the *CANT1* spectrum, I hypothesized that the level would be between 20 and 50% of wild type and endeavored to determine the level of enzymatic activity resulting from the p.Ile109Lys substitution in MED case R92-280. Using Epstein Barr Virus transformed lymphoblastoid cell lines for both affected individuals in family R92-280, positive control cells of DBQD patients with *CANT1* mutations, and unaffected negative control cells, I attempted to assay the enzymatic activity of CANT1. However, due to the low expression of *CANT1* in the lymphocyte cells, I was unable to detect CANT1 activity in

the cells. Additional studies using the *in vitro* system described in Furuichi et al., 2011 could be used to determine how the p.Ile109Lys mutation affects CANT1.

Additional studies of *CANT1* using primary cultures of DBQD patient fibroblasts have shown that CANT1 is involved in the posttranslational modification of proteoglycans (PGs), specifically in the synthesis of glycosaminoglycan (GAG) side chains [5]. Subsequent sequencing studies in DBQD patients negative for mutations in *CANT1* identified a second locus for DBQD, *XYLT1*, the gene encoding xylosyltransferase 1, which catalyzes the chain initiation for posttranslational GAG synthesis [6]. Analysis of the GAG content in the DBQD patients positive for *XYLT1* mutations determined that the proteoglycans primarily affected by the loss of xylosyltransferase activity were chondroitin sulfate proteoglycans (CSPGs), and not heparin sulfate proteoglycans (HSPGs) [6]. As these studies have not been conducted in patients with *CANT1* mutations, further examination of the proteoglycan and GAG content in cases with *CANT1* mutations, including MED cases, could aid in understanding the underlying mechanism that results in the spectrum of CANT1 phenotypes. I attempted to assay the GAG levels in cells from affected individuals in family R92-280, but I encountered the similar issue of low gene expression of *CANT1* in lymphocytes that hindered the enzymatic activity assay. Using a xyloside treatment to initiate GAG synthesis, as observed in both Nizon et al. 2012 [5] and Bui et al. 2014 [6], could assist in overcoming the low expression in non-cartilaginous tissues. I might then be able to assay the GAG levels and determine the PG content for CSPGs and HSPGs using chondroitinase and heparanase treatments, providing additional insight into the pathophysiology of disease in MED due to *CANT1* mutations.

Col9a2 and Type IX Collagen Trimerizaton

In Chapter 3, I assessed the biochemical role of α2(IX) in the trimerization of type IX collagen using the *in vivo* model of the *Col9a2* knockout mouse. Based on my analysis, I determined the following:

- The α2(IX) procollagen chain is essential to the trimerization of type IX collagen, and absence of this subunit results in a functional knockout.
- In mice, the loss of type IX collagen results in mild short stature, short limbs, mild craniofacial defects, hearing loss, and early-onset joint degeneration, a phenotype that resembles Stickler syndrome (STL).
- The loss of type IX collagen alters growth plate architecture and chondrocyte morphology. Chondrocytes were irregularly shaped, displayed a loss of polarity, and exhibited endoplasmic reticulum (ER) distention.

I was able to assess the skeletal and auditory phenotypes in the *Col9a2* knockout mice, but further analysis is required to fully comprehend the pathophysiology of disease. Using transmission electron microscopy (TEM), I identified severe ER distention, suggesting the possibility that the unincorporated procollagen chains are triggering ER stress and an unfolded protein response (UPR). This phenomenon has been observed with other structural proteins of the cartilage ECM, such as COMP, matrilin-3, type II collagen and type X collagen, providing precedent for this potential cellular response [7-10]. However, I have not conducted assays to determine whether a UPR was activated. To determine if one consequence of the loss of type IX collagen is UPR, assays could detect the levels of UPR markers from the three main signaling pathways, the PERK, ATF6, and IRE1 pathways [9]. If there are elevated levels of key UPR markers, such as the chaperone proteins BiP and Grp94, or pro-apoptotic marker CHOP, either

via mRNA, protein, or both, I can conclude that the observed growth plate phenotype is due in part from ER stress[9].

References

1. Huber C, Oulès B, Bertoli M, Chami M, Fradin M, Alanay Y, Al-Gazali LI, Ausems MGEM, Bitoun P, Cavalcanti DP *et al*: **Identification of CANT1 Mutations in Desbuquois Dysplasia**. *The American Journal of Human Genetics* 2009, **85**(5):706-710.

2. Furuichi T, Dai J, Cho T-J, Sakazume S, Ikema M, Matsui Y, Baynam G, Nagai T, Miyake N, Matsumoto N *et al*: **CANT1 mutation is also responsible for Desbuquois dysplasia, type 2 and Kim variant**. *Journal of Medical Genetics* 2011, **48**(1):32-37.

3. Dai J, Kim O-H, Cho T-J, Miyake N, Song H-R, Karasugi T, Sakazume S, Ikema M, Matsui Y, Nagai T *et al*: **A founder mutation of CANT1 common in Korean and Japanese Desbuquois dysplasia**. *J Hum Genet* 2011, **56**(5):398-400.

4. Kim O-H, Nishimura G, Song H-R, Matsui Y, Sakazume S, Yamada M, Narumi Y, Alanay Y, Unger S, Cho T-J *et al*: **A variant of Desbuquois dysplasia characterized by advanced carpal bone age, short metacarpals, and elongated phalanges: Report of seven cases**. *American Journal of Medical Genetics Part A* 2010, **152A**(4):875-885.

5. Nizon M, Huber C, De Leonardis F, Merrina R, Forlino A, Fradin M, Tuysuz B, Abu-Libdeh BY, Alanay Y, Albrecht B *et al*: **Further delineation of CANT1 phenotypic spectrum and demonstration of its role in proteoglycan synthesis**. *Human Mutation* 2012, **33**(8):1261-1266.

6. Bui C, Huber C, Tuysuz B, Alanay Y, Bole-Feysot C, Leroy JG, Mortier G, Nitschke P, Munnich A, Cormier-Daire V: **XYLT1 Mutations in Desbuquois Dysplasia Type 2**. *The American Journal of Human Genetics*, **94**(3):405-414.

7. Nundlall S, Rajpar M, Bell P, Clowes C, Zeeff L, Gardner B, Thornton D, Boot-Handford R, Briggs M: **An unfolded protein response is the initial cellular response to the expression of mutant matrilin-3 in a mouse model of multiple epiphyseal dysplasia**. *Cell Stress and Chaperones* 2010, **15**(6):835-849.

8. Cameron TL, Bell KM, Tatarczuch L, Mackie EJ, Rajpar MH, McDermott BT, Boot-Handford RP, Bateman JF: **Transcriptional Profiling of Chondrodysplasia Growth Plate Cartilage Reveals Adaptive ER-Stress Networks That Allow Survival but Disrupt Hypertrophy**. *PLoS ONE* 2011, **6**(9):e24600.

9. Patterson SE, Dealy CN: **Mechanisms and models of endoplasmic reticulum stress in chondrodysplasia**. *Developmental Dynamics* 2014, **243**(7):875-893.

10. Holden P, Keene DR, Lunstrum GP, Bächinger HP, Horton WA: **Secretion of Cartilage Oligomeric Matrix Protein Is Affected by the Signal Peptide**. *Journal of Biological Chemistry* 2005, **280**(17):17172-17179.

CHAPTER FIVE

Conclusions

Through the study of the chondrodysplasias, I have gained a basic understanding of the structure and function of the cartilage extracellular matrix, but the knowledge in this area is still limited. Continued identification and characterization of the mutations that result in these inherited disorders will help improve the understanding of complex developmental processes, such as ECM biosynthesis, that are involved in skeletal growth.

Exome Sequencing in Multiple Epiphyseal Dysplasia

With the discovery and widespread use of next generation sequencing, I was able to address many questions about my cohort of MED patients by conducting exome sequencing: 1) Are these patients positive for a mutation in a known locus? 2) Is the diagnosis based on the radiographic data accurate? 3) Is a novel locus responsible for the molecular basis of disease? Even with a small sequencing cohort of 15 families, I was able to successfully resolve these questions in the majority of the cases.

As described in Chapter 2, I identified mutations in the known MED loci in 6 cases. Among those 6 cases, 3 of these cases had been previously screened for mutations in the known MED loci, while 3 cases had not. While Sanger sequencing is a very powerful and cost-efficient tool for screening a small number of genes with a few exons, in cases like MED where there is significant locus heterogeneity and the genes are large, as in the case of *COMP* with 19 exons and the type IX collagen genes with 35+ exons, this tool is not ideal[1]. Also, with some difficult PCR reactions, it is challenging to obtain good quality sequencing reads to accurately determine the mutation status of cases. However, using exome sequencing, I was able to overcome the limitations of Sanger sequencing by screening the unknown cases and identifying 2 *COMP* mutations and 1 *COL9A2* mutation, and in the hypothesized "negative" cases, I identified 1 *COMP* and 2 *MATN3* mutations, which were likely missed due to sequencing issues. In cases such as these, exome sequencing proved to be a valuable tool.

In addition to the mutations identified in the known MED loci, exome sequencing also identified 3 apparent MED cases with mutations in known skeletal dysplasia loci—*COL2A1*, *GNPTAB*, and *CANT1*. In the case of *COL2A1* and *GNPTAB*, the identified mutations demonstrated that during childhood there is radiographic similarity of MED to related but generally more severe skeletal dysplasias, and how temporal-dependent radiographic manifestations of disease can present an impediment in making accurate diagnoses. In both of these cases, the radiographic images were obtained during early adolescence prior to complete development of the disease, and the phenotype appeared to be MED. Through the use of exome sequencing, I was able to accurately identify the causative mutations, and in the case of the *GNPTAB* mutations, the MLIII diagnosis. There is some debate on whether *COL2A1* is a locus for MED, so the identification of mutations in the gene could be viewed as unsurprising but provides further evidence justifying screening *COL2A1* in MED cases[2]. The study also illustrated how identifying the mutation, in this case through exome sequencing, can assist families by determining the correct inheritance pattern, as the MLIII case was hypothesized to be sporadic and dominant, while the data proved it was actually recessive. Because of these benefits, clinical exome sequencing is becoming more prominent as a tool for molecular diagnostics[1].

Finally, one of the most promising benefits of exome sequencing is the ability to identify rare novel loci in small families[3]. In the case of the novel *CANT1* mutation, I was able to use exome sequencing to identify the pathogenic mutation, even though I was limited to a single case. Combining exome sequencing with other genetic tools such as homozygosity mapping in recessive cases or filtering for *de novo* changes in dominant disorders has and will continue to aid in determining the molecular basis of disease in rare cases.

Just like any novel tool, exome sequencing is not without limitations. I was unable to identify the molecular basis of disease in 6 cases, and this was due in part to some of the limitations of exome sequencing. Since exome sequencing targets only the coding regions, my approach would have missed a molecular defect due to an intronic splicing variant outside the targeted regions of the exome, which might be present in a known MED locus or a novel locus. I also cannot rule out novel mechanisms that could produce MED, including regulatory mutations or copy number variations, neither of which would be detected by exome sequencing. Combining techniques such as RNA-sequencing to detect altered gene expression levels and whole genome sequencing to ensure complete coverage could aid in overcoming the shortcomings of capturing and sequencing just the exome[4].

Type IX Collagen in Humans and Mice

In Chapter 3, I focused on resolving the ambiguity revolving around type IX collagen trimerization and whether the α2(IX) chain was required for this biological process. Because *in vitro* biochemical data suggested that α2(IX) was dispensable and the *in vivo* human data from the STL family were limited, represented by a single case of *COL9A2* STL, there was an opportunity to resolve the question using a mouse model. Analysis of the mouse *Col9a2* knockout mouse established that α2(IX) is essential for trimerization.

One of the major challenges of studying a mild disease, such as STL or MED, is the inability to obtain patient specimens. Because the phenotype is very mild, invasive procedures such as cartilage or even a skin biopsy are not routinely performed. Also, since many of the associated genes are highly and/or selectively expressed in cartilage, studies in cell types other than chondrocytes do not accurately mimic the mechanism of disease pathogenesis. In cases such as these, mouse models prove invaluable since we are able to study and analyze the

pathophysiology of disease using an *in vivo* model. Using this rationale, my study of the *Col9a2* $^{-/-}$ mouse enabled us to determine the mechanism of disease in *COL9A2* STL, which will make a contribution to the literature on this topic. For this reason, mouse models will continue to aid in research on rare diseases and their mechanisms.

Through my study of MED and type IX collagen, I was able to successfully determine the molecular basis of disease in 11 unresolved cases of MED using a combination of exome and Sanger sequencing. With the identification of the clinically distinct *CANT1* recessive MED, I have expanded the number of known loci for the disease. Using the *Col9a2* -/- mouse I was able to determine that the alpha-2 chain of type IX collagen is required for trimerization, and the mechanism of disease in *COL9A2* STL is the result of a functional knockout of type IX collagen. A continued use of next-generation sequencing tools and mouse genetics will aid in the study of chondrodysplasias of the cartilage ECM.

References

1. Fogel BL, Lee H, Strom SP, Deignan JL, Nelson SF: **Clinical exome sequencing in neurogenetic and neuropsychiatric disorders**. *Annals of the New York Academy of Sciences* 2016, **1366**(1):49-60.

2. Jackson GC, Mittaz-Crettol L, Taylor JA, Mortier GR, Spranger J, Zabel B, Le Merrer M, Cormier-Daire V, Hall CM, Offiah A *et al*: **Pseudoachondroplasia and multiple epiphyseal dysplasia: A 7-year comprehensive analysis of the known disease genes identify novel and recurrent mutations and provides an accurate assessment of their relative contribution**. *Human Mutation* 2012, **33**(1):144-157.

3. Geister KA, Camper SA: **Advances in Skeletal Dysplasia Genetics**. *Annual Review of Genomics and Human Genetics* 2015, **16**(1):199-227.

4. Meynert AM, Ansari M, FitzPatrick DR, Taylor MS: **Variant detection sensitivity and biases in whole genome and exome sequencing**. *BMC Bioinformatics* 2014, **15**(1):1-11.